

ABSTRACT

Title of Document: CHARACTERIZING FOREST DISTURBANCE
DYNAMICS IN THE HUMID TROPICS USING
OPTICAL AND LIDAR REMOTELY SENSED
DATA SETS

Alexandra Tyukavina, Ph.D., 2015

Directed by: Professor Matthew C. Hansen, Department of
Geographical Sciences

Human-induced tropical deforestation and forest degradation are widely recognized as major environmental threats, negatively affecting tropical forest ecosystem services, such as biodiversity and climate regulation. To mitigate the effects of forest disturbance, particularly carbon emissions, national forest monitoring systems are being established throughout the tropics. Multiple good practice guidelines aimed at developing accurate, compatible and cost-effective monitoring systems have been issued by IPCC, UNFCCC, GFOI and other organizations. However, there is a lack of consensus in characterization of

the baseline state of the forests and carbon stocks. This dissertation is focused on the improvement of the current methods of remotely-sensed forest area and carbon loss estimation. A sample-based estimation method employing Landsat-based forest type and change maps and GLAS Lidar-modeled carbon data was first prototyped for the Democratic Republic of the Congo (DRC), and then applied for the entire pan-tropical region. The DRC study found that Landsat-scale (30m) map-based forest loss assessments unadjusted for errors may lead to significant underestimation of forest aboveground carbon (AGC) loss in the environments with small-scale land cover change dynamics. This conclusion was supported by the pan-tropical study, which revealed that Landsat-based mapping omitted almost half (44%) of forest loss in Africa compared to the sample-based estimate (sample-based estimate exceeded map-based by 78%). Landsat performed well in Latin America and Southeast Asia (sample-based estimate exceeded map-based by 15% and 6% respectively), where forest dynamics are dominated by large-scale industrial forest clearings. The pan-tropical validation sample also allowed disaggregating forest cover and AGC loss by occurrence in natural- (primary and mature secondary forests, and natural woodlands) or human-managed (tree plantations, agroforestry systems, areas of subsistence agriculture with rapid tree cover rotation) forests. Pan-tropically, 58% of AGC loss came from natural forests, with proportion of natural AGC loss being the highest in Brazil (72%) and the lowest in the humid tropical Africa outside of the DRC (22%). The pan-tropical study employed a novel forest stratification for carbon estimation based on forest structural characteristics (canopy cover and height) and intactness, which aided in reducing standard errors of the sample-based estimate (SE of 4% for the pan-tropical gross forest loss area estimate). Such a stratification also allowed for the quantification of forest

degradation by delineating intact and non-intact forest areas with different carbon content. This indirect approach to quantify forest degradation was advanced in the last research chapter by automating the process of intact (hinterland) forest mapping. Hinterland forests are defined as forest patches absent of and removed from disturbance in near-term history. Their utility in using spatial context to map structurally different (degraded and non-degraded) forests points a way forward for improved stratification of forest carbon stocks. Conclusions from the dissertation summarize strengths and challenges of sample-based area estimation in monitoring forest carbon stocks and the possible use of such estimates in the revision of spatially explicit maps by adjusting them to match the unbiased sample-based estimates. Hinterland forest maps, in addition to providing a valuable stratum for sample-based carbon monitoring, may serve as a baseline for the near real-time monitoring of remaining ecologically intact tropical forests.

CHARACTERIZING FOREST DISTURBANCE DYNAMICS IN THE HUMID
TROPICS USING OPTICAL AND LIDAR REMOTELY SENSED DATA SETS

by

Alexandra Tyukavina

Dissertation submitted to the Faculty of the Graduate School of the
University of Maryland, College Park, in partial fulfillment
of the requirements for the degree of
Doctor of Philosophy
2015

Dissertation Examining Committee:
Professor Matthew C. Hansen, Chair
Dr. Scott Goetz
Professor Christopher O. Justice
Research Assoc. Prof. Peter V. Potapov
Professor Joseph Sullivan

© Copyright by
Alexandra Tyukavina
2015

Foreword

Chapters 2-4 contain jointly authored work in which Alexandra Tyukavina is the primary author. Methods development, data processing, analysis of the findings and manuscript writing is led by Alexandra Tyukavina with the contributions from other co-authors, who are named in the corresponding chapters.

Acknowledgements

I'm very grateful to my advisor, Dr. Matthew Hansen, who is a wonderful teacher and friend, for keeping me motivated, and constantly providing support and feedback on my research. Thank you for giving me the opportunity to work on exciting projects and for showing me tropical forests.

It's a pleasure to thank the members of my dissertation committee for directing the path of my research and helping me get through the thorny peer-review process.

I want to express my deepest gratefulness to our research group, which is like a family to me. I feel blessed being the part of this wonderful team. My research wouldn't be possible without everyday guidance and support of Peter Potapov, Sveta Turubanova and Alexander Krylov. Peter and Sveta were the ones who initially believed in me and introduced me to the team, for which I'm sincerely thankful. I also thank LeeAnn King, Belinda Margono, Yolande Munzimi, Yamile Talero, Janet Nackoney, Sam Jantz, Patrick Lola Amani, Guiseppe Molinario, Alice Altstatt for friendly support and intellectually stimulating discussions. Special thanks to Allison Gost whose excellent organization skills allowed me to concentrate on my research instead of worrying about paperwork. Thank you to Alice Altstatt for proofreading my dissertation.

I thank colleagues from the Woods Hole Research Center, namely Dr. Scott Goetz, Dr. Richard Houghton and Dr. Alessandro Baccini, for significantly contributing to my research by sharing data and ideas, and jointly working on the manuscripts.

I'm thankful to Dr. James R. Kellner for giving an excellent introduction to the theory and practice of science, which initiated fruitful discussions in class and stimulated my development as a scientist outside of class. I also thank the members of my Portfolio committee, Dr. Stephen Prince and Dr. Eric Kasischke for making me think about my professional and research goals.

And last but not least I thank my family and friends for supporting me along the way. To my parents, thank you for approving all my decisions and being proud of my work more than I am myself. To Pasha, thank you for helping me look at my problems and worries from a different angle, constantly caring about me and connecting me to the place inside myself that is love.

Table of Contents

Foreword	ii
Acknowledgements	iii
List of Tables	vi
List of Figures	viii
Chapter 1: Introduction	1
1.1 Background of the research.....	1
1.1.1 Current state of remotely sensed characterization of tropical forest disturbance and related carbon loss.....	1
1.1.2 Advances and challenges in mapping tropical forest degradation.....	9
1.2 Research goals and objectives.....	11
1.3 Structure of the dissertation.....	13
Chapter 2: National-scale estimation of gross forest aboveground carbon loss: a case study of the Democratic Republic of the Congo	16
2.1. Introduction.....	16
2.2. Data.....	20
2.2.1. Activity data.....	20
2.2.2. Carbon data.....	21
2.2.3. Validation data.....	23
2.3. Methods.....	24
2.3.1. Uncertainties from activity data.....	24
2.3.1.1. Sampling design and sample size.....	24
2.3.1.2. Estimating area of forest loss and its uncertainty.....	28
2.3.2. Uncertainties from carbon data.....	32
2.3.3. Combination of the uncertainties.....	32
2.4. Results.....	35
2.5. Discussion.....	39
2.6. Conclusion.....	45
Chapter 3: Aboveground carbon loss in natural and human-modified tropical forests from 2000 to 2012	49
3.1. Introduction.....	49
3.2. Data and Methods.....	53
3.2.1. Study region.....	53
3.2.2. Approach to estimating gross aboveground carbon loss.....	54
3.2.3. Pan-tropical forest cover stratification (year 2000).....	55
3.2.4. Height model.....	57
3.2.5. Forest cover loss data.....	57
3.2.6. Carbon density data.....	67
3.3. Results.....	69
3.4. Discussion and Conclusions.....	74
Chapter 4: Indirect mapping of forest degradation in the tropics	81
4.1. Introduction.....	81
4.2. Data and Methods.....	85
4.2.1. Definitions.....	85
4.2.2. Data.....	87

4.2.3. Hinterland forest mapping.....	88
4.2.4. Forest degradation mapping.....	89
4.3. Results.....	91
4.3.1. Hinterland forest and degradation mapping.....	91
4.3.2. Comparison with GLAS.....	98
4.3.3. Comparison with the IFL map.....	99
4.4. Discussion and Conclusions.....	101
Chapter 5: Summary of findings, significance and future research directions.....	105
5.1. Sample-based approach to forest loss area estimation and its implications for carbon monitoring.....	105
5.2. Potential of hinterland forest mapping in stratification for forest carbon loss estimation and in forest degradation assessment.....	108
5.3. Future research directions.....	109
Bibliography.....	113

List of Tables

Table 2.1 Distribution of samples among forest types using proportional and arbitrary sample allocation strategies for stratified random sampling.....	26
Table 2.2 Allocation of sample size among validation strata.....	27
Table 2.3 Error matrix of sample counts for map-scale and sub-grid area estimates.....	28
Table 2.4 Parameters for the calculation of error-adjusted area of forest cover loss within <i>terra firma</i> primary forests (map-scale estimate).....	31
Table 2.5 GLAS-based AGC density estimates for the DRC forest types. Mean AGC densities are given with \pm 95% CI.....	32
Table 2.6 Original FACET and error-adjusted estimates of 2000-2010 forest cover loss within DRC forest types (\pm 95% CI).....	35
Table 2.7 Gross AGC loss estimates (2000-2010) with the uncertainty measures for DRC forest types (\pm is the 95% CI).....	39
Table 2.8 Comparison of forest cover and carbon loss estimates for the DRC (\pm 95% CI).....	40
Table 3.1 Sample size allocation per stratum for the stratified random sample. Forest strata codes are from figure 3: 1 – low cover; 2 – medium cover short; 3 – medium cover tall; 4 – dense cover short; 5 – dense cover short intact; 6 – dense cover tall; 7 – dense cover tall intact.....	60
Table 3.2 Error matrix of sample counts. 1-pixel buffer sub-stratum includes mapped no loss pixels adjacent to pixels of mapped loss.....	60
Table 3.3 Sample size allocation per countries and country groups (figure 3.1) for the final reporting.....	62

Table 3.4 2000-2012 forest cover and aboveground carbon (AGC) loss estimates. Estimates are produced within the continental strata (see figure 3.3). Uncertainty is expressed as a 95% confidence interval.....	65
Table 3.5 2000-2012 forest cover loss and aboveground carbon (AGC) loss estimates. The “Sample estimate” value is computed using an unbiased estimator of forest cover loss area applied to data obtained from a probability sampling design (see Data and Methods). Uncertainty is expressed as a 95% confidence interval (CI). For the boundaries of the regions see figure 3.1.....	70
Table 3.6 Comparison of gross carbon loss estimates. AGC stands for aboveground carbon; BGC – belowground carbon. Range of uncertainty represents the 95% confidence interval for the current study; 90% prediction interval derived from Monte Carlo simulations and including all critical sources of uncertainty for Harris et al. (2012), and uncertainty range derived from a sensitivity analysis related to the bias in carbon density maps for Achard et al. (2014).....	75
Table 3.7 Comparison of methodology in the current study, Harris et al. (2012) and Achard et al. (2014).....	77
Table 4.1 Estimated extent of 2007-2012 forest degradation (hinterland forest loss) in the study regions.....	95
Table 4.2 2007 forest cover, 2007 hinterland forest extent and 2007-2012 hinterland forest loss by country. 2007 forest cover is derived from year 2000 canopy cover (Hansen et al., 2013) by thresholding (>25%) and subtracting 2000-2006 forest cover loss.....	95
Table 4.3 Sources of disagreement between the 2010 IFL map (Potapov <i>et al</i> 2008b) and 2011 hinterland forest map (current study).....	100

List of Figures

Figure 1.1 Conceptual diagram of dissertation research.....	13
Figure 2.1 FACET forest cover and forest cover loss (Potapov <i>et al</i> 2012) combined with DRC wetland map (Bwangoy <i>et al</i> 2010): a) forested area; b) woodlands.....	21
Figure 2.2 2004-2008 GLAS shots color-coded by the FACET forest type (Potapov <i>et al</i> 2012) combined with wetland map (Bwangoy <i>et al</i> 2010).....	22
Figure 2.3 Example of sample block visual interpretation; for the map-scale estimate, 0.5 loss is treated as no loss. The black stripe in the 2010 Landsat loss sample is a data gap due to the Landsat 7 scan-line corrector malfunction.....	29
Figure 2.4 Forest cover loss (2000-2010) within DRC forest types; error bars are the 95% CIs.....	36
Figure 2.5 Comparison of the AGC density estimates from the published datasets (error bars are the 95% CIs) and the current study.....	37
Figure 2.6 Forest type and strata averages, aggregated to a 5-km grid: a) year 2000 AGC; b) map-scale estimate of 2000-2010 gross AGC loss; c) sub-grid estimate of 2000-2010 AGC loss; d) difference between sub-grid and map-scale estimates. Water bodies are shown in grey. Note that AGC values for both b) and c) are the same for the respective forest types.....	38
Figure 3.1 Boundaries of reporting units. A) Democratic Republic of the Congo; B) Humid tropical Africa; C) The rest of Sub-Saharan Africa; D) Brazil; E) Pan-Amazon; F) The rest of Latin America; G) Indonesia; H) Mainland South and Southeast Asia (includes southern China up to 40°N); I) Insular Southeast Asia.....	54

Figure 3.2 Forest cover stratification thresholds. Terminal node values are mean strata AGC density values (MgC/ha).....	56
Figure 3.3 Forest cover stratification. a) Africa; b) South and Southeast Asia; c) Latin America; numbers in the legend refer to forest strata: 1 – low cover; 2 – medium cover short; 3 – medium cover tall; 4 – dense cover short; 5 – dense cover short intact; 6 – dense cover tall; 7 – dense cover tall intact.....	56
Figure 3.4 Validation samples: a-g – natural forest loss in Mato Grosso, Brazil; h-n – plantation clearing and regrowth in Parana, Brazil; a-f and h-k are Landsat multitemporal composites for years circa 2000, 2003, 2006, 2009, 2012 and 2000-2012 maximal composite; g and n – high resolution imagery from Google Earth™.....	63
Figure 3.5 GLAS samples (2003-2009) attributed with aboveground carbon (AGC) densities. Each circle on the map corresponds to a ~65 m diameter circular GLAS lidar footprint with the modeled AGC density (MgC/ha) value (Baccini et al., 2012).....	68
Figure 3.6 Mean AGC densities (\pm 95% CI) for forest strata 1-7 within the 3 study regions, derived from GLAS-modeled biomass samples (Baccini et al., 2012)).....	68
Figure 3.7 Forest strata average aboveground carbon (AGC) density and loss: a-c, year 2000 aboveground carbon (AGC) density; d-f, estimated 2000-2012 AGC loss. Data are aggregated to 5 km for display purposes.....	71
Figure 3.8 Forest loss in natural and managed forests. Sample locations classified as reference loss within natural and managed forests for each of the seven forest type strata (see figure 3.3): 1 – low cover; 2 – medium cover short; 3 – medium cover tall; 4 – dense	

cover short; 5 – dense cover short intact; 6 – dense cover tall; 7 – dense cover tall intact.....72

Figure 3.9 Difference between sample and map-based (Hansen et al., 2013) aboveground carbon (AGC) loss estimates. Positive values correspond to the areas where the sample estimate exceeds the map-based estimate. Difference map was derived by calculating the difference between sample- and map-based AGC loss estimates for each stratum and aggregating to a 5 km resolution for display.....74

Figure 4.1 Hinterland forest criteria: a) distance to forest cover loss and gain (>1 km); b) minimal patch size (100 km²); c) minimal corridor width (2 km). Red is forest cover loss; blue – forest cover gain; dark green – hinterland forests; light green – other forests after subtracting 1-km buffer around change.....86

Figure 4.2 Hinterland forest mapping workflow. Input parameters: start and end years (year1 and year2) and forest canopy cover threshold (X%).....89

Figure 4.3 2007-2012 forest degradation (hinterland forest loss) mapping. Background image is a year 2000 Landsat composite (Hansen et al. 2013), band combination 5-4-3....90

Figure 4.4 Results of the visual assessment of 2007-2012 forest degradation patches with the area <100km². Blue represents inclusion threshold: all polygons < 0.13km² were considered incorrect (noise) and excluded from the final forest degradation map. X axis (area) has log scale.....91

Figure 4.5 Hinterland forests 2007: a) Latin America; purple inset – Para, Brazil; red – Chaco woodlands; b) Africa; yellow inset – Kisangani, DRC; c) Southeast Asia; cyan inset – coast of Sumatra, Indonesia.....92

Figure 4.6 Forest degradation (2007-2012): a) Latin America; purple inset – Urucu natural gas field, Amazonas, Brazil; red – Chaco woodlands large-scale agricultural clearing, Santa Cruz, Bolivia and Boqueron and Alto Paraguay, Paraguay; b) Africa; yellow inset – smallholder-dominated agriculture, Likuuala, RoC and Equateur, DRC; c) Southeast Asia; cyan inset – logging in Central Kalimantan, Indonesia and Sarawak, Malaysia.....93

Figure 4.7 Percent of hinterland forests 2007 from total forest cover (>25%) vs. percent 2007-2013 hinterland forest loss from 2007 hinterlands. Circle size represents 2007 hinterland forest area (diameter is proportional to the square root of the area). DRC stands for the Democratic Republic of the Congo, CAR for Central African Republic. Tropical countries with hinterland forest extent <200 ha (Bangladesh, Benin, Burkina Faso, Burundi, El Salvador, Gambia, Guinea-Bissau, Haiti, Malawi, Togo) and Rwanda, which lost all of its hinterland forests by 2013, are excluded from the graph.....97

Figure 4.8 Histograms of year 2007 GLAS-estimated tree heights within and outside 2007 hinterland forests.....99

Figure 4.9 Comparison of 2010 Intact forest landscapes (IFL) map and 2011 hinterland forest map.....101

Figure 5.1 Number of cloud-free observations for each 30-m pixel during the first 288 days of the year 2014 within a hinterland forest mask in Peru.....112

Chapter 1: Introduction

1.1 Background of the research

Awareness of the potential effects of tropical deforestation and forest degradation on the global climate, on biodiversity and on livelihoods of people living off the forests has resulted in the emergence of research and policy initiatives aimed to reduce the rate of tropical forest loss. The REDD+ (Reducing Emissions from Deforestation and Forest Degradation + Conservation and Sustainable Development) mechanism under the United Nations Framework Convention on Climate change (UNFCCC), in order to compensate developing countries for avoided carbon emissions from deforestation and potential social and environmental co-benefits, calls for valid and up-to-date data on the rates and spatial distribution of deforestation and forest degradation (UNFCCC 2014).

Food and Agriculture Organization of the United Nations (FAO) publishes reports on the state of the forests (Forest Resources Assessment) every five years based on the statistics provided by individual countries and derived using different methodological approaches. Forest in these reports is defined based on land use (FAO 2012), and only the net value of forest area change is reported (FAO 2010). All of this makes inter-country comparison of forest disturbance rates and the analysis of global and regional trends in forest cover ambiguous.

Remote sensing, on the contrary, enables large scale, objective forest dynamics assessments independent of country politics and culture. Remotely sensed forest change detection is based on the physical signal determined by the presence or absence of tree cover and reflecting the change of land cover rather than land use, and could therefore be

delivered in a more consistent definitional framework, as opposed to the variety of official forestry inventory data provided by the countries. Moreover, remotely sensed data are synoptic, covering areas where field inventories are either impractical or non-existent, such as remote areas of Central Africa where expansion of small-scale slash-and-burn agriculture encroaches into primary tropical forests (Potapov *et al* 2012). These factors determined the focus of current dissertation research on the existing remotely sensed data products and their use for the characterization of forest dynamics and quantification of the resulting change in forest carbon stocks.

1.1.1 Current state of remotely sensed characterization of tropical forest disturbance and related carbon loss

From a remotely sensed perspective, forest disturbance is defined as the loss of tree canopy cover detectable in the imagery. I intentionally avoid the term “deforestation” further in this dissertation to avoid confusion, because the term usually implies a land use change, which I do not intend to characterize in the current research:

“Deforestation – the conversion of forest to other land use or the permanent reduction of the tree canopy cover below the minimum 10 percent threshold” (FAO 2012)

Global Forest Observations Initiative recently published a review of the methods of remotely sensed forest change area (“activity data” in the Intergovernmental Panel on Climate Change (IPCC) terminology) estimation (table 7, GFOI 2014) in the REDD+ framework, which indicates that both optical and synthetic aperture radar (SAR) satellite data could be used in the operational mode for forest cover and change mapping at national and sub-national (project) levels. Although SAR data are unaffected by cloud

coverage, and their utility for forest cover and change mapping has been demonstrated in a number of case studies (Walker *et al* 2010, Thiel *et al* 2009, Lehmann *et al* 2012), forest monitoring SAR-based systems are currently not used operationally, and subsequently in this section I will focus on optical remotely sensed data for forest change area estimation.

Initially global and large-regional forest cover and forest change estimates were based on optical satellite data with coarse spatial resolution ranging from hundreds of meters to kilometers, such as data from Advanced Very High Resolution Radiometer (AVHRR) and Moderate-Resolution Imaging Spectroradiometer (MODIS) sensors (Hansen and DeFries 2004, Achard *et al* 2007). Medium resolution (10x meters) optical data, e.g. from Landsat Thematic Mapper (TM) and Enhanced Thematic Mapper Plus (ETM+) sensors, were later used in a combination with coarser resolution data for the purposes of forest monitoring (Hayes and Cohen 2007, Hansen *et al* 2008), but utility of this approach was limited at the time due to high costs of Landsat-resolution data. The establishment of two Landsat-based national monitoring systems, Brazilian National Institute for Space Research (INPE) PRODES system (INPE 2008, Shimabukuro *et al* 1998) and Australian National Carbon Accounting System (NCAS) (Caccetta *et al* 2007), was facilitated by the availability of free Landsat imagery from the countries' ground receiving stations. These national systems are based on a single-date, cloud-free image availability. The situation dramatically changed with the opening of Landsat archive in 2008 (Wulder *et al* 2012). Free access to the longest unbroken data record of earth observations (a result of Landsat's global acquisition strategy) has enabled large-scale wall-to-wall mapping. Several regional-scale Landsat mapping projects based on the analysis of multitemporal image composites have been implemented since then (Potapov

et al 2011, 2012), followed by the publishing of the first 30-m resolution global forest cover change map (Hansen *et al* 2013). High resolution (<10 meters) optical imagery, due to its cost and absence of global acquisition plans, is currently used mostly for the local mapping projects or for the validation of medium- and coarse-resolution maps. The public archive of dated high resolution imagery provided by GoogleEarth™ is one of the major sources of such data. The launch of high resolution microsatellites by Planet Labs and Skybox (Butler 2014) may change the situation providing near real-time low cost high resolution imagery, but the utility of these data in scientific applications still needs to be investigated.

Medium resolution wall-to-wall forest cover and change maps represent the state of the art in remotely sensed forest monitoring, and therefore the current dissertation research is based on such products: the Democratic Republic of the Congo (DRC) Forêts d'Afrique Centrale Evaluées par Télédétection (FACET) map (Potapov *et al* 2012) and the global 30-m forest cover change map (Hansen *et al* 2013). The obvious advantage of wall-to-wall maps is the ability to analyze patterns and temporal trends of forest cover and change distribution within any areal unit. However, due to the errors inevitably resulting from the mapping process, estimates of area should be based on validation sample data (Stehman 2013), rather than counting pixels of the map:

“A key strength of remote sensing is that it enables spatially exhaustive, wall-to-wall coverage of the area of interest. However, as might be expected with any mapping process, the results are rarely perfect. Placing spatially and categorically continuous conditions into discrete classes may result in confusion at the categorical transitions. Error can also result from the change mapping process, the data used, and analyst biases (Foody, 2010). Change detection and mapping approaches using remote sensing are increasingly robust, with improvements aimed at the mitigation of these sources of error. However, any map made from remotely sensed data can be assumed to contain some error, with the areas calculated from the map (e.g. pixel counting) also potentially subject

to bias. An accuracy assessment identifies the errors of the classification, and the sample data can be used for estimating both accuracy and area along with the uncertainty of these estimates.” (Olofsson *et al* 2014)

A recommended approach is therefore to use a stratified random sample with strata being map classes to produce an unbiased area estimate based on the reference classification of sample units (Olofsson *et al* 2013, 2014, Stehman and Czaplewski 1998). Following these good practice recommendations, I have implemented the sample-based approach to estimating forest cover loss area from the map in Chapters 2 and 3.

Sample-based forest cover and change analysis not based on wall-to-wall maps is also suitable (GOFC-GOLD 2013), though it lacks spatial continuity inherent in wall-to-wall mapping. In this case the recommended sampling approaches are systematic sampling or stratified sampling with the strata based on auxiliary information, e.g. derived from coarse resolution satellite data or existing GIS datasets (GOFC-GOLD 2013). Broich *et al.* (2009) have shown that both stratified and systematic sampling designs yield smaller standard errors than simple random sampling, and stratified sampling yields smaller standard errors than systematic with the same sample size. Systematic sampling of Landsat-resolution data was implemented to estimate forest cover change rates in the Congo basin (Céline *et al* 2013) and in the entire tropical region (Achard *et al* 2014). The examples of forest dynamics studies using stratified sampling of medium-resolution data are the pan-tropical assessment based on 1-km² forest cover and expert-identified deforestation risk stratification (Achard *et al* 2002) and the global assessment based on MODIS-indicated forest cover loss stratification (Hansen *et al* 2010).

The IPCC identifies two basic approaches to quantify land-cover (including forest) carbon stock change (Volume 4, Chapter 2, eq. 2.4 and 2.5, IPCC 2006): Gain-Loss (G-L) and Stock-Difference (S-D) methods. In the G-L approach, *activity data* on the extent of gains (e.g. forest regrowth, forest planting) and losses (e.g. logging, fires) of a given land cover class are related to the corresponding increases in biomass and *emission factors* (carbon emissions per unit activity). In the S-D approach carbon stocks at two points of time are measured, and the change in carbon stocks for the given period is measured as the difference between the two. In terms of the methods of satellite-based carbon mapping and monitoring, Goetz et al. (2009) distinguish three major approaches: Stratify and Multiply (SM), where a single carbon stock value is assigned to each land cover or land cover change class derived from satellite data; Combine and Assign (CA) method, similar to SM, but making use of a large variety of spatial data, including existing maps and GIS datasets; and Direct Remote Sensing (DR), in which carbon stock estimates (derived from the field surveys or using field-calibrated models based on remotely sensed data) are directly related to satellite measurements to produce carbon density maps. The SM approach is the simplest and requires the least amount of data processing, while the DR usually employs complicated modelling and requires significant computational resources. The SM, CA and DR approaches all could be used to quantify carbon stock change using both G-L and S-D IPCC methods. For example, to quantify forest carbon loss using the G-L approach, SM would assign emissions factors to existing land cover change map classes, CA would enhance this approach by using additional information of adjacency to cities and roads and other factors that may have an impact on emission factors, and DR would directly map gains and losses of forest

carbon by relating known values of carbon loss and gain with remotely sensed data (optical, Light Detection and Ranging (LIDAR), SAR). For the S-D approach, SM, CA and DR would be used to produce forest carbon density or carbon stock maps for time 1 and time 2, which then would be compared to estimate change in carbon stocks.

The IPCC also classifies methodological approaches to carbon stock change estimation into three Tiers (IPCC 2003b, 2006, GFOI 2014). The simplest, Tier 1, employs the G-L approach with the default emission factors, and could be implemented using SM or CA methods with published coarse-resolution maps. Tier 2 is similar to Tier 1, but uses country-specific emission factors and more detailed spatial information. Tier 3 may employ G-L or S-D approaches and more complex CA and DR mapping methods together with models linking carbon dynamics in various carbon pools (e.g. in biomass and soils). Transition from Tiers 1 to Tier 3 also implies reduction of estimate uncertainty and a more rigorous estimation of uncertainties.

The method of forest aboveground carbon loss estimation presented in Chapters 2 and 3 corresponds to the “loss” component of the G-L approach and uses the SM method, and could be used for the regional, national and sub-national Tier 2 and Tier 3 assessments (in Chapter 3 – closer to CA because of the use of multiple parameters for forest type stratification instead of a single forest type map).

The major sources of emission factors are published tabular data (Gibbs 2006, Gibbs and Brown 2007, FAO 2010), carbon density maps derived using remote sensing (Saatchi *et al* 2011, Baccini *et al* 2012), field-calibrated LIDAR-modeled biomass estimates (Baccini *et al* 2012), National Forest Inventory (NFI) data for the countries with the established national forest monitoring systems, and other field biomass

estimates. Tabular data are useful for the Tier 1 estimates and have a limited capability to account for the spatial heterogeneity of land cover classes. NFI and other field data are the most precise, though influenced by measurement errors, the choice of allometric equations, and the uncertainties related to the field plot size and sample representativeness (Chave *et al* 2004). These data are expensive and labor-consuming to acquire, and, as a result, scarce or nonexistent for many regions of the world, especially for those with poor infrastructure, like Central Africa. Remote sensing enables extrapolation of field measurements to other locations. The first level of abstraction is to use field biomass measurements to calibrate LIDAR metrics of vertical canopy structure (Baccini *et al* 2012, Popescu *et al* 2011). High resolution airborne LIDAR data could be used to estimate aboveground biomass at the individual tree level (Popescu 2007) with high accuracy, but such data are very expensive and not acquired over large regions in a systematic manner. Data from spaceborne Geoscience Laser Altimeter System (GLAS) LIDAR, which was operating onboard ICESAT-1 satellite between 2003 and 2009, though having a coarser resolution (~70 m elliptical footprint), were acquired globally in a regular grid of tracks, which enabled Baccini *et al.* (2012) to model aboveground biomass over the entire tropical region using co-located field measurements to calibrate GLAS data. At the next level of abstraction, field-calibrated GLAS biomass estimates are related to optical (Baccini *et al* 2012) or optical and radar (Saatchi *et al* 2011) satellite data to produce spatially continuous biomass maps. These maps currently have a relatively low spatial resolution compared to the best available activity data (500 m – 1 km), and were shown to provide realistic carbon stock estimates when aggregated over large regions, but to have high uncertainties in the spatial distribution of biomass

(Mitchard *et al* 2013). One of the limitations of biomass modeling using optical imagery is its sensitivity primarily to the density of vegetative cover, e.g. dense forest stands (100% canopy cover) with different biomass would be indistinguishable on an optical image. LIDAR-based estimates and continuous carbon maps derived from these estimates are based on canopy vertical structure and do not account for the species-specific differences in wood density, observed in the field and significantly affecting biomass estimates (Mitchard *et al* 2014). Despite these fundamental limitations of modeling biomass from the space, field-calibrated LIDAR estimates are the best available proxy for forest inventory data over the large regions, and were subsequently employed to estimate emission factors in Chapters 2 and 3.

1.1.2 Advances and challenges in mapping tropical forest degradation

Forest degradation, though contributing to carbon emissions, habitat and biodiversity loss, is harder to characterize and map than the stand-replacement forest disturbance discussed in the previous section, as it implies a forest remaining as a forest in terms of retaining minimum cover and height criteria. There is no agreement in defining forest degradation (IPCC 2003a), but most commonly it represents human-induced changes of forest cover (e.g. partial crown removal, fragmentation or altered species composition), which lead to the long-term reduction in forest productivity and carbon stocks. Herold et al. (2011) delineate three major drivers of forest degradation: extraction of forest products for subsistence and local markets; industrial (commercial) extraction of forest products; and uncontrolled anthropogenic wildfire. Forest degradation is estimated to account for at least 15% of total emissions from land cover

and land use change (Houghton 2013). Its relative contribution varies from country to country, e.g. selective logging accounts for less than 10% of emissions from deforestation in the countries with high forest loss rates, such as Indonesia and Brazil, and for up to 50-70% in the countries with relatively low forest loss (Pearson *et al* 2014). Annual carbon loss due to the long-term edge effects resulting from tropical forest fragmentation alone is estimated to comprise from 9 to 24% of the annual carbon emissions from deforestation (Pütz *et al* 2014).

There are two main approaches to remotely sensed forest degradation monitoring: direct and indirect (GOFC-GOLD 2013). Direct detection using a variety of high resolution optical, SAR and airborne LIDAR data is well suited to monitor forest degradation activities leading to significant canopy damage, such as industrial selective logging (Asner *et al* 2005), charcoal production (Rembold *et al* 2013) or small-scale mining, but has a very limited utility in monitoring low intensity degradation not necessarily associated with immediate canopy cover loss, such as harvesting of non-timber products, artisanal logging, understory thinning or exotic species invasion (Herold *et al* 2011).

Indirect approaches are focused on the identification of intact areas, and defining forest degradation as transition from intact to non-intact state. The definition of intact forest landscapes (IFL) includes the criteria of adjacency to human infrastructure (at least 1 km from settlements and roads), absence of recent disturbances and fragmentation (forest patch area at least 500km², corridor width at least 2 km) (Potapov *et al* 2008b). Though IFL criteria are not universal (for example, a more or less conservative minimum patch area criterion may be useful for different applications) and the original IFL

methodology involves visual image interpretation and is therefore quite labor-intensive, IFL maps have been suggested as the recommended data input for the indirect degradation mapping within national forest monitoring systems (Maniatis and Mollicone 2010, GOFC-GOLD 2013). The utility of this approach was demonstrated at the national scale by Margono et al. (2014, 2012) to quantify the extent of primary forest degradation in Indonesia. Chapter 4 of the current dissertation research is focused on advancing the methods of indirect forest degradation monitoring by developing an automated successor to the IFL mapping method. Changes in IFL could subsequently be used in the method developed in Chapters 2 and 3 as strata in assessing carbon emissions due to forest degradation.

1.2 Research goals and objectives

This research seeks to develop a scalable method for forest loss area and carbon loss assessment, combining existing remotely sensed data products (Hansen *et al* 2013, Baccini *et al* 2012, Potapov *et al* 2012) with the recommended statistical approaches to uncertainty and area estimation (Olofsson *et al* 2014, Stehman 2013, IPCC 2006). Specifically, forest cover loss and related loss of carbon in humid tropical forests is estimated via probability sampling with forest type and forest loss maps employed as sampling strata. The research is also aimed at developing methods to stratify forest cover for carbon loss estimation based on structural characteristics (percent canopy cover and height) and intactness, in the event forest cover type maps for a specific region are absent or do not agree in quality or spatial resolution with data on forest cover loss and carbon density. An automated method is developed to map recently undisturbed high biomass

hinterland forests and identify areas of forest degradation with reduced carbon stocks, which may be used to improve stratifications for the sample-based carbon loss assessments. Furthermore, the current research demonstrates the utility of point-based LIDAR forest carbon density estimates as a substitute of ground forest inventory data for carbon monitoring.

The major research objectives are the following:

1. Prototype a method to estimate national and continental-scale gross forest cover loss and aboveground carbon (AGC) loss and to quantify associated uncertainties, using existing data for the Democratic Republic of the Congo;
2. Produce a pan-tropical forest AGC loss estimate by creating a pan-tropical stratification of forest cover based on tree cover density, height and forest intactness, and applying the method, developed in objective 1;
3. Map potential forest degradation areas pan-tropically using an indirect mapping method based on the identification of intact areas rather than directly mapping degradation.

1.3 Structure of the dissertation

The three research components of the dissertation addressing the aforementioned research objectives are covered in Chapters 2 - 4 (figure 1.1). Chapter 2 and 3 are use a similar “Stratify and Multiply” methodological approach to quantify forest aboveground carbon loss at two scales: national (the DRC case study, Chapter 2) and pan-tropical (Chapter 3). Chapter 4 complements forest cover stratification for carbon estimation from Chapter 3 by developing an automated method to map recently undisturbed (hinterland)

forests and areas of potential forest degradation. It provides a baseline to quantify small-scale forest disturbances not captured by the national- and global-scale Landsat-based (30m resolution) forest cover change maps and associated carbon loss.

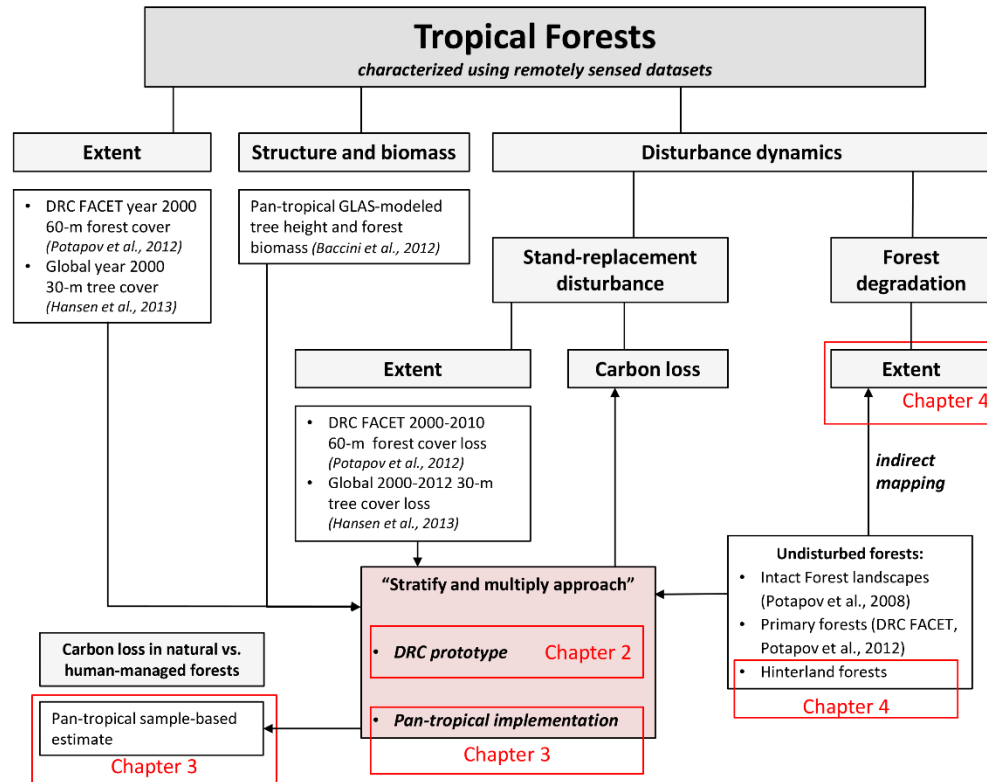


Figure 1.1 Conceptual diagram of dissertation research.

Chapter 2 uses off-the-shelf Landsat-based (60-m resolution) forest cover type and forest loss maps for the Democratic Republic of the Congo (Potapov *et al* 2012) to prototype a method of a national-scale forest aboveground carbon (AGC) loss assessment. The challenge of working in environments such as the DRC is a virtual absence of infrastructure and, hence, there are no reliable and consistent ground inventory data on carbon stocks and validation data for the forest cover loss maps. Therefore Chapter 2 illustrates the use of publicly available medium and high resolution satellite data (30m Landsat time series data and sub-meter resolution data from Google Earth™)

for the validation of the forest loss map and sample-based loss area assessment, and the use of point-based (circa 60-m diameter) GLAS LIDAR AGC estimates (Baccini *et al* 2012) in place of yet non-existent national forest inventory data.

Chapter 3 extends the methodology developed in Chapter 2 to a pan-tropical scale, using the same GLAS LIDAR AGC dataset (Baccini *et al* 2012) and the global 30-m Landsat-based forest cover change map (Hansen *et al* 2013). In contrast with the DRC, forest cover type maps, readily available, methodologically consistent and comparable in spatial resolution with forest loss and carbon data, are nonexistent for the entire tropical region. Hence, one of the focuses of Chapter 3 is to create a pan-tropical stratification of forest cover for the sample-based estimation of AGC loss aimed to minimize within-stratum variance of GLAS-modeled forest carbon density. Such a stratification is based on structural parameters of forest cover as characterized by the 30-m Landsat-based tree canopy cover (Hansen *et al* 2013) and height (current research) maps, as well as forest intactness (Potapov *et al* 2008b). The sample-based forest loss area assessment aims to identify how well Landsat-based maps capture forest loss in various regions across the tropics and, hence, how reliable are loss area estimates derived by counting pixels from such maps. Visual interpretation of the pan-tropical validation sample also aims to disaggregate loss into occurring in natural- (primary and mature secondary forests, and natural woodlands) or human-managed (tree plantations, agroforestry systems, areas of subsistence agriculture with rapid tree cover rotation) forests.

Chapter 4 returns to the idea of stratification for carbon estimation, offering an extension of the Intact forest landscapes (IFL) mapping methodology of Potapov *et al.* (2008) by automating the mapping of recently undisturbed (hinterland) forests which

likely have higher carbon stock compared to the disturbed and degraded forests. It also aims to develop a method to map degraded forests (fragmented and located in the adjacency with the stand-replacement forest disturbances), where small-scale disturbances, undetectable with Landsat, are likely to occur. The resulting map of degraded forests may be used as a baseline for a sample-based degradation assessment, either via remotely sensed data (e.g. high resolution optical and airborne LIDAR) acquisition, or targeted field surveys.

Chapter 5 summarizes the findings from the three research Chapters (2-4), provides a discussion of strengths and limitations of developed methods, and places the current study in the framework of the future research.

Chapter 2: National-scale estimation of gross forest aboveground carbon loss: a case study of the Democratic Republic of the Congo¹

2.1 Introduction

The United Nations Reducing Emissions from Deforestation and forest Degradation (UN-REDD) program seeks to compensate developing countries for avoiding emissions due to likely future forest clearing and logging (Houghton 2012) through the emerging REDD+ mechanism. The success of REDD+ will be defined by confirmed reductions in rates of deforestation and forest degradation. A program requirement is the capability to accurately map and monitor changes in forest carbon by estimating gross emissions as a function of area of forest loss and density of carbon stocks within areas of forest loss.

National Forest Inventories (NFIs) could provide detailed and comprehensive information to produce national-scale carbon stock and change estimates. However, NFIs have not been established in many developing countries that participate in the UN-REDD program (Romijn et al 2012). The United Nations Food and Agriculture Organization (FAO) and the UN-REDD are working on the general guidelines for implementing multi-objective NFIs in these countries (UN-REDD 2011). Meanwhile, alternative methods of national-scale carbon stocks assessment independent of the availability of systematically collected ground-based forest inventory data are being investigated and prototyped

¹ The presented material has been previously published in Tyukavina A, Stehman S V, Potapov P V, Turubanova S A, Baccini A, Goetz S J, Laporte N T, Houghton R A and Hansen M C 2013 National-scale estimation of gross forest aboveground carbon loss: a case study of the Democratic Republic of the Congo *Environmental Research Letters* **8** 1–14

(GOFC-GOLD 2010). Goetz et al (2009) provided an overview of the satellite-based methods of mapping and monitoring carbon stocks, and identified 3 general approaches: Stratify and Multiply (SM), when a single carbon density value is assigned to each land cover type; Combine and Assign (CA), extending the SM approach by adding various ancillary spatial data layers; and Direct Remote Sensing (DR) approach, aimed to derive the carbon stock estimates from machine learning algorithms based on satellite observations and other detailed spatial data coupled with field measurements. The last approach requires acquisition and processing of large volumes of data to produce a national-scale carbon stock or loss estimate. The first approach, SM, also referred to as the “biome-average approach” (Gibbs *et al* 2007), is relatively easy to implement using a limited set of published data available at low or no cost. Although this approach is fairly generalized, in that it does not capture finer scale spatial heterogeneity of carbon stocks, the accuracy of the estimates can be increased via data refinements and overlays with other data sets in a CA approach.

For a national-level aboveground carbon (AGC) loss assessment, SM approaches require a national-scale land cover change dataset (*activity data* in the IPCC terminology (IPCC 2006)) and mean AGC density estimates for each land cover type (IPCC *emission factors*, here referred to as *carbon data*). Modifying the basic IPCC equation used to calculate carbon emissions (IPCC 2006, vol.1, ch.1.2), the equation to estimate gross AGC loss within a study region or a country is the following:

$$AGC\ loss = \sum_{i=1}^n \Delta AD_i * CD_i \quad (2.1)$$

where ΔAD_i (*activity data*) denotes the change in the extent of a given land cover type i , and CD_i (*carbon data*) represents average vegetation carbon content per land cover type.

Carbon data that are required for the national-scale AGC loss assessments in an SM approach could be derived from field inventory data (e.g. tree DBH and height measurements) converted to aboveground biomass using allometric equations (e.g. for tropical forests – from Brown 1997 and Chave *et al* 2005) or existing databases and maps of biomass carbon density (e.g. Zheng *et al* 2003, Gibbs 2006, FAO 2010, Malhi *et al* 2006). Alternatively, biomass carbon content can be mapped using multi-source LIDAR and radar data that are capable to capture vertical tree canopy structure (Goetz and Dubayah 2011, Treuhaft *et al* 2009). Several regional and global-scale carbon stock maps have been created recently using the synergy of field measurements, optical, LIDAR and radar remotely sensed data (Saatchi *et al* 2011, Baccini *et al* 2012). Another approach, presented here, is to calibrate LIDAR data using co-located field measurements (Baccini *et al* 2012). In this approach, a model is derived to convert LIDAR waveforms into biomass estimates. The derived model is then extrapolated to a much larger population of LIDAR shots, providing a biomass database for assigning carbon density values to mapped forest cover types.

For REDD+ countries, deforestation is likely to be the key category for greenhouse gas emissions estimates. A good practice for these countries is to use at least IPCC Tier 2 or 3 level assessments for this category of emissions, which implies reporting uncertainties (Maniatis and Mollicone 2010). AGC stock and loss uncertainty estimates are also crucial if these datasets are to be used as inputs to carbon cycle and

biosphere models. However, published land cover change datasets that may be used as activity data often lack key accuracy assessment information (e.g. description of sampling design, original error matrix, area of each map category, etc.) that would permit error-adjusted estimates of the change area (Olofsson *et al* 2013). The objectives of the current analyses are: (i) to illustrate the process of activity data accuracy assessment on the national level, applicable when using already published land cover data or when creating a new data set, (ii) to integrate uncertainties from activity and carbon data in a national-level forest AGC loss estimate.

In this chapter, I implemented a SM (Stratify and Multiply) approach for assessing gross forest AGC loss in the Democratic Republic of the Congo (DRC), where forest cover change is dominated by smallholder land use and industrial selective logging (Laporte *et al* 2007). Due to the aftermath of two civil wars, persistent political unrest and lack of infrastructure, the DRC does not collect NFI data required for ground-based estimates of AGC stock and its change. This approach employs the best available activity and carbon data at the national scale - forest extent and loss maps derived from Landsat imagery (Potapov *et al* 2012) and AGC estimates derived from GLAS-based canopy vertical structure metrics (Baccini *et al* 2012). Results include new estimates of error-adjusted area of forest cover loss between 2000 and 2010, gross AGC loss, and associated uncertainties.

2.2 Data

2.2.1 Activity data

To estimate the area of forest loss, I used Landsat-based year 2000 forest cover and 2000-2010 forest cover loss data from the Forêts d'Afrique Centrale Evaluées par Télédétection (FACET) product, available on-line (<ftp://congo.iluci.org/FACET/DRC/>). FACET data processing and mapping methodology are described in Potapov *et al* (2012). The FACET dataset provides forest cover and gross forest cover loss for three forest types: primary humid tropical forests, defined as mature humid tropical forest with canopy cover >60%; secondary forests, defined as regrowing forest with canopy cover >60%; and woodlands, defined as forested areas with canopy cover 30-60%. The spatial resolution of FACET data is 60m per pixel. I further separated these three forest types into *terra firma* (dryland) and wetland sub-classes using the DRC wetland map of Bwangoy *et al* (2010), resulting in six forest types in total. FACET forest cover loss was attributed to these new forest classes (figure 2.1). In this manner, the different carbon content of the antecedent forest cover could be directly related to disturbance dynamics in *terra firma* and wetland forested ecosystems. In this chapter, I conduct an explicit statistical validation of FACET forest cover loss for each of these forest types and derive the error-adjusted estimate of changed area based on the validation sample.

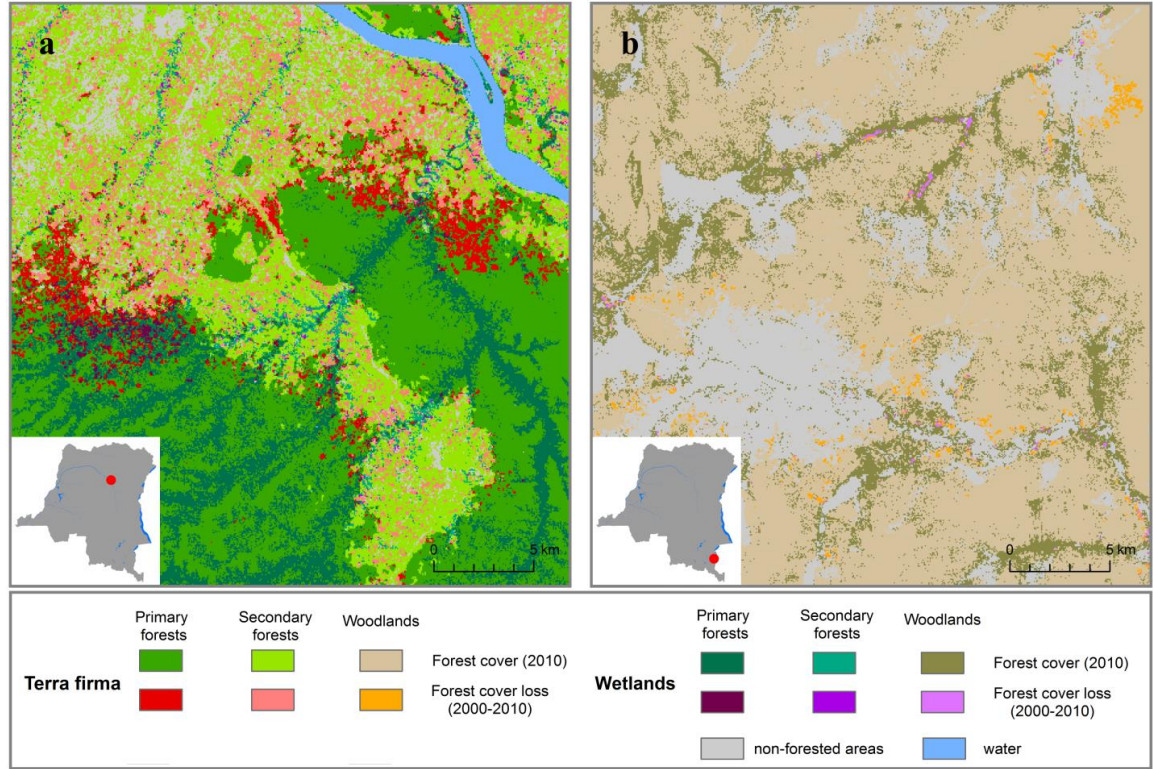


Figure 2.1 FACET forest cover and forest cover loss (Potapov *et al* 2012) combined with DRC wetland map (Bwangoy *et al* 2010): a) forested area; b) woodlands.

2.2.2 Carbon data

Mean AGC density values for each of the forest types were derived from GLAS-based biomass estimates. Baccini *et al* (2012) developed a statistical model to predict AGC densities observed in the field using GLAS LIDAR energy metrics in order to estimate biomass per 65m diameter GLAS shot. The model was based on nearly 300 field sites located in 12 countries across the tropics. GLAS-predicted AGC explained 83% of variance in the field-measured carbon density at the GLAS-footprint scale with a standard error of 22.6 Mg C ha⁻¹ (Baccini *et al* 2012). For this study, I employed the GLAS-derived biomass data as if they were field inventory data and did not incorporate this model uncertainty in downstream calculations. After screening GLAS data for noise and

filtering for slope ($\leq 10^\circ$), 371,458 AGC-estimated GLAS-shots for the years 2004-2008 (figure 2.2) were analyzed together with the combined FACET forest cover and DRC wetland maps to calculate mean AGC density values for the six target forest classes. Only shots within the forested areas that did not experience forest cover loss between 2000 and 2010 according to FACET were used for these calculations. The use of a large number of GLAS-estimated biomass values to calculate biome-average AGC densities helps avoid biases often inherent in estimates based on the compilation of point-based field measurements (i.e. paucity of sites over large areas, inadequate stratification to capture variability, and other factors that limit their spatial representativeness).

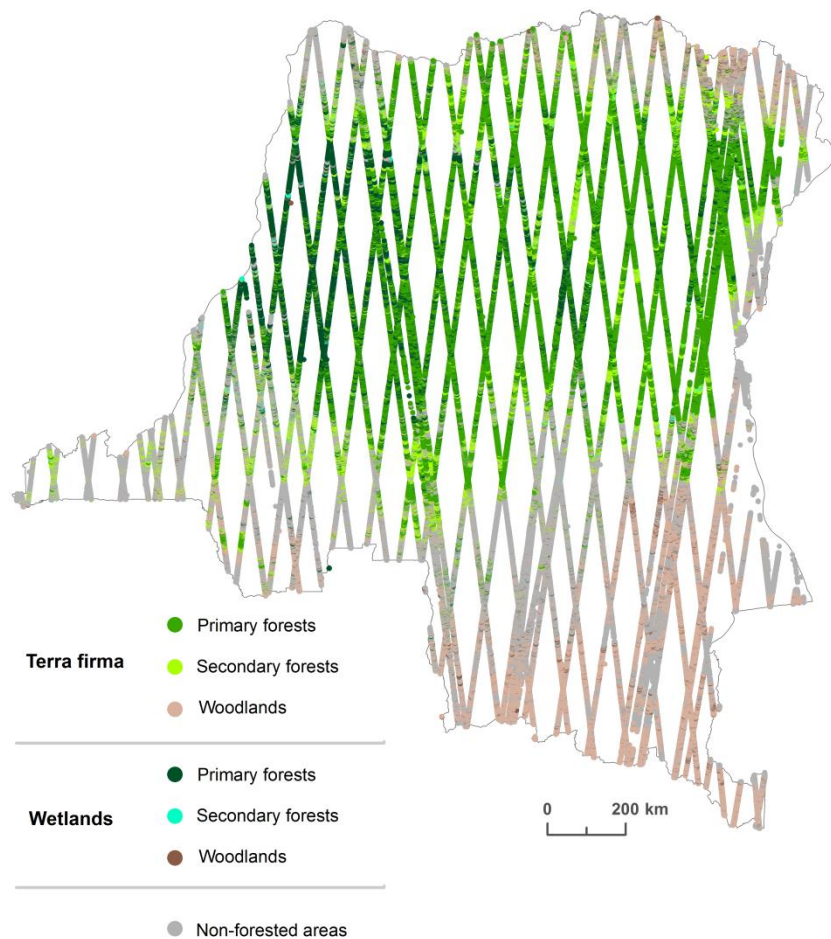


Figure 2.2 2004-2008 GLAS shots color-coded by the FACET forest type (Potapov *et al* 2012) combined with wetland map (Bwangoy *et al* 2010).

2.2.3 Validation data

For the purposes of activity data validation, namely the uncertainty estimation for the FACET forest cover loss, I used all available original L1T Landsat images for years 2000 and 2010 available at no charge from USGS archives (<http://glovis.usgs.gov/>) and annual Landsat composites for circa 2000, 2005 and 2010 (Potapov *et al* 2012). Year 2005 composite images helped identify forest cover loss in the early 2000s that might be difficult to detect in 2010 Landsat images due to rapid vegetation regeneration in the tropics.

In addition to the use of Landsat images for the validation (reference) classification, I also employed visual interpretation of very high spatial resolution images available for the study region through Google EarthTM and through a partnership between NASA and NGA that provides access to unclassified commercial high spatial resolution satellite data from NGA archives for NASA Earth Science Investigators (<http://cad4nasa.gsfc.nasa.gov/>). A total of 1689 high resolution images from multispectral and panchromatic sensors (Ikonos, WorldView-1, WorldView-2, Quickbird, Orbview-5) for 2008-2011 time interval were used for the visual assessment of validation samples. In total, 503 out of a final 1061 validation samples had at least one matching high resolution image available between 2000 and 2013, either from Google EarthTM or from the NGA archive. These images facilitated the forest cover loss validation, providing information about forest cover type on date 1 (2000) or date 2 (2010).

2.3 Methods

2.3.1 *Uncertainties from activity data*

The key objective of activity data validation is to estimate error-adjusted area of forest cover loss for each forest type and to quantify its uncertainty. Error-adjusted area estimation uses validation sample data to adjust area of forest cover loss due to classification errors (including omission errors and excluding commission errors) present in the map product (Olofsson *et al* 2013). The choice of sampling design is determined by this objective, as well as by feasibility issues and time constraints.

2.3.1.1 *Sampling design and sample size*

The target activity data class, forest cover loss, is relatively small compared with the unchanged forest areas; the sampling design should increase the sample representation of this rare class in order to achieve a precise estimate of forest cover loss accuracy (Khorram 1999). Moreover, the current objective is forest type-specific loss area estimation and its accuracy; stratified random sampling is an appropriate choice in this case (Stehman 2009).

Initially, two strata within each forest type class were considered: “no loss” (forests, undisturbed between 2000 and 2010) and “loss” (2000-2010 forest cover loss). However, sufficient estimation of loss omission error within the large “no loss” stratum requires special attention. Given a simple “loss” and “no loss” stratification, rates of false negatives (change omission errors) could be poorly characterized (Khorram 1999). Furthermore, the FACET national-scale forest cover loss product is likely to be conservative, i.e. omitting forest cover loss in comparison to committing forest loss. To

address this issue I identified an additional “probable loss” stratum within each forest type class. This stratum was constructed to target omitted forest cover loss in order to improve the loss area estimate for the AGC loss calculation. The “probable loss” stratum is defined here as a 1-km radius circular region around forest cover loss, assuming that omission of loss is likely to occur in proximity to mapped loss. The choice of the 1-km wide “probable loss” stratum is supported by the evidence that increased tree mortality in temperate and tropical forests is generally observed up to 1 km from the forest edge (Broadbent *et al* 2008).

A total of 18 strata were analyzed: “loss”, “probable loss”, and “no loss” for each of the six forest types (*terra firma* and wetland primary forests, *terra firma* and wetland secondary forests, *terra firma* and wetland woodlands). Allocation of samples among these strata should effectively address the current validation objective (see paragraph 2.3.1) of minimizing standard errors (SEs) of error-adjusted estimators of forest cover loss area (Stehman 2012).

When considering allocation of samples among forest types, I examined both the area of forest type and the area of the target class (forest loss) within each forest type. Proportional allocation of samples among forest types based on the forest type area would lead to small sample sizes from secondary forest, woodlands and wetland forests: almost half of all samples in this case fall into the dense forest class (table 2.1). Although forest cover loss in dense forests that have high biodiversity and other high-value ecosystem services is important to estimate correctly, the majority of mapped forest cover loss occurred in secondary forests. However, allocation of samples based on the forest cover loss area leads to the majority of samples being located in secondary forests. In order to

find a compromise between preserving a sufficient number of samples in the strategically important dense forest class while adequately representing the relatively small classes with high proportional forest cover change (secondary forest, woodlands), I implemented an arbitrary allocation that was close to proportional by forest type area, but adjusted for forest loss area (table 2.1).

Table 2.1. Distribution of samples among forest types using proportional and arbitrary sample allocation strategies for stratified random sampling.

Forest type	Proportional allocation (% samples):		Arbitrary allocation (% samples):
	based on forest area	based on loss area	
Primary forest	46	25	33
Secondary forest	11	55	17
Woodlands	21	13	25
Wetland primary forest	19	3	17
Wetland secondary forest	1	3	4
Wetland woodlands	2	1	4

The sample size allocation to the three strata within each forest type was determined as follows. Because it is equally important for the primary validation objective (estimation of forest loss area for each forest type based on an error matrix) to account for committed and omitted loss area, I addressed the need to account for omission errors by creating the separate “probable loss” strata within the original “no loss” class. Therefore, when allocating samples among loss strata, I chose to have an allocation closer to equal, which helped to target errors of commission (Stehman 2012) among the “no loss”, “probable loss” and “loss” strata. A total sample size of 1000 was projected as feasible to be visually interpreted by expert analysts. I imposed the condition that a sample size greater than 50 was required for the major forest types (primary, secondary

forests, woodlands, wetland primary forests), the allocation of sample size per stratum (the sampling unit is one 60m FACET pixel) was implemented as shown in table 2.2.

Table 2.2 Allocation of sample size among validation strata.

Forest type	No loss	Probable loss	Loss	Total
Primary forest	200	70	63	333
Secondary forest	30	87	50	167
Woodlands	100	90	60	250
Wetland primary forest	80	30	57	167
Wetland secondary forest	15	15	12	42
Wetland woodlands	15	15	12	42

For the chosen sample allocation I calculated SEs of the estimated area of change using hypothetical omission and commission error rates in order to confirm that the chosen allocation would not lead to inflated standard errors. I compared arbitrary allocation to proportional among forest allocation with equal and proportional allocation among loss strata and found that the arbitrary allocation performed as well or better than the other options. The equation used to calculate SEs of the estimated area of change for each forest type is similar to equation 3 from Olofsson *et al* (2013). However, after the assignment of reference values to the samples during expert validation, I found out that the “probable loss” stratum contributed 35% of the total variance in primary forest, 50% of the variance in secondary forest, and 20% of the variance in woodlands. Additional random samples were added to the “probable loss” stratum of *terra firma* primary, secondary forests and woodlands (20, 30 and 10 samples respectively) in order to minimize the total SE of the loss area estimate.

2.3.1.2 Estimating area of forest loss and its uncertainty

Visual interpretation of validation samples was performed at a 30m spatial resolution, enabling map-scale and sub-grid error assessments (FACET was made at a 60m spatial resolution using resampled 30m Landsat time-series imagery). I produced two forest loss area estimates for the DRC for the last decade (2000-2010): a map-scale estimate accounting for whole-pixel classification errors in the 60-m resolution FACET forest cover change product, and a sub-grid estimate that took into account 60m cells that experienced partial forest loss (table 2.3). For the map-scale estimate I treated a 60m validation pixel as “loss” only if the reference forest loss fraction detected using 30m Landsat and/or high spatial resolution was $\geq 75\%$ of pixel area. For the sub-grid estimate, three gradations of reference loss fraction per pixel were used: 1 (loss) with reference loss $\geq 75\%$ of pixel area; 0.5 (mixed pixels) with reference loss between 75% and 25%; and 0 (no loss) otherwise (figure 2.3).

Table 2.3 Error matrix of sample counts for map-scale and sub-grid area estimates.

Forest type	Map strata	Reference strata				N of pixels in each stratum
		Map-scale estimate		Sub-grid estimate		
		no loss	loss	no loss	loss	
Primary forest	no loss	200	0	200	0	147,647,298
	no loss - probable loss	89	1	86.5	3.5	56,158,987
	loss	3	60	3	60	2,638,342
Secondary forest	no loss	30	0	30	0	5,720,568
	no loss - probable loss	107	10	98.5	18.5	35,535,337
	loss 00-10	3	47	3	47	5,619,034
Woodlands	no loss	100	0	100	0	51,491,436
	no loss - probable loss	98	2	97	3	39,725,284
	loss 00-10	7	53	7	53	1,374,079
Wetland primary forest	no loss	80	0	80	0	67,675,696
	no loss - probable loss	30	0	30	0	15,706,036
	loss 00-10	9	48	9	48	326,316

Forest type	Map strata	Reference strata				N of pixels in each stratum
		Map-scale estimate		Sub-grid estimate		
		no loss	loss	no loss	loss	
Wetland secondary forest	no loss	15	0	15	0	1,506,946
	no loss - probable loss	15	0	14.5	0.5	2,176,786
	loss 00-10	4	8	4	8	255,498
Wetland woodlands	no loss	15	0	15	0	7,003,885
	no loss - probable loss	15	0	15	0	2,477,979
	loss 00-10	2	10	2	10	97,176

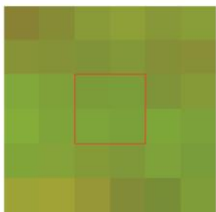
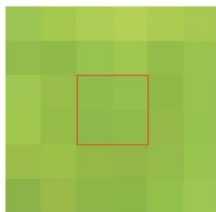

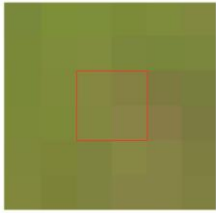
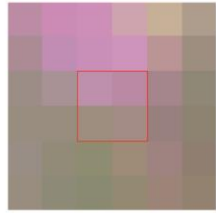

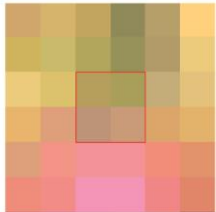
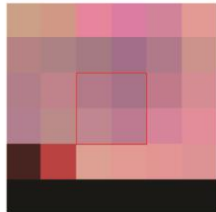

2000 Landsat	2010 Landsat	2009-2011 VHR imagery	Reference loss
			0 (no loss)
			0.5
			1 (loss)

Figure 2.3 Example of sample block visual interpretation; for the map-scale estimate, 0.5 loss is treated as no loss. The black stripe in the 2010 Landsat loss sample is a data gap due to the Landsat 7 scan-line corrector malfunction.

When the sampling strata and map classes being validated are the same, equations 2, 3 and 4 from Olofsson *et al* (2013) should be used to calculate error-adjusted area of forest cover loss and its standard error based on a validation confusion matrix. In

this case, there was a mismatch between sampling strata (“no loss”, “probable loss”, “loss”) and map classes (“loss” and “no loss”) within each forest cover type arising from the attempt to target omitted forest cover loss by creating the additional “probable loss” stratum. Based on sampling theory (Cochran 1977), the following equation was employed to produce an unbiased estimator of the area of forest cover loss within each of the forest cover types when validation strata and map classes do not match (Stehman 2013):

$$\hat{A} = A_{tot} * \frac{\sum_{h=1}^H N_h \bar{y}_h}{N} \quad (2.2)$$

where A_{tot} – total area of the forest cover type;

$y_u = 0.5$ or 1 if pixel u (or it’s half) is in reference class “forest cover loss”, and $y_u = 0$ otherwise;

$\bar{y}_h = \frac{\sum_{u \in h} y_u}{n_h}$, the sample mean of the y_u values in stratum h ;

n_h – sample size in stratum h ;

N_h – number of pixels in stratum h ;

N – total number of pixels within the forest cover type.

The standard error of the error adjusted estimate of the forest cover loss is:

$$SE(\hat{A}) = A_{tot} * \sqrt{\frac{\sum_{h=1}^H N_h^2 \left(1 - \frac{n_h}{N_h}\right) \frac{s_{yh}^2}{n_h}}{N^2}} \quad (2.3)$$

where $s_{yh}^2 = \frac{\sum_{u \in h} (y_u - \bar{y}_h)^2}{n_h - 1}$, the sample variance for stratum h .

A 95% confidence interval (assuming normal distribution) is:

$$\hat{A} \pm 1.96 * SE(\hat{A}) \quad (2.4)$$

An example of the forest cover loss area estimation for *terra firma* primary forests (map-scale estimate) is presented in table 2.4 and equations 2.5 – 2.7.

Table 2.4 Parameters for the calculation of error-adjusted area of forest cover loss within *terra firma* primary forests (map-scale estimate).

Primary forest	$\sum_{u \in h} y_u$	n_h	\bar{y}_h	N_h	Map area (ha)	s_{yh}^2
no loss	0	200	0/200	147,647,298	53,153,027	0.000000000
no loss - probable loss	1	90	1/90	56,158,987	20,217,235	0.011111111
loss	60	63	60/63	2,638,342	949,803	0.046082949
			<i>total</i>	206,444,627	74,320,066	

$$\hat{A} = 74,320,065.72 * \frac{0 * 147,647,298 + \frac{1}{90} * 56,158,987 + \frac{60}{63} * 2,638,342}{206,444,627} = 1,129,210 \text{ ha} \quad (2.5)$$

$$SE(\hat{A}) = 74,320,065.72 * \sqrt{\frac{147,647,298^2 \left(1 - \frac{200}{147,647,298}\right) \frac{0.0}{200} + 56,158,987^2 \left(1 - \frac{90}{56,158,987}\right) \frac{0.011111111}{90} + 2,638,342^2 \left(1 - \frac{63}{2,638,342}\right) \frac{0.046082949}{63}}{206,444,627^2}} \quad (2.6)$$

226,099 ha

$$\hat{A} = 1,129,210 \pm 443,156 \text{ ha} \quad (2.7)$$

2.3.2 Uncertainties from carbon data

Table 2.5 presents the mean and population standard deviation (STD) derived from the number of GLAS shots per forest type. Using the SM (Stratify and Multiply) approach a single mean AGC density value was assigned to each of the forest type classes to estimate gross AGC loss. To quantify the uncertainty of this estimate, I employed the standard deviation of the sample-mean's estimate of a population mean, the standard error of the mean (SEM). According to the central limit theorem, the distribution of sample estimates of the mean is normally distributed, enabling us to calculate the 95% confidence interval (CI) of mean AGC density estimates as $\pm 1.96\text{SEM}$. Table 2.5 shows mean AGC densities of target forests classes along with their 95% CIs.

Table 2.5 GLAS-based AGC density estimates for the DRC forest types. Mean AGC densities are given with $\pm 95\%$ CI.

Forest type	Mean AGC density (Mg C ha ⁻¹)	Number of GLAS samples	STD
Primary forest	156.8 \pm 0.4	115,566	67.03
Secondary forest	94.8 \pm 0.7	31,443	67.45
Woodlands	71.2 \pm 0.2	121,671	44.24
Wetland primary forest	128.9 \pm 0.4	85,923	55.29
Wetland secondary forest	90.7 \pm 2.3	3,148	65.83
Wetland woodlands	66.5 \pm 0.8	13,707	45.81

2.3.2 Combination of the uncertainties

When calculating AGC loss for each forest type using equation 1, uncertainty comes both from activity data (in this case - forest cover loss) and emission factors (carbon data). In order to combine uncertainties from these quantities, the multiplication

approach from the recent IPCC Guidelines for National Greenhouse Gas Inventories (IPCC 2006, vol.1, ch.3, p.28, eq.3.1) was used:

$$U_{total} = \sqrt{U_1^2 + U_2^2 + \dots + U_n^2} \quad (2.8)$$

where U_{total} is the percentage uncertainty in the product of the quantities (half the 95% confidence interval divided by the total and expressed as a percentage);

U_i is the percentage uncertainties associated with each of the quantities.

For example, for the primary forest stratum, the calculation of the U_{total} (using the map-scale ΔAD estimate) is the following:

$$U_{total} = \sqrt{\left(\frac{SE(\hat{A})}{\hat{A}} * 100\right)^2 + \left(\frac{AGC\ SEM}{Mean\ AGC} * 100\right)^2} = \sqrt{\left(\frac{226,099.75}{1,129,210} * 100\right)^2 + \left(\frac{0.2}{156.83} * 100\right)^2} = 20.02\% \quad (2.9)$$

When calculating total gross AGC loss within the DRC (summing AGC loss values for all forest types), the addition and subtraction approach from the IPCC Guidelines (IPCC 2006, vol.1, ch.3, p.28, eq.3.2) was used to estimate the uncertainty of the resulting quantity:

$$U_{total\ DRC} = \frac{\sqrt{(U_1 * x_1)^2 + (U_2 * x_2)^2 + \dots + (U_n * x_n)^2}}{|x_1 + x_2 + \dots + x_n|} \quad (2.10)$$

where U_{total} is the percentage uncertainty in the sum of the quantities (half the 95% confidence interval divided by the total and expressed as percentage);

x_i and U_i are the uncertain quantities and percentage uncertainties associated with them.

Thus, the overall uncertainty of gross AGC loss estimate for the entire DRC is:

$$\begin{aligned}
& U_{total\ DRC} \\
& = \frac{\sqrt{(U_{total1} * \Delta AGC_1)^2 + (U_{total2} * \Delta AGC_2)^2 + \dots + (U_{totaln} * \Delta AGC_n)^2}}{|\Delta AGC_1 + \Delta AGC_2 + \dots + \Delta AGC_n|} \quad (2.11)
\end{aligned}$$

where numbers (1 through n) stand for the six forest cover types.

2.4 Results

Applying the approach of adjustment for the classification errors described in the Methods section, I produced estimates of forest cover loss within target DRC forest classes (table 2.6). Error-adjustment significantly increased estimated areas of forest loss in *terra firma* forest classes (primary, secondary forests and woodlands); omission errors prevailed over commission errors (figure 2.4). In the wetland forests and woodlands, on the contrary, more loss was committed in the map product; error-adjusted loss area estimates were smaller than those prior to adjustment. SE was highest in wetland secondary forests and *terra firma* woodlands. High uncertainty in the wetland secondary forests is associated with it being the smallest and spatially discontinuous class. Woodland is a challenging forest type to map and monitor due to the gradients of tree canopy cover and seasonality as well as the comparatively uneven intensity of disturbance events, all of which contributes to larger SEs.

Table 2.6 Original FACET and error-adjusted estimates of 2000-2010 forest cover loss within DRC forest types (\pm 95% CI).

Forest type	2000-2010 forest cover loss (ha)		
	error-adjusted		FACET map
	map-scale estimate	sub-grid estimate	
Primary forest	1,129,210 \pm 443,156	1,690,800 \pm 645,694	949,803
Secondary forest	2,994,876 \pm 664,625	3,924,262 \pm 736,673	2,022,852
Woodlands	722,979 \pm 396,475	865,990 \pm 439,210	494,668
Wetland primary forest	98,925 \pm 11,218	98,925 \pm 11,218	117,474
Wetland secondary forest	87,440 \pm 78,014	87,441 \pm 78,014	91,979
Wetland woodlands	29,153 \pm 7,704	29,153 \pm 7,704	34,983

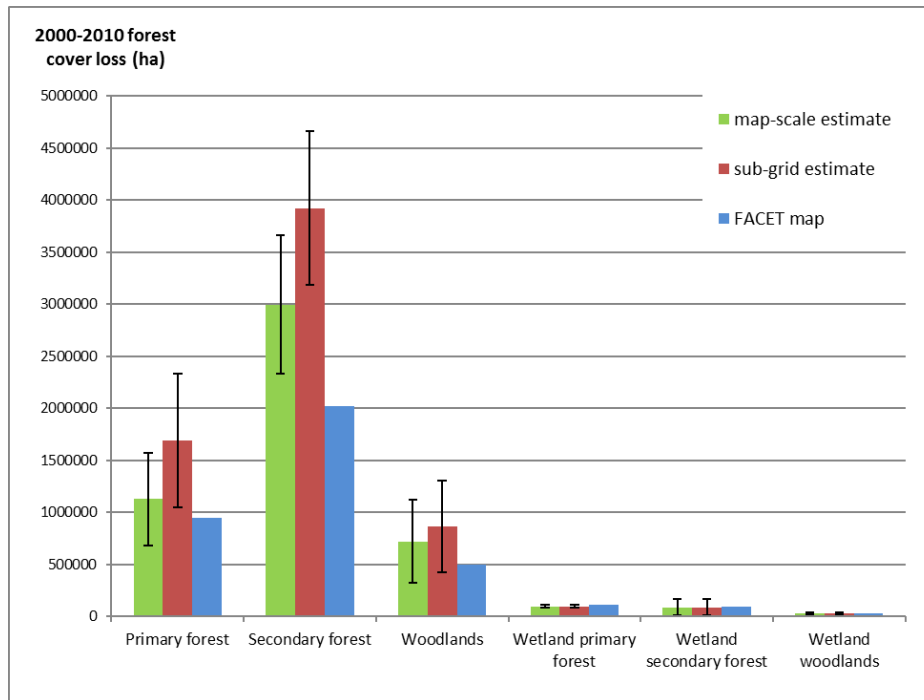


Figure 2.4 Forest cover loss (2000-2010) within DRC forest types; error bars are the 95% CIs.

To compare AGC density estimates for the target forest classes with published estimates, I calculated average AGC densities within the 6 DRC forest types using available spatially explicit vegetation carbon density products (Baccini *et al* 2012, Saatchi *et al* 2011, Gibbs and Brown 2007, Kindermann *et al* 2008) and compared them with the GLAS-based estimates of the current study (figure 2.5). This comparison provides a general understanding of how well the current estimates correspond to existing knowledge. Examination of figure 2.5 shows that GLAS-based AGC density estimates are generally higher than those modeled using optical remotely sensed data (Baccini *et al* 2012, Saatchi *et al* 2011, Gibbs and Brown 2007), probably because of spatial averaging (Goetz and Dubayah 2011, Zolkos *et al* 2013), but don not exceed the estimates

of Kindermann *et al* (2008) who employed FAO 2005 Forest Resources Assessment statistics.

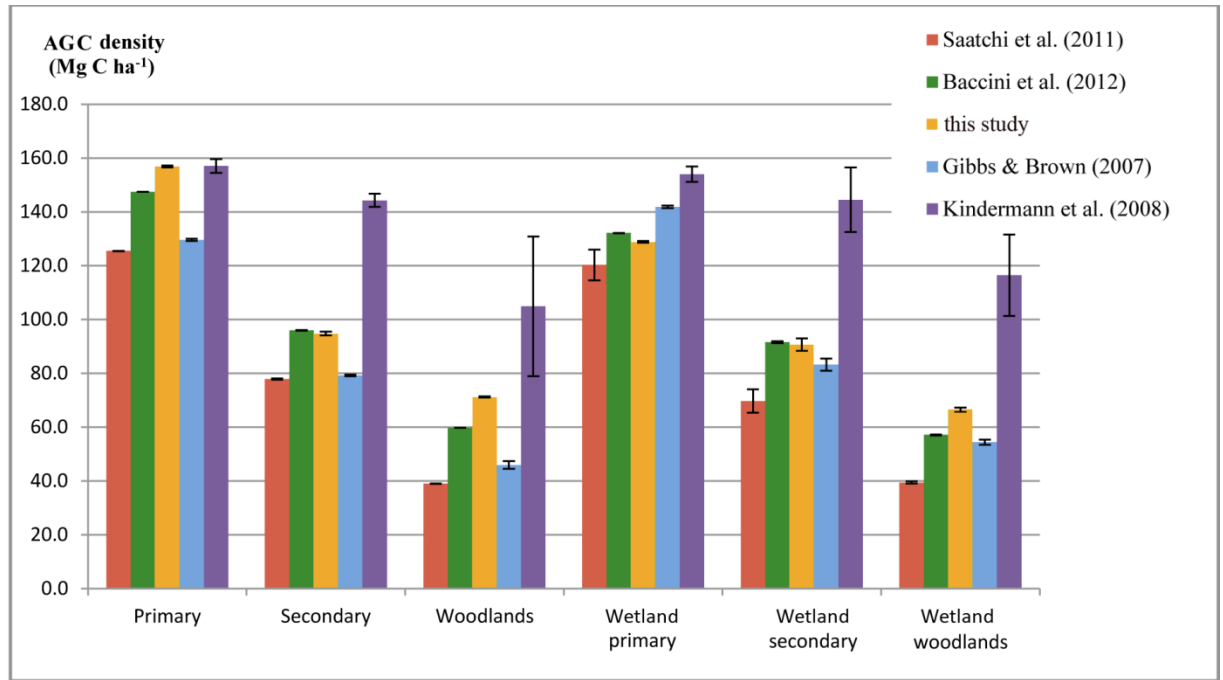


Figure 2.5 Comparison of the AGC density estimates from the published datasets (error bars are the 95% CIs) and the current study.

Sub-grid gross AGC loss estimates were 20-50% higher than map-scale ones for the major *terra firma* forests (primary, secondary forests and woodlands) and nearly equal for the less widespread wetland forests (table 2.7, figure 2.6b-c). Differences between these estimates are mostly associated with the “loss” and “probable loss” strata, particularly in regions where primary and secondary forest loss predominate. There are no significant differences in the forests and woodlands of the “no loss” strata (figure 2.6d). For the whole of the DRC, the sub-grid AGC loss estimate was 35% higher than the map-scale estimate (table 2.7).

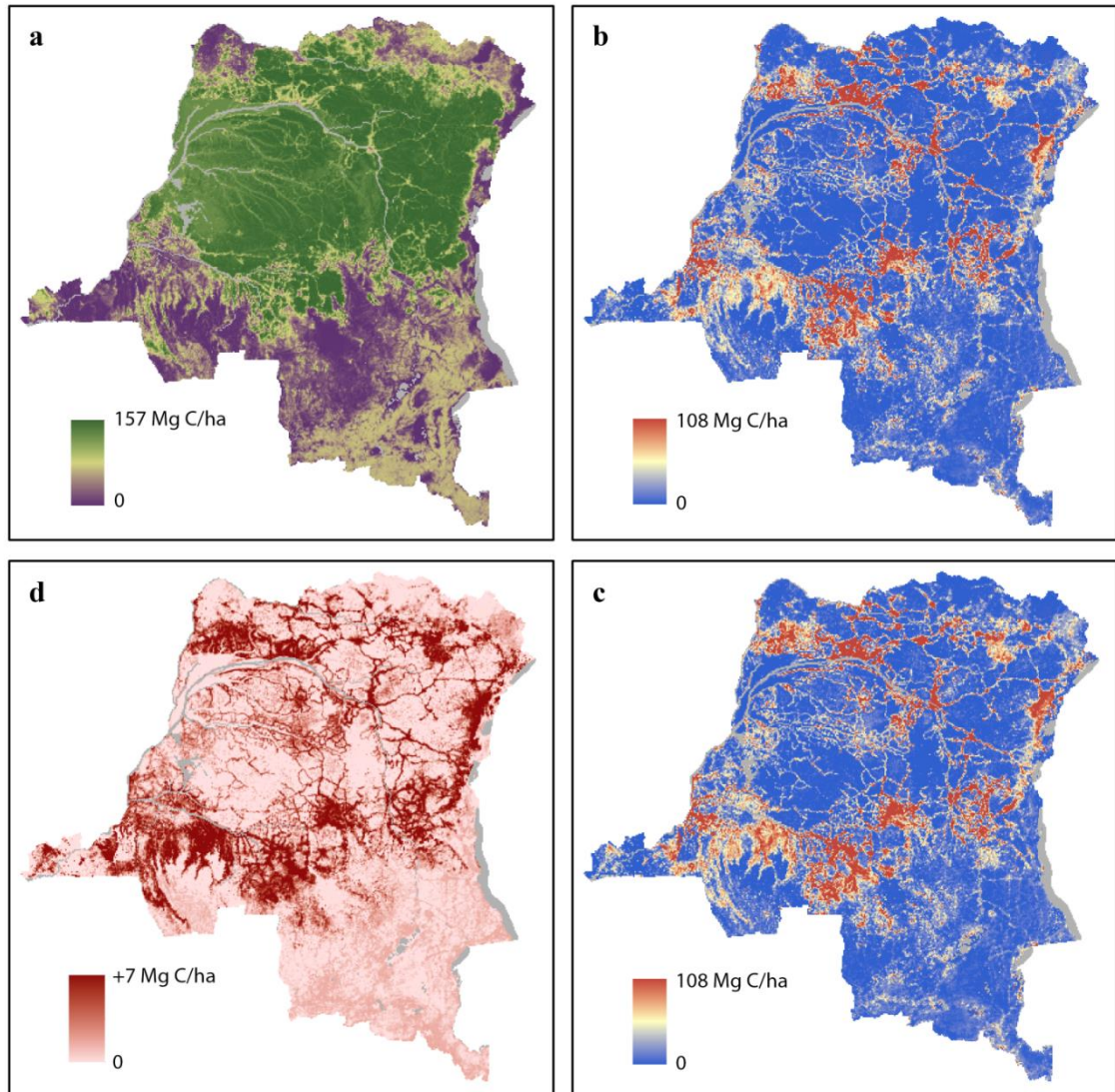


Figure 2.6 Forest type and strata averages, aggregated to a 5-km grid: a) year 2000 AGC; b) map-scale estimate of 2000-2010 gross AGC loss; c) sub-grid estimate of 2000-2010 AGC loss; d) difference between sub-grid and map-scale estimates. Water bodies are shown in grey. Note that AGC values for both b) and c) are the same for the respective forest types.

Table 2.7 Gross AGC loss estimates (2000-2010) with the uncertainty measures for DRC forest types (\pm is the 95% CI).

Forest type	Map-scale loss area estimate		Sub-grid loss area estimate	
	U_{total} (%)	gross AGC loss 2000-2010 (Pg C)	U_{total} (%)	gross AGC loss 2000-2010 (Pg C)
Primary forest	20.0	0.177 ± 0.070	19.5	0.265 ± 0.101
Secondary forest	11.3	0.284 ± 0.063	9.6	0.372 ± 0.070
Woodlands	28.0	0.051 ± 0.028	25.9	0.062 ± 0.031
Wetland primary forest	5.8	0.013 ± 0.001	5.8	0.013 ± 0.001
Wetland secondary forest	45.5	0.006 ± 0.005	45.5	0.008 ± 0.007
Wetland woodlands	13.5	0.002 ± 0.001	13.5	0.002 ± 0.001
DRC total	9.4	0.533 ± 0.098	9.0	0.721 ± 0.127

The comparison of gross forest cover loss and gross AGC rates from this study with published estimates is presented in table 2.8. Here annual forest cover loss rates are reported separately for primary and secondary forests, excluding woodlands (table 2.8) to best match the definition of forests employed in the most recent regional sample-based forest cover loss estimate by Ernst *et al* (2013) (all tropical moist forests, excluding woodland savannahs and tropical dry forests).

2.5 Discussion

The results reported in table 2.8 need to be considered in the context of inconsistencies in methodologies, definitions, and areas of analysis (a direct consequence of the differences in the definitions of forest and woodlands). The current map-scale 2000-2010 annual forest cover loss estimate within dense forests ($0.35\% \pm 0.03\%$) agrees well with the estimates of Ernst *et al* (2013) for the first half of the decade ($0.32\% \pm 0.05\%$) and of Hansen *et al* (2013) for 2000-2012 (0.34%). Map-scale estimate also falls within the confidence interval of the global sample-based estimate of Hansen *et al* (2010),

but is significantly higher than the FACET map-based estimate without error-adjustment (Potapov *et al* 2012).

Table 2.8 Comparison of forest cover and carbon loss estimates for the DRC (\pm 95% CI).

Source		Extent	2000-2005 Annual <i>gross</i> forest cover loss (% of the forest area)	2005-2010
current study	map-scale	forests + woodlands	0.32% \pm 0.03%	
	sub-grid	forests + woodlands	0.42% \pm 0.03%	
	map-scale	forests	0.35% \pm 0.03%	
	sub-grid	forests	0.47% \pm 0.04%	
FACET map Potapov <i>et al</i> (2012) – 60m		forests + woodlands	0.22%	0.25%
Hansen <i>et al</i> (2013) – 30m		forests + woodlands	0.34%	
Ernst <i>et al</i> (2013)		forests	0.32% \pm 0.05%	–
Hansen <i>et al</i> (2010)		forests + woodlands	0.12% \pm 0.23%	–
			Annual <i>net</i> forest cover loss (% of the forest area)	
FAO (2010)		forests + woodlands	0.20%	0.20%
Ernst <i>et al</i> (2013)		forests	0.22%	0.22%
			Annual <i>gross</i> AGC loss (Tg C year ⁻¹)	
current study	map-scale	forests + woodlands	53.3 \pm 9.8	
	sub-grid	forests + woodlands	72.1 \pm 12.7	
			Annual <i>gross</i> carbon loss (Tg C year ⁻¹)	
Harris <i>et al</i> (2012)		forests + woodlands	23	–

The sub-grid estimate, accounting for the finer-scale forest disturbance, is 30-40% higher than published estimates for the DRC, and points to the difficulty of mapping forest change in a landscape where smallholder shifting cultivation predominates. For example, FACET forest cover loss has a mean patch area of 1.4ha (Potapov *et al* 2012). While patch size is not the same as field size, it is worth noting that typical shifting cultivation practices in the tropics employ field sizes well under 1ha (Aweto 2013). The quantification of such change is challenging and represented by the comparatively large

presence of mixed pixels in the FACET data. The difference of two methodologically consistent loss area estimates based on input data of different resolutions (60-m FACET and 30-m Hansen *et al* (2013), table 2.8) prior to error-adjustment illustrates the issue: the 30-m product depicts 1.5 times more change than the 60-m one. Any binary (yes/no) change map will have scale-dependent omission errors. These “cryptic disturbances” have been reported to add more than 50% of forest cover loss to existing Landsat-scale forest disturbance classifications for the Amazon Basin (Asner *et al* 2005).

Table 2.8 reflects a second type of omission error related to algorithmic and/or data limitations. Estimates of forest loss derived at a 30m spatial resolution, particularly the Hansen *et al* (2013) and Ernst *et al* (2013) products, have comparable gross forest cover loss rates, 0.34% and 0.32% +/-0.05%. However, the 30m validation estimate is 0.47% +/-0.04%. Large area mapping algorithms are often conservatively implemented in attempting to avoid commission error. For validation, the determination of loss/no loss is performed independently per sample and is free of this consideration. Differences between the Hansen *et al* (2013) 30m map and the Ernst *et al* (2013) 30m sample estimates could be due to this fact. However, the estimate of Ernst *et al* (2013) was also sample based. The additional loss found in the current validation effort compared to Ernst *et al* (2013), while partially due to the use of very high spatial resolution data for a portion of the reference samples, is not easily explained and may be more related to definitional differences or other methodological factors. In summary, the difference between the 60m FACET loss rates of 0.22% and 0.25% and the 30m loss rates of 0.34% and 0.32% is most likely related to the differing scales of measurement. The difference between the 30m loss rates of 0.34% and 0.32% and the validation rate of 0.47% is most likely related

to limitations in mapping versus sampling or to other methodological factors. The discrepancy between map-scale and sub-grid estimates emphasizes the issue of scale in change area estimation for smallholder dominated landscapes like the DRC.

The approach for validating activity data employed in this study is relatively straightforward and easy to implement. The method allows for the generation of error-adjusted loss area estimates from the existing land cover and vegetation maps. This approach doesn't require large volumes of data processing and is therefore not limited by computational facilities. The use of open access medium- and high-resolution imagery for map product validation (USGS Landsat archive, Google Earth™ high resolution imagery) allows defining reference values of validation samples without *in situ* measurements. Despite its advantages, the method is sensitive to sampling design and the associated decision of how to allocate the sample size among validation strata. For the strata and sample size allocation implemented in this study, the decisions were advantageous; for the four largest forest types, the reduction in standard error attributable to the stratification was substantial. Specifically, the gain in precision due to stratification can be computed from the sample data (Cochran 1977, sec. 5A.11) as the ratio of the standard error that would have been obtained from simple random sampling to the standard error obtained from the stratified design implemented (same sample size for both designs). For the four largest forest types, these ratios were 1.42 for primary forest, 1.10 for secondary forest, 1.32 for woodlands, and 23.21 for wetland primary forest (the latter estimate is likely inflated by the fact that two of the three strata had 0% forest loss). The methodology is also highly dependent on the knowledge base of the remote sensing experts performing visual interpretation of validation samples. Finally, it is a function of

the quality of the reference imagery and the resulting clarity or conversely ambiguity in assigning change per validation sample. The map-scale and sub-grid estimates reflect the importance of this issue.

A further consideration in assessing the results concerns the reference data and the potential volatility of the sample-based estimate itself. Table 2.4 illustrates this issue. The “loss” stratum records 60 of 63 samples as having experienced *terra firma* primary forest cover loss, representing 905,574 ha of error-adjusted forest loss area. For the “probable loss” stratum, 1 of 90 samples was interpreted as having experienced forest cover loss. Due to the much larger size of this stratum, this one sample accounts for an estimated 224,635ha of error-adjusted forest loss area, or fully 20% of *terra firma* primary forest cover loss. Without the use of the “probable loss” stratum and the inclusion of this single sample of commission error, results would indicate a slight underestimate of *terra firma* forest cover loss. Validation studies should formally consider likely regions of false negatives of forest change in developing stratified sampling methods for error-adjusted area estimation. The validity of the sample-based estimate is a function of many factors, including the vagaries of any individual sample data set used in creating the error-adjusted estimates.

Estimates of carbon density derived using different methods can vary considerably within the same region (Houghton *et al* 2001), introducing uncertainty to the carbon loss estimation. However, recent published estimates of carbon loss from deforestation differ primarily due to major disagreements in the quantification of the areal extent of forest cover loss (Pan *et al* 2011, Harris *et al* 2012). The DRC gross AGC loss estimates from the current study (map-scale and sub-grid) are 2 to 3 times higher than

the biomass carbon loss (total carbon, above- and belowground) estimate of Harris *et al* (2012) (table 2.8) due primarily to differences in the estimated area of forest cover loss. The Harris *et al* (2012) estimate is based on a global forest cover loss product by Hansen *et al* (2010) that is highly uncertain in the DRC (SE=100%, see table 2.8). Hansen *et al* (2010) employed a pan-tropical MODIS-based stratification to target sample allocation with only seven samples located in the DRC. The small sample size resulted in a high standard error (table 2.8). Harris *et al* (2012) reported a 90% carbon loss prediction interval for the DRC, based on a Monte Carlo approach: 16 - 32 Tg C year⁻¹; the current DRC gross AGC loss estimates, map-scale (53.3 Tg C year⁻¹) and sub-grid (72.1 Tg C year⁻¹), are not within this interval.

In the current analysis, DRC gross forest AGC loss assessment consists only of stand-replacement forest disturbance that can be observed at the mapping scale and in reference data. However, forest degradation processes that do not lead to the complete loss of tree canopy or cause small-scale canopy openings, and can be detected only in the field or using dense series of sub-meter remotely sensed data may result in significant AGC loss at the national scale (IPCC 2003a, Schoene *et al* 2007). One possible approach to assess the loss of biomass from these disturbances could be based on monitoring changes in the area of intact forest landscapes (Potapov *et al* 2008b) and assigning an AGC loss value to the forests that have undergone the transition from intact primary to primary degraded and secondary forests (Margono *et al* 2012, Zhuravleva *et al* 2013). For countries such as the DRC, where large-scale agro-industrial forest disturbance is largely absent, the question of scale and its impact on AGC loss due to deforestation and degradation remains an important line of scientific inquiry.

I employed GLAS-based AGC estimates as a proxy for the ground-based NFI data. There are some known issues and limitations concerning the estimation of biomass from GLAS metrics. For example, GLAS-estimated vegetation heights often used in AGC models have on average 2-3 meter error when compared with USDA Forest Inventory and Analysis (FIA) and other field-measured heights (Pflugmacher *et al* 2008, Lefsky *et al* 2005, Sun *et al* 2008). GLAS-derived biomass estimates are also known to be affected by the season of data acquisition and terrain slope (Sun *et al* 2008). In total, GLAS-based AGC models explain from 73% (Lefsky *et al* 2005, Pflugmacher *et al* 2008) to 83% (current study; Baccini *et al* 2012) of the variance in field-estimated biomass. Regional forest inventory data are required to calibrate and validate the current forest-type GLAS-based estimates. Additional field data collection could further refine the estimates but, unfortunately, GLAS observations are not available after 2009, posing a near-term challenge for improved AGC mapping and monitoring beyond the current models. As part of the process of establishing an NFI for the DRC continues, other sources of remotely-sensed data characterizing vegetation vertical structure, such as airborne LIDAR or spaceborne radar data, can bridge the gap until systematic spaceborne LIDAR measurements become available to the scientific and REDD+ implementation communities.

2.6 Conclusion

I applied a method of error-adjustment of forest cover loss area to produce a national-scale gross forest AGC loss estimate for the DRC based on a published forest cover loss dataset. I employed field-calibrated GLAS LIDAR-derived biomass carbon

densities as a substitute for NFI data, which do not exist for the territory of the DRC. Two realizations of the resulting DRC gross AGC loss estimate, map-scale and sub-grid, were produced. The sub-grid AGC loss estimate accounted for disturbances finer than the map grid scale of 60m and was higher than published estimates, highlighting issues of scale and spatial averaging in AGC estimation. Omitted disturbances were largely related to smallholder agriculture land cover change, the detection of which is scale-dependent. For the FACET product, the input Landsat imagery were averaged to 60m and then classified, leading to the estimated scale-related omission error. Other processing steps can lead to change omission, either through the algorithm itself, for example image segmentation, post-processing of the output classification, or the application of a minimum mapping unit. In Brazil, where agro-industrial land conversion results in large forest disturbances, the Brazilian Space Agency's PRODES product 6.25 ha minimum mapping unit (the equivalent of approximately 69 Landsat pixels) (INPE 2012), provides a viable deforestation monitoring approach. However, a 6.25 ha minimum mapping unit for the DRC would omit the majority of change. For heterogeneous landscapes with change dynamics at or finer than the resolution of Landsat data, higher spatial resolution imagery to directly map such changes, or indirect methods to delimit degraded areas and subsequently relate to *in situ* measurements, are required.

The current study also illustrates the importance of reference forest state in assessing carbon dynamics, as with the primary, secondary and woodland forest types presented here. The Brazilian PRODES product, the current standard for national-scale forest monitoring, quantifies only the loss of primary forest in the Legal Amazon. While reducing primary humid tropical forest loss is the main focus of climate mitigation

strategies such as REDD+, other forest types and even trees outside of forests will be part of national carbon accounting schemes. This study underscored the importance of monitoring other forest dynamics, as AGC loss in secondary forests was found to be 140% that of primary forests. The reuse of secondary forests remains a challenge to carbon monitoring and the development of appropriate strategies for reducing emissions, but monitoring all relevant forest types and dynamics is required as national-scale programs are developed and implemented.

REDD+ mechanisms will rely on accurate mapping and monitoring of AGC (Houghton *et al* 2010). However, scientific, technical and operational aspects of AGC mapping and monitoring are still in their infancy. Results from this study have significant implications for policy initiatives like REDD+. It is clear that the spatial scale of forest change characterization, reference information on forest type and carbon stock, and sample representativeness, can all dramatically impact AGC loss estimation. For example, considering change at a 30m validation scale, an extra 35% of AGC loss was estimated compared to the 60m spatial scale; *terra firma* secondary forest cover loss accounted for 40% more AGC loss than that of *terra firma* primary forest loss; a single validation sample added 20% to map-scale *terra firma* primary forest cover loss area. The volatility of results within this study indicates the DRC to be a challenging environment for quantifying changes to forest carbon stocks, with implications for other countries as well. Eventual national monitoring systems will need to demonstrate spatio-temporal consistency given the various factors that impact AGC loss estimation. While absolute accuracies may differ due to some of the aforementioned factors, relative consistency for any particular set of observations and spatial scale should be achievable

and implementable. Demonstrating such consistency will be a proof of readiness for REDD+ monitoring.

Chapter 3: Aboveground carbon loss in natural and human-modified tropical forests from 2000 to 2012²

3.1 Introduction

Deforestation and degradation of tropical forests constitute the second largest source of anthropogenic emissions of carbon dioxide after fossil fuel combustion (van der Werf *et al* 2009). Policy initiatives have been proposed to reduce the rate of tropical forest loss, which would have the co-benefit of preserving other unique tropical ecosystem services such as biodiversity richness (Jantz *et al* 2014). The REDD+ mechanism under the United Nations Framework Convention on Climate change (UNFCCC) seeks to compensate developing countries for avoided emissions that would have otherwise occurred under business as usual scenarios. To do so, methodologically consistent baseline estimates of forest carbon stocks and forest loss area within different forest types are required as a part of national forest monitoring systems, which is underlined by the recent decision of the UNFCCC Conference of the Parties 19 (COP 19) on “Modalities for national forest monitoring systems” (UNFCCC 2014). Existing estimates of gross carbon loss derived from carbon stock and forest area loss data vary greatly (from 0.81 to 2.9 PgC annually (Harris *et al* 2012, Pan *et al* 2011, Achard *et al* 2014)) with the greatest variance found between studies that employ remotely sensed-

² The presented material is under review: Tyukavina A, Baccini A, Hansen M C, Potapov P V, Stehman S V, Houghton R A, Krylov A M, Turubanova S, Goetz S J (*in review*) Aboveground carbon loss in natural and managed tropical forests from 2000 to 2012. *Environmental Research Letters*

derived data versus those that use forest inventory and other tabular reference data. Aggregate emissions from deforestation based largely on satellite-derived products are similar (~ 0.81 PgC) despite regional differences (Houghton 2013) in pan-tropical carbon density reference data, forest cover change estimates, and the carbon pools included (IPCC 2013, Houghton 2013, Saatchi *et al* 2011, Mitchard *et al* 2013, Ometto *et al* 2014).

Activity data represent human activities that result in greenhouse gas emissions and removals and are reported in units of area. Activity data are combined with emissions factors to generate emissions estimates. If a map is to be used to estimate activity data, its accuracy must be quantified. Good practice guidance from the Intergovernmental Panel on Climate Change (IPCC) requires emissions data to “satisfy two criteria: (1) neither over- nor under-estimates so far as can be judged, and (2) uncertainties reduced as far as is practicable (Penman *et al.*, 2003). To satisfy these criteria, compensation should be made for classification errors when estimating activity areas from maps and uncertainties should be estimated using robust and statistically rigorous methods. The primary means of estimating accuracies, compensating for classification errors, and estimating uncertainty is via comparisons of map classifications and reference observations for an accuracy assessment sample” (GFOI 2014). To this end, I demonstrate a generic and cost-effective approach for estimating forest cover loss activity data that follows good practice guidance (Olofsson *et al* 2014, IPCC 2006, GFOI 2014). Probability-based samples, required in order to meet the standard of statistical rigor, are used to quantify forest cover loss area and associated uncertainty. Samples are allocated to forest carbon stock strata (emissions factors) to estimate aboveground carbon

(AGC) loss pan-tropically. The demonstrated approach represents the most rigorous assessment of pan-tropical forest loss activity data to date.

Gross carbon loss due to removal of aboveground forest biomass in 2000-2012 is quantified in a “stratify and multiply” (stock-difference) approach (Goetz *et al* 2009) in which area of forest loss is first estimated and then the aboveground carbon density associated with loss areas quantified. In this study, the strata of the “stratify and multiply” approach were forest strata based on canopy structure as defined by percent cover (Hansen *et al* 2013) and height, and intactness (Potapov *et al* 2008b). The area of forest loss was estimated from a probability sample for which forest loss was determined using visual interpretation of Landsat time series and high resolution imagery from Google EarthTM at each sample location, and the 30-m forest cover map of Hansen et al. (2013) was used via a stratified estimator to reduce the standard error of the area estimate. The aboveground carbon density estimates were obtained based on field-calibrated LIDAR estimates of aboveground biomass (Baccini *et al* 2012). This approach was prototyped earlier at the national scale for the Democratic Republic of the Congo (Tyukavina *et al* 2013), and can be implemented at various geographic scales given the appropriate data on forest type, forest loss and carbon density, which makes it potentially useful for national forest monitoring systems. The data used in the analysis are freely available, obviating the need for commercial data sets that are often too costly and consequently impractical to incorporate into operational national-scale forest monitoring programs.

This study defines forest as any vegetation taller than 5m with canopy cover \geq 25% (both natural forests and plantations); this corresponds to the forest definition agreed under the UNFCCC (UNFCCC 2006) except for the minimum area and potential for

growth criteria: “*Forest’ is a minimum area of land of 0.05–1.0 hectare with tree crown cover (or equivalent stocking level) of more than 10–30 per cent with trees with the potential to reach a minimum height of 2–5 metres at maturity in situ.*” Forest cover loss is defined as any stand-replacement disturbance (Hansen *et al* 2013), both semi-permanent conversion of forest cover into other land cover and land use types (“deforestation” as defined by FAO (FAO 2012) and under the UNFCCC (UNFCCC 2006)) and temporary forest disturbances followed by tree regeneration. Gross forest cover and AGC loss is further disaggregated into loss in natural (primary and mature secondary forests, and natural woodlands) and managed (tree plantations, agroforestry systems, areas of subsistence agriculture with rapid tree cover rotation) forests (see Data and Methods and figure 3.4). Natural forest cover loss represents forests cleared for the first time in recent history and is the primary target of initiatives such as UN-REDD. This category of AGC loss can be applied to cases where natural forests are replaced by non-forestry land uses (deforestation), such as the conversion of Amazonian rainforests to pastures, and where natural forests are replaced by forestry land uses, such as the conversion of Sumatran rainforests to forest plantations.

Here I estimate gross AGC loss due to stand-replacement disturbance mapped at a 30-m resolution and add a modeled belowground carbon loss (BGC) estimate in order to compare results with other contemporary remote-sensing based studies. Forest disturbances often associated with forest degradation include burning, selective logging, forest fuelwood removal, and charcoal production (Cochrane and Schulze 1999). The current study quantifies these dynamics where observable, including forest loss due to fire and the building of roads and other infrastructure associated with selective logging, but

doesn't account for the finer scale disturbances that cannot be directly mapped using Landsat data, largely selective removals due to logging. Pearson et al. (2014) recently found that in countries with high rates of deforestation such as Indonesia and Brazil, carbon emissions from selective logging account for ~12% of emissions from deforestation, including losses due to infrastructure.

3.2 Data and Methods

3.2.1. Study region

The study region includes biomes within tropical, subtropical and portions of the temperate climate domains in Latin America between 30°N and 60°S, in Sub-Saharan Africa between 30°N and 40°S and in South and Southeast Asia between 40°N and 20°S. Forest cover stratification in the current research was produced within this area. For the final forest cover loss area and aboveground carbon (AGC) loss estimation, the study area was limited to the following countries and country groups (figure 3.1):

- 1) Africa: Democratic Republic of the Congo, humid tropical Africa, the rest of Sub-Saharan Africa;
- 2) Latin America: Brazil, Pan-Amazon, the rest of Latin America;
- 3) South and Southeast Asia: Indonesia, mainland South and Southeast Asia, insular Southeast Asia.

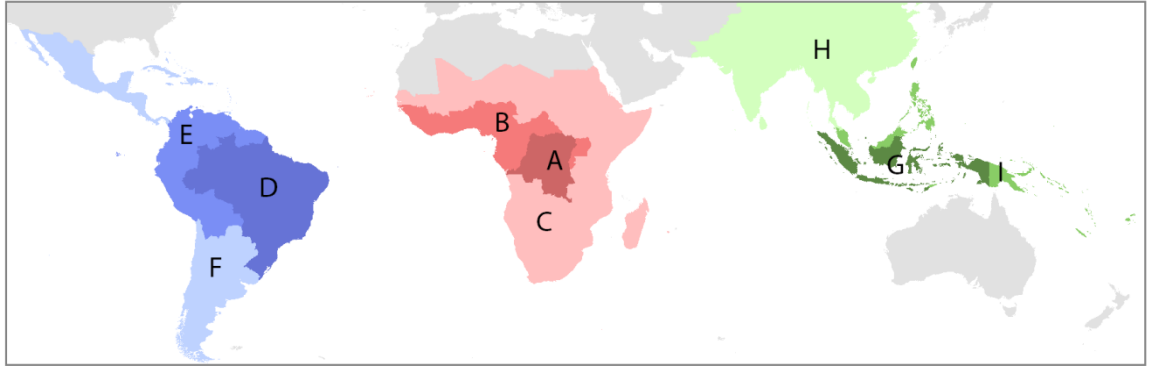


Figure 3.1 Boundaries of reporting units. A) Democratic Republic of the Congo; B) Humid tropical Africa; C) The rest of Sub-Saharan Africa; D) Brazil; E) Pan-Amazon; F) The rest of Latin America; G) Indonesia; H) Mainland South and Southeast Asia (includes southern China up to 40°N); I) Insular Southeast Asia.

3.2.2. Approach to estimating gross aboveground carbon loss

The Stratify and Multiply approach (Goetz *et al* 2009) to estimating gross 2000-2012 AGC loss was implemented using equation 2.1. (Chapter 2) and the following data:

- 1) Forest cover type stratification for year 2000 (prior to disturbance);
- 2) Forest cover loss map (*activity data*) and validation sample data;
- 3) Mean carbon density estimate for each forest stratum (*emission factors* or *carbon data*).

Uncertainties from both activity and carbon data were estimated and incorporated into the final AGC loss estimates using the recommended Approach 1 (Propagation of Error) from the IPCC Guidelines (IPCC 2006).

3.2.3. *Pan-tropical forest cover stratification (year 2000)*

The purpose for stratifying forest cover was to delineate regions (strata) associated with different carbon stock reference values. However, consistently characterized pan-tropical forest type maps are not available at the 30-m spatial resolution corresponding to the Hansen *et al.* (2013) forest loss data. Characterizing forest cover based on complex multi-parameter definitions (e.g. “primary forests”, “secondary forests”, “woodlands”) as was performed at a national scale (Potapov *et al* 2012) is not easily achieved at a biome scale. Instead, I defined tropical forest strata using remotely sensed-derived structural characteristics of tree canopy (year 2000 percent tree canopy cover (Hansen *et al* 2013)), tree height (current study) and forest intactness (Potapov *et al* 2008b).

Stratification thresholds were developed to minimize within-strata AGC variance using a statistical regression tree approach with point-based GLAS carbon estimates (Baccini *et al* 2012) for the period 2003 - 2008 as the dependent variable. When building a tree, the highest priority was assigned to tree canopy cover, with height and intactness as auxiliary variables having lower weights in the model. Figure 3.2 shows the resulting regression tree. Only areas where tree canopy cover was $\geq 25\%$ were considered forest cover and included in the final stratification (figure 3.3).

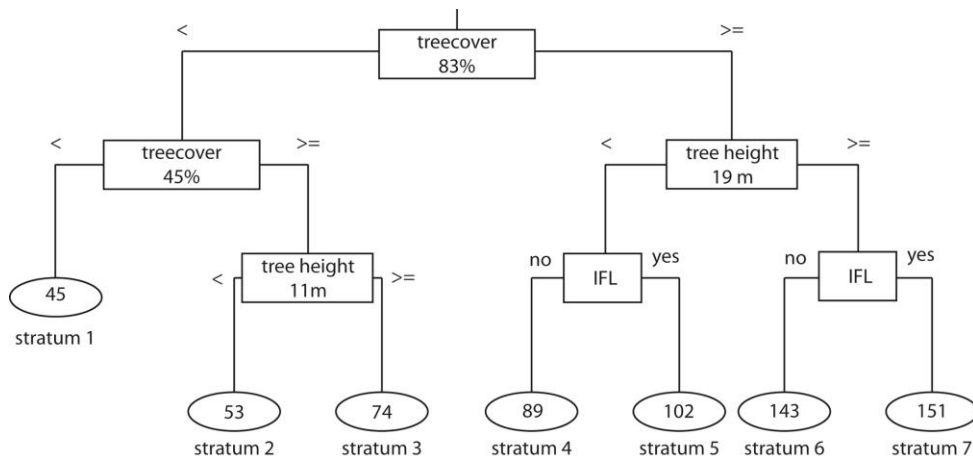


Figure 3.2 Forest cover stratification thresholds. Terminal node values are mean strata AGC density values (MgC/ha).

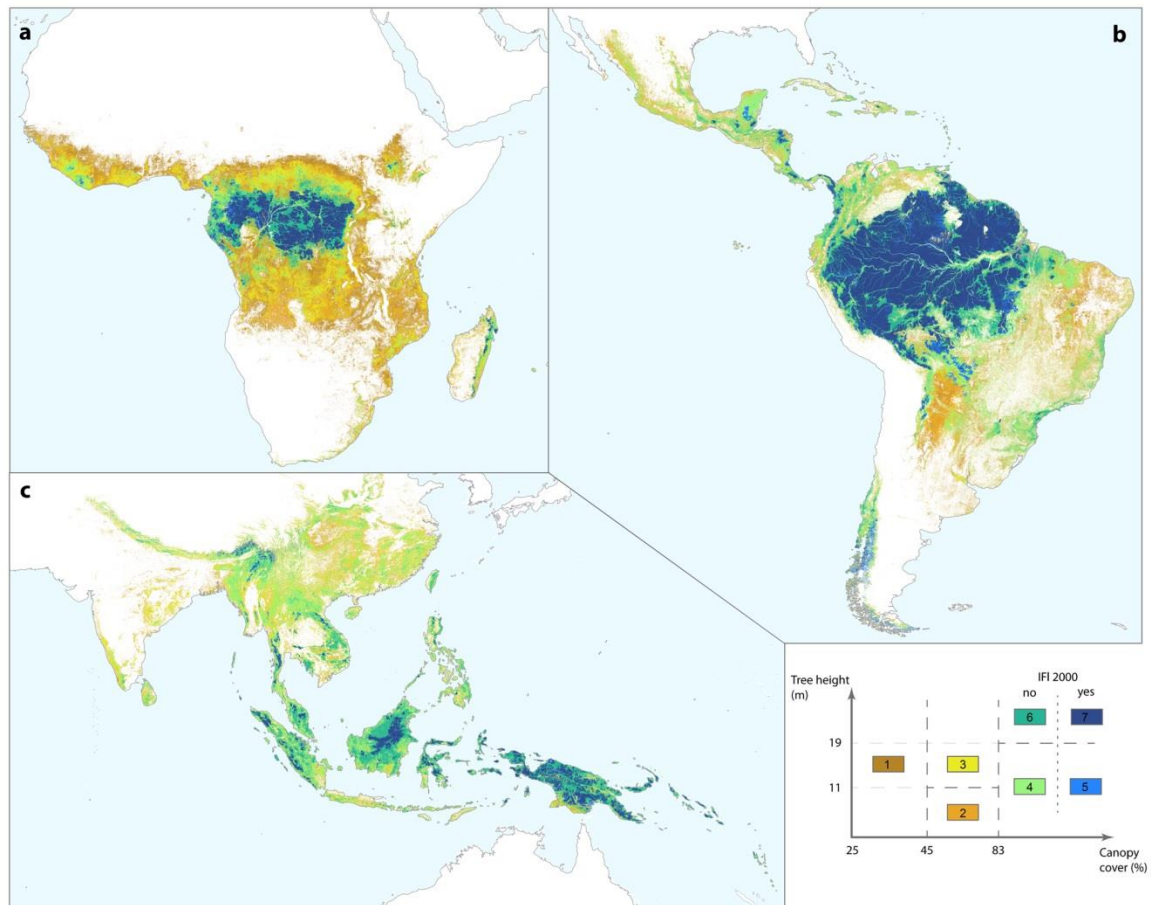


Figure 3.3 Forest cover stratification. a) Africa; b) South and Southeast Asia; c) Latin America; numbers in the legend refer to forest strata: 1 – low cover; 2 – medium cover short; 3 – medium cover tall; 4 – dense cover short; 5 – dense cover short intact; 6 – dense cover tall; 7 – dense cover tall intact.

3.2.4. Height model

Tree height map was generated using a regression tree model which related GLAS-derived tree height estimates (Baccini *et al* 2012) to Landsat time-series metrics. Landsat 7 Enhanced Thematic Mapper Plus (ETM+) growing season images were processed to create a per-pixel set of cloud-free land observations which in turn were used to assemble the time-series metrics (Potapov *et al* 2012). Circa year 2000 tree height was derived by taking the maximum of 5 annual height models (2000-2004). A random subset of 90% of the available GLAS data was used to train models with the remaining 10% of the data set aside for cross-validation. For the study region the resulting 5 year maximum height model has root mean square error (RMSE) of 8.1 m and mean absolute error (MAE) of 5.9 m; within forests (crown cover >25%) RMSE = 6.5 m and MAE = 4.7 m.

3.2.5. Forest cover loss data

The global 2000-2012 forest cover loss map (Hansen *et al* 2013) includes all stand-replacement disturbances of vegetation taller than 5m observable at a 30-m resolution. For the current analysis I considered only forest cover loss within target forest strata (figure 3.3) with crown cover $\geq 25\%$.

A sample-based approach (Cochran 1977) was implemented to estimate map errors within forest strata and to estimate area of gross forest cover loss (Stehman 2013) as suggested by good practice recommendations (Olofsson *et al* 2014). Commission and omission errors inherent in the Hansen et al. (2013) map likely introduce bias to the map-

based forest loss area estimates. Consequently, the current area estimates are based on the reference condition of each pixel selected in the sample where the reference condition is considered the most accurate available assessment of forest loss (the protocol for determining the reference condition or classification is described later in this subsection). In the previous validation effort (Hansen *et al* 2013), a sample of 300 120-m x 120-m sample units was allocated to the tropical biome to assess the accuracy of the forest cover map. However, this sample was deemed inadequate for the current analysis because several smaller forest strata would have insufficient sample sizes and consequently large standard errors for the forest cover loss area estimates. A new stratified random sample of 3000 30-m pixels was selected from the three study regions with the sample size allocated to each region roughly proportionally to the area of forest cover loss, with 1200 sample pixels allocated to Latin America, and 900 sample pixels each to Africa and Asia. Within each of the three regions, the sample was further stratified by forest type (figure 3.3). Separate per-continent sample allocations reduced continent-level standard errors for estimates of area of forest cover loss and overall accuracy (Stehman 2009). Forest types covering relatively small areas were combined into larger strata (table 3.1) for selecting the sample. Estimates of forest cover loss area were still obtained for every forest type displayed in figure 3.3. The Hansen et al. (2013) map played a key role in the sample-based forest loss area estimation protocol as the mapped loss data were used to create sub-strata per each carbon stock stratum shown in figure 3.3. The loss data were employed in stratified estimators that yielded substantially reduced standard errors relative to what would have resulted without stratification.

Each sampling stratum had two sub-strata: one-pixel buffered forest cover loss (i.e., all map forest loss pixels and any pixels adjacent to a mapped loss pixel) and no

loss (table 3.1). A one-pixel buffer was created around mapped loss to target forest loss omission error pixels that commonly occur at the boundary of map loss pixels. The Hansen et al. (2013) forest cover loss map in the tropical domain had higher omission error (producer's accuracy of 83.1% vs. user's accuracy of 87.0%) and a previous study in Central Africa (Tyukavina *et al* 2013) showed that Landsat-based forest cover change was more likely to omit forest cover loss along the boundaries of mapped forest cover loss. The prevalence of boundary loss omission was also observed in the present validation effort: 92% of the sample pixels with loss omission error (78 out of 85) came from the one-pixel boundary around mapped loss (table 3.2).

A stratified estimator (Cochran 1977) was used to produce the final forest cover loss area estimates for the countries and country groups (see figure 3.1). These estimates were based on 2936 of the sample pixels; 64 sample pixels (15 in America and 49 in Asia) were excluded as they were outside of the countries of interest. Table 3.3 shows the sample size for each country and country group.

Table 3.1 Sample size allocation per stratum for the stratified random sample. Forest strata codes are from figure 3.3: 1 – low cover; 2 – medium cover short; 3 – medium cover tall; 4 – dense cover short; 5 – dense cover short intact; 6 – dense cover tall; 7 – dense cover tall intact.

Forest type strata	sub-strata	
	no loss	1-pixel buffered loss (2000-2012)
Africa		
1,2	130	60
3	130	60
4	130	60
5,7	90	50
6	130	60
<i>total sample size</i>	900	
Latin America		
1,2,3	245	105
4,6	350	150
5,7	245	105
<i>total sample size</i>	1200	
South and Southeast Asia		
1,2	65	25
3	135	45
4	185	90
5,7	105	50
6	135	65
<i>total sample size</i>	900	

Table 3.2 Error matrix of sample counts. 1-pixel buffer sub-stratum includes mapped no loss pixels adjacent to pixels of mapped loss.

Forest strata	Mapped loss sub-strata		Reference loss		Natural forest loss (from total reference loss)	Sample size	Strata area (Mha)
			no loss	loss			
Africa							
1	no loss		76	1	1	77	198.6
	buffered	1-pix buffer	14	9	4	23	10.1
	loss	mapped loss	1	11	4	12	3.5
2	no loss		52	1	0	53	148.0
	buffered	1-pix buffer	19	3	2	22	9.3
	loss	mapped loss	0	3	0	3	3.5
3	no loss		128	2	0	130	150.9
	buffered	1-pix buffer	34	8	3	42	13.2
	loss	mapped loss	2	16	6	18	6.2
4	no loss		130	0	0	130	64.8
	buffered	1-pix buffer	30	4	2	34	7.0
	loss	mapped loss	0	26	15	26	4.1
5	no loss		11	0	0	11	10.4

Forest strata	Mapped loss sub-strata		Reference loss		Natural forest loss (from total reference loss)	Sample size	Strata area (Mha)
			no loss	loss			
6	buffered loss	1-pix buffer mapped loss	8	0	0	8	0.1
			0	1	1	1	0.0
	no loss		130	0	0	130	68.8
7	buffered loss	1-pix buffer mapped loss	31	6	5	37	5.0
			0	23	18	23	3.2
	no loss		79	0	0	79	86.5
	buffered loss	1-pix buffer mapped loss	27	1	1	28	0.5
			1	12	12	13	0.2
South America							
1	no loss		68	2	1	70	88.8
	buffered loss	1-pix buffer mapped loss	16	8	4	24	5.2
			1	3	1	4	2.8
2	no loss		113	0	0	113	132.3
	buffered loss	1-pix buffer mapped loss	21	9	3	30	10.8
			1	14	10	15	9.0
3	no loss		62	0	0	62	57.5
	buffered loss	1-pix buffer mapped loss	24	0	0	24	4.9
			8	0	5	8	3.6
4	no loss		204	0	0	204	223.9
	buffered loss	1-pix buffer mapped loss	48	8	6	56	24.5
			1	45	24	46	27.1
5	no loss		37	0	0	37	49.7
	buffered loss	1-pix buffer mapped loss	17	3	3	20	0.8
			1	13	13	14	0.8
6	no loss		146	0	0	146	144.7
	buffered loss	1-pix buffer mapped loss	19	1	1	20	8.2
			2	26	25	28	13.0
7	no loss		208	0	0	208	383.2
	buffered loss	1-pix buffer mapped loss	30	2	2	32	1.7
			0	39	39	39	2.0
South and Southeast Asia							
1	no loss		29	0	0	29	44.4
	buffered loss	1-pix buffer mapped loss	4	3	1	7	1.6
			0	2	0	2	0.3
2	no loss		36	0	0	36	47.6
	buffered loss	1-pix buffer mapped loss	11	2	0	13	2.7
			0	3	1	3	0.8
3	no loss		135	0	0	135	129.7
	buffered loss	1-pix buffer mapped loss	23	2	1	25	10.0
			3	17	9	20	4.5
4	no loss		184	1	1	185	164.9
	buffered loss	1-pix buffer mapped loss	49	6	2	55	19.5
			3	32	15	35	16.3
5	no loss		25	0	0	25	13.8
	buffered loss	1-pix buffer mapped loss	13	1	1	14	0.2
			1	3	3	4	0.1
6	no loss		135	0	0	135	115.9
		1-pix buffer	35	0	0	35	8.4

Forest strata	Mapped loss sub-strata		Reference loss		Natural forest loss (from total reference loss)	Sample size	Strata area (Mha)
			no loss	loss			
7	buffered loss	mapped loss	1	29	24	30	11.8
	no loss		80	0	0	80	50.7
	buffered loss	1-pix buffer	22	0	0	22	0.5
	loss	mapped loss	0	10	10	10	0.3

Table 3.3 Sample size allocation per countries and country groups (figure 3.1) for the final reporting.

Reporting units	N of samples
Democratic Republic of the Congo	328
Humid tropical Africa	298
The rest of Sub-Saharan Africa	274
Brazil	603
Pan-Amazon	337
The rest of Latin America	245
Indonesia	248
Mainland South and Southeast Asia	430
Insular Southeast Asia	173

The reference 2000-2012 forest cover loss condition (i.e., loss or no loss) was assigned to each sample pixel based on the visual interpretation of Landsat multitemporal composites for years circa 2000, 2003, 2006, 2009, 2012 and 2000-2012 maximal reflectance value composite, and high resolution imagery available through Google EarthTM. Of the 3000 sampled pixels, 1042 had at least one high resolution image available for the study period, 438 sample pixels had at least 2 images, and 219 sample pixels had 3 or more images. The validation process is illustrated schematically in figure 3.4.

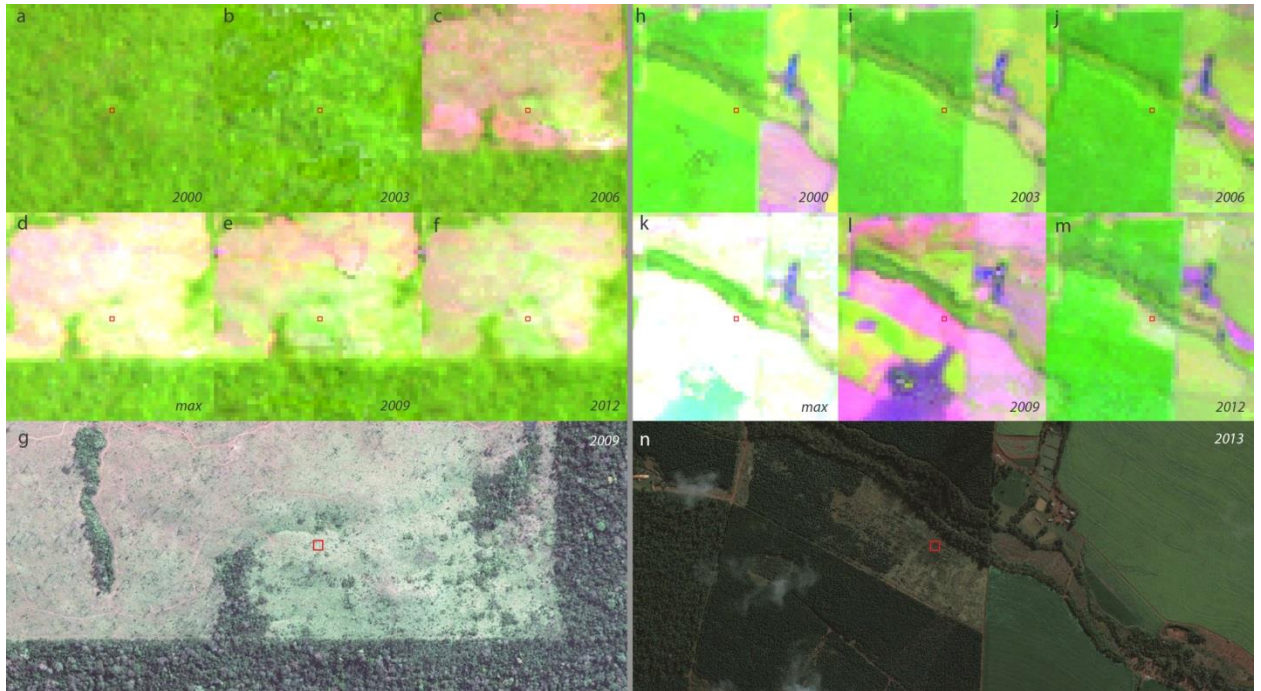


Figure 3.4 Validation samples: a-g – natural forest loss in Mato Grosso, Brazil; h-n – plantation clearing and regrowth in Parana, Brazil; a-f and h-k are Landsat multitemporal composites for years circa 2000, 2003, 2006, 2009, 2012 and 2000-2012 maximal composite; g and n – high resolution imagery from Google EarthTM.

The sample data were used to estimate area of forest loss by the seven forest cover types per continent (table 3.4), country and country group (table 3.5), and to calculate standard errors and the corresponding 95% confidence intervals of the estimates (Cochran 1977). The sample data were also used to estimate the proportion of loss occurring within natural forests (tables 3.4, 3.5). To obtain the latter estimates, each sample pixel that was identified as 2000-2012 loss was characterized as having occurred within “natural” or “managed” forest based on interpretation of Landsat time-series, high resolution data, and ancillary land cover information (figure 3.4). The “natural” forest category included all primary and mature secondary forests and natural woodlands without evidence of prior disturbances. The “managed” forest category included forest plantations, agroforestry systems and areas of subsistence farming due to shifting

cultivation practices. In Landsat imagery, dense natural tropical forests with large crowns have coarser texture, while the texture of dense plantations composed of more uniform stands is comparatively smoother (figure 3.4). In the dry tropics, plantations often have denser canopy cover than natural vegetation and look brighter and more uniform in satellite imagery.

Table 3.4 2000-2012 forest cover and aboveground carbon (AGC) loss estimates. Estimates are produced within the continental strata (see figure 3.3). Uncertainty is expressed as a 95% confidence interval.

	strata	Gross forest cover loss			Accuracy of forest cover loss map (%)		Natural forest cover loss	AGC density	Gross AGC loss	Natural forest AGC loss	BGC density	Gross BGC loss	Gross AGC+BGC loss
		Area (Mha)		Difference between sample and map estimates (%)			Area (Mha)	(MgC/ha)	Annual (TgC/yr)	Annual (TgC/yr)	(MgC/ha)	Annual (TgC/yr)	Annual (TgC/yr)
		Map (Hansen et al., 2013)	Sample estimate		User's	Producer's							
Africa	1	3.5	9.4 ± 5.8	↑ 170	93	32	5.0 ± 2.9	45.2 ± 0.1	35 ± 22	19 ± 11	13.5 ± 6.1	11 ± 8	46 ± 23
	2	3.5	7.9 ± 6.0	↑ 128	100	37	1.2 ± 1.8	57.9 ± 0.1	38 ± 29	6 ± 9	16.8 ± 7.6	11 ± 10	49 ± 30
	3	6.2	10.5 ± 3.9	↑ 69	91	54	2.5 ± 1.4	72.1 ± 0.1	63 ± 23	15 ± 9	20.4 ± 9.3	18 ± 11	81 ± 26
	4	4.1	4.8 ± 0.7	↑ 19	100	84	2.5 ± 1.0	104.8 ± 0.2	42 ± 6	21 ± 9	28.5 ± 12.9	11 ± 6	54 ± 9
	5	0.0	0.0 ± 0.0	0	100	100	0.0 ± 0.0	150.5 ± 0.9	0 ± 0	0 ± 0	39.3 ± 17.9	0 ± 0	0 ± 0
	6	3.2	4.0 ± 0.6	↑ 25	100	80	3.0 ± 0.7	155.8 ± 0.3	51 ± 7	39 ± 9	40.5 ± 18.4	13 ± 6	65 ± 10
	7	0.2	0.3 ± 0.1	↑ 9	93	93	0.3 ± 0.0	166.1 ± 0.3	4 ± 1	4 ± 0	42.9 ± 19.5	1 ± 0	5 ± 1
	total	20.7	36.9 ± 9.2	↑ 78	96	52	14.5 ± 4.9	-	234 ± 44	104 ± 21		65 ± 19	300 ± 48
Latin America	1	2.8	6.9 ± 3.9	↑ 150	89	34	2.8 ± 2.2	38.7 ± 0.1	22 ± 13	9 ± 7	11.7 ± 5.3	7 ± 5	29 ± 13
	2	9.0	11.7 ± 2.2	↑ 30	92	75	7.2 ± 2.5	41.8 ± 0.1	41 ± 8	25 ± 9	12.6 ± 5.7	12 ± 6	53 ± 10
	3	3.6	3.5 ± 0.5	↓ 2	100	89	2.6 ± 1.2	56.8 ± 0.2	17 ± 3	12 ± 6	16.5 ± 7.5	5 ± 2	22 ± 3
	4	27.1	30.4 ± 2.9	↑ 12	98	89	17.5 ± 4.4	77.9 ± 0.1	197 ± 19	114 ± 28	21.8 ± 9.9	55 ± 26	252 ± 32
	5	0.8	0.9 ± 0.2	↑ 10	93	87	0.9 ± 0.0	94.2 ± 0.2	7 ± 1	7 ± 0	25.9 ± 11.8	2 ± 1	9 ± 2
	6	13.0	11.8 ± 2.0	↓ 9	93	97	11.1 ± 1.4	134.9 ± 0.2	133 ± 22	125 ± 16	35.6 ± 16.2	35 ± 17	168 ± 28
	7	2.0	2.1 ± 0.2	↑ 2	100	96	2.1 ± 0.0	147.0 ± 0.1	25 ± 2	25 ± 0	38.5 ± 17.5	7 ± 3	32 ± 4
	total	58.3	67.3 ± 6.1	↑ 15	96	83	44.0 ± 5.7	-	442 ± 33	316 ± 35		123 ± 32	564 ± 46
	1	0.3	1.2 ± 0.7	↑ 256	100	33	0.2 ± 0.3	64.5 ± 0.3	6 ± 4	1 ± 2	18.5 ± 8.4	2 ± 1	8 ± 4
	2	0.8	1.1 ± 0.5	↑ 32	100	64	0.2 ± 0.4	71.2 ± 0.3	6 ± 3	1 ± 2	20.2 ± 9.2	2 ± 1	8 ± 3

strata	Gross forest cover loss						Natural forest cover loss	AGC density	Gross AGC loss	Natural forest AGC loss	BGC density	Gross BGC loss	Gross AGC+BGC loss
	Area (Mha)		Difference between sample and map estimates (%)	Accuracy of forest cover loss map (%)		Area (Mha)	(MgC/ha)	Annual (TgC/yr)	Annual (TgC/yr)	(MgC/ha)	Annual (TgC/yr)	Annual (TgC/yr)	
	Map (Hansen et al., 2013)	Sample estimate		User's	Producer's								
South and Southeast Asia	3	4.5	4.7 ± 1.3	↑ 4	89	82	1.0 ± 0.5	90.3 ± 0.2	35 ± 10	8 ± 3	24.9 ± 11.3	10 ± 5	45 ± 11
	4	16.3	17.6 ± 3.3	↑ 8	88	82	4.3 ± 3.7	103.4 ± 0.2	152 ± 28	37 ± 32	28.1 ± 12.8	41 ± 20	193 ± 35
	5	0.1	0.1 ± 0.0	↓ 34	74	82	0.1 ± 0.0	120.7 ± 1.0	1 ± 0	1 ± 0	32.3 ± 14.7	0 ± 0	1 ± 0
	6	11.8	11.4 ± 0.8	↓ 3	97	100	9.3 ± 1.7	148.2 ± 0.3	141 ± 10	115 ± 22	38.7 ± 17.6	37 ± 17	178 ± 19
	7	0.3	0.3 ± 0.0	↑ 8	100	100	0.3 ± 0.0	176.9 ± 0.6	5 ± 0	5 ± 0	45.4 ± 20.6	1 ± 1	6 ± 1
	total	34.2	36.4 ± 3.8	↑ 6	92	86	18.9 ± 4.5	-	346 ± 32	167 ± 39		93 ± 27	439 ± 42

3.2.6. Carbon density data

Baccini et al. (2012) employed field data and co-located GLAS lidar data to convert GLAS waveform metrics into biomass estimates. The field-calibrated statistical relationships were then applied to approximately 9 million tropical GLAS shots between 23°N and 23°S in a semi-regular grid of ICESat tracks (figure 3.5). I employed the field-calibrated GLAS-derived biomass data to calculate continent-specific mean strata AGC densities (figure 3.7a-c, figure 3.6 and table 3.4). In effect, the GLAS biomass data in this study were treated as a substitute for field inventory data. Model errors (of 22.6 MgC/ha; 5.5%) were not incorporated into calculations; the uncertainty of mean strata AGC estimates was characterized by their standard errors calculated from GLAS samples. The biomass data used in this study are not from the map product of Baccini et al. (2012), but from the population of GLAS shots converted to biomass used in generating the carbon stock map of Baccini et al. (figure 3.5).

My main result is AGC loss, for which I employ a source of aboveground carbon stock in the form of biomass-calibrated lidar data; these data serve as a surrogate for forest inventory measurements with mean and variance calculated per mapped carbon stock strata. Though there are no analogous observational data for belowground carbon, I further estimated per-stratum belowground carbon (BGC) densities and BGC loss in order to make the current results comparable to those of Harris et al. and Achard et al. Stratum-specific belowground carbon (BGC) densities were estimated from AGC densities using equation 1 from Mokany et al. (2006), and uncertainty of BGC using equation S7 from Saatchi et al. (2011).

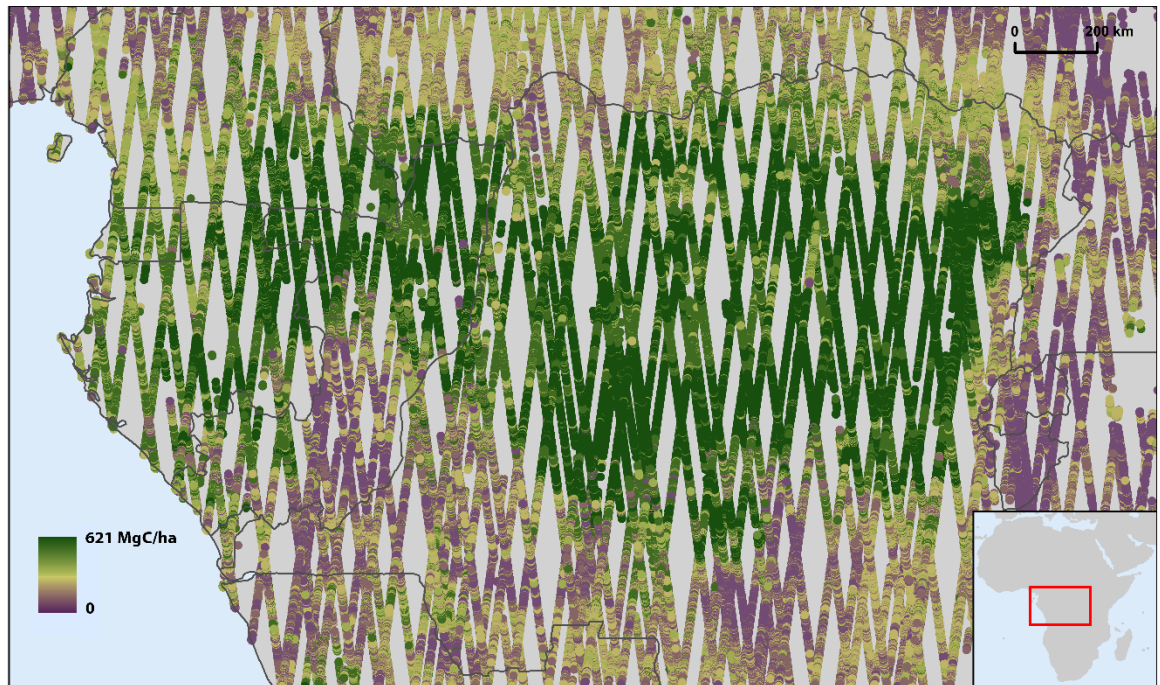


Figure 3.5 GLAS samples (2003-2009) attributed with aboveground carbon (AGC) densities. Each circle on the map corresponds to a ~65 m diameter circular GLAS lidar footprint with the modeled AGC density (MgC/ha) value (Baccini et al., 2012).

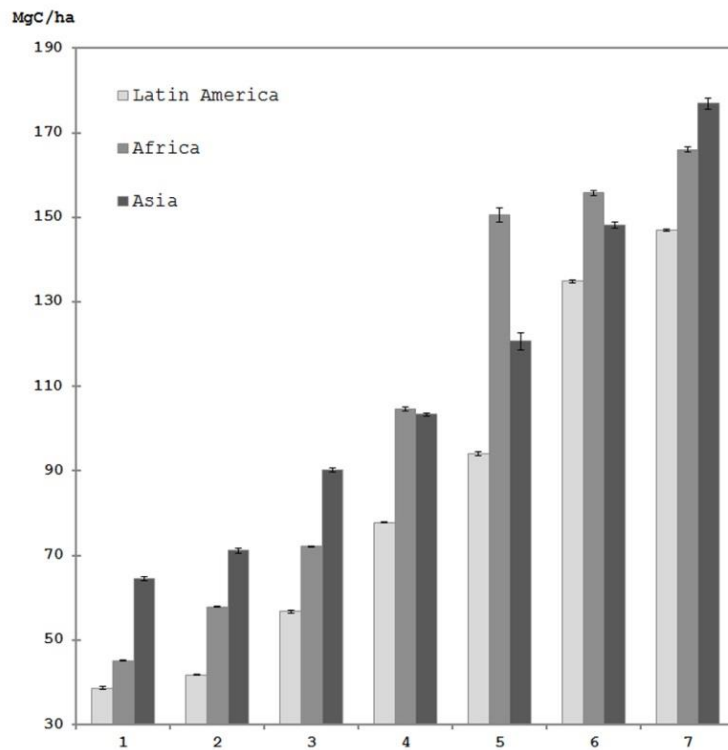


Figure 3.6 Mean AGC densities (\pm 95% CI) for forest strata 1-7 within the 3 study regions, derived from GLAS-modeled biomass samples (Baccini et al., 2012)).

3.3 Results

In this chapter I estimated gross aboveground carbon (AGC) loss in the entire pan-tropical region to be 1022 ± 64 TgC/yr (table 3.5, figure 3.7d-f). AGC loss within natural forests accounted for 58% of the estimated total pan-tropical AGC loss and differed among the study regions (table 3.5, figure 3.8) with the highest losses in the Amazon basin and the lowest in Central Africa. Latin America experienced the highest AGC loss of the three regions of study, accounting for 43% of gross and 54% of natural forest pan-tropical AGC loss. Brazil alone accounted for 26% of pan-tropical gross forest AGC loss and 34% of natural forest AGC loss. Africa experienced the least AGC loss among continents, totaling one-half of Latin America's gross and one-third of its natural AGC loss. AGC loss within intact forests (strata 5 and 7, see table 3.4) accounted for 11% of the pan-tropical total, 70% of which occurred in Latin America.

AGC loss is dominant in dense forests (strata 4-7, see table 3.4), which accounted for 82% of gross forest AGC loss and 86% of natural forest AGC loss in Latin America, and 86% of gross and 95% of natural forest AGC loss in South and Southeast Asia. Dense forests in Africa accounted for 41% of gross and 62% of African natural forest AGC loss, meaning AGC loss in savanna woodlands is comparable to that of humid tropical forests in Africa. Proportional AGC loss per unit area of forest is higher in natural forests for all humid tropical-dominated regions. The three sub-regions with significant dry tropical forest and woodland cover (regions C, F and H (figure 3.1); table 3.5) have proportionately less AGC loss within natural forests compared to managed systems, likely reflecting the presence of plantations with higher carbon stock than native tree cover.

Table 3.5 2000-2012 forest cover loss and aboveground carbon (AGC) loss estimates. The “Sample estimate” value is computed using an unbiased estimator of forest cover loss area applied to data obtained from a probability sampling design (see Data and Methods). Uncertainty is expressed as a 95% confidence interval (CI). For the boundaries of the regions see figure 3.1.

	Gross forest cover loss			Natural forest cover loss		Gross AGC loss	Natural forest AGC loss	
	Area (Mha)		Difference between sample and map estimates (%)	Area (Mha)	% of sample gross forest loss estimate	Annual (TgC/yr)	Annual (TgC/yr)	% of gross AGC loss
	Map (Hansen et al., 2013)	Sample estimate						
DRC	5.9	9.7 ± 3.1	↑ 65	4.3 ± 1.9	45	86 ± 19	46 ± 12	53
Humid Tropical Africa	5.1	9.8 ± 6.2	↑ 92	1.2 ± 0.8	12	56 ± 29	12 ± 2	22
The rest of Sub-Saharan Africa	9.7	17.4 ± 6.2	↑ 79	9.0 ± 3.4	52	92 ± 27	47 ± 15	50
Africa total	20.7	36.9 ± 9.2	↑ 78	14.5 ± 4.9	39	234 ± 44	104 ± 21	45
Brazil	34.4	37.6 ± 3.0	↑ 9	25.1 ± 3.8	67	266 ± 18	202 ± 12	76
Pan-Amazon	9.0	10.8 ± 1.8	↑ 21	7.5 ± 2.1	70	76 ± 14	58 ± 2	76
The rest of Latin America	14.9	18.8 ± 4.1	↑ 27	11.6 ± 3.6	62	99 ± 25	55 ± 15	56
Latin America total	58.3	67.3 ± 6.1	↑ 15	44.0 ± 5.7	65	442 ± 33	316 ± 21	72
Indonesia	15.7	14.4 ± 2.0	↓ 9	7.5 ± 2.2	52	151 ± 14	88 ± 21	59
Mainland South and Southeast Asia	12.3	16.3 ± 2.8	↑ 32	10.3 ± 2.2	63	136 ± 23	90 ± 17	66
Insular Southeast Asia	6.1	5.5 ± 1.3	↓ 9	2.7 ± 1.5	49	58 ± 12	32 ± 15	54
South and Southeast Asia total	34.2	36.4 ± 3.8	↑ 6	18.9 ± 4.5	52	346 ± 32	167 ± 39	48
Pan-tropical total	113.1	140.5 ± 11.6	↑ 24	77.5 ± 8.8	55	1022 ± 64	588 ± 49	58

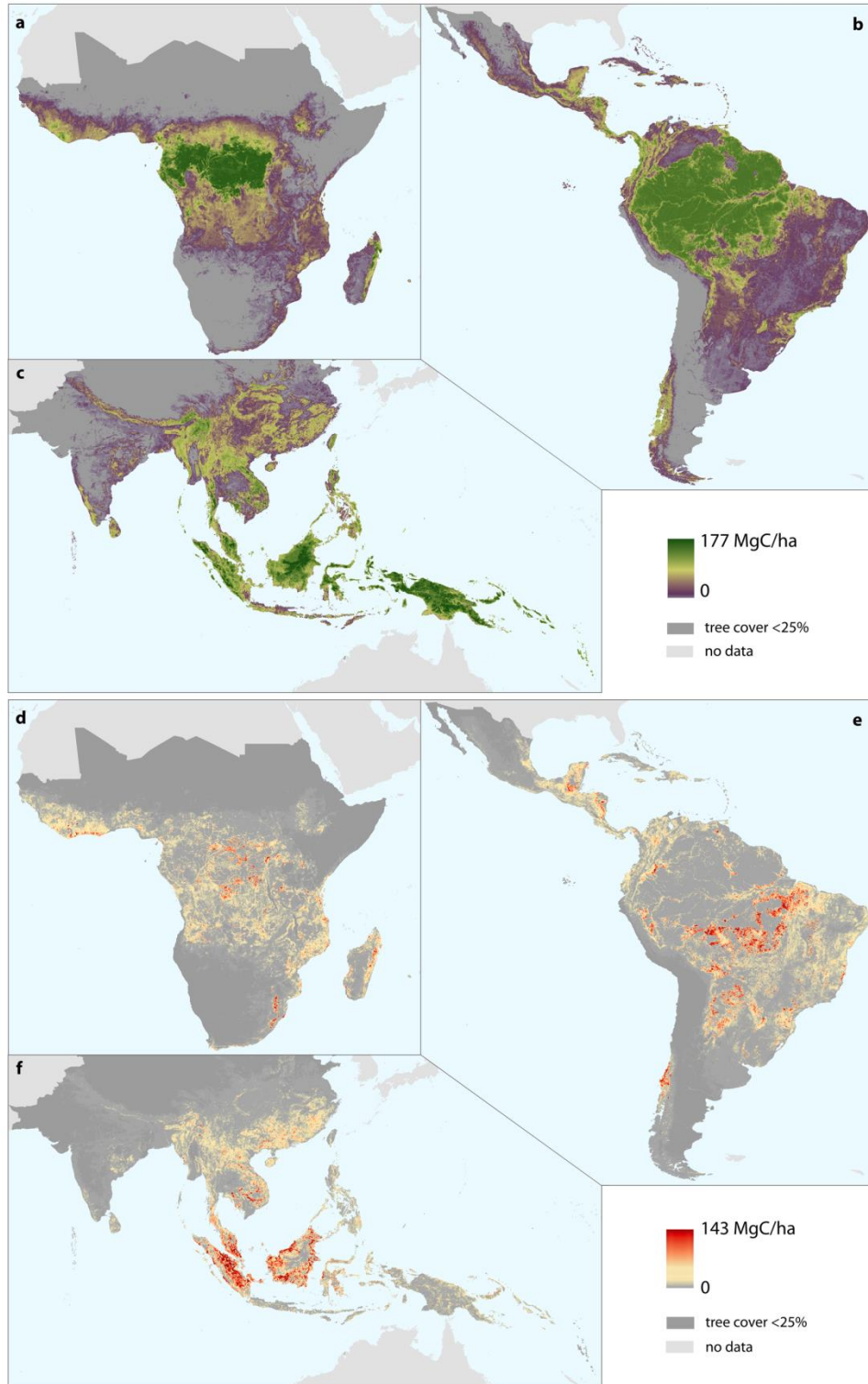


Figure 3.7 Forest strata average aboveground carbon (AGC) density and loss: a-c, year 2000 aboveground carbon (AGC) density; d-f, estimated 2000-2012 AGC loss. Data are aggregated to 5 km for display purposes.

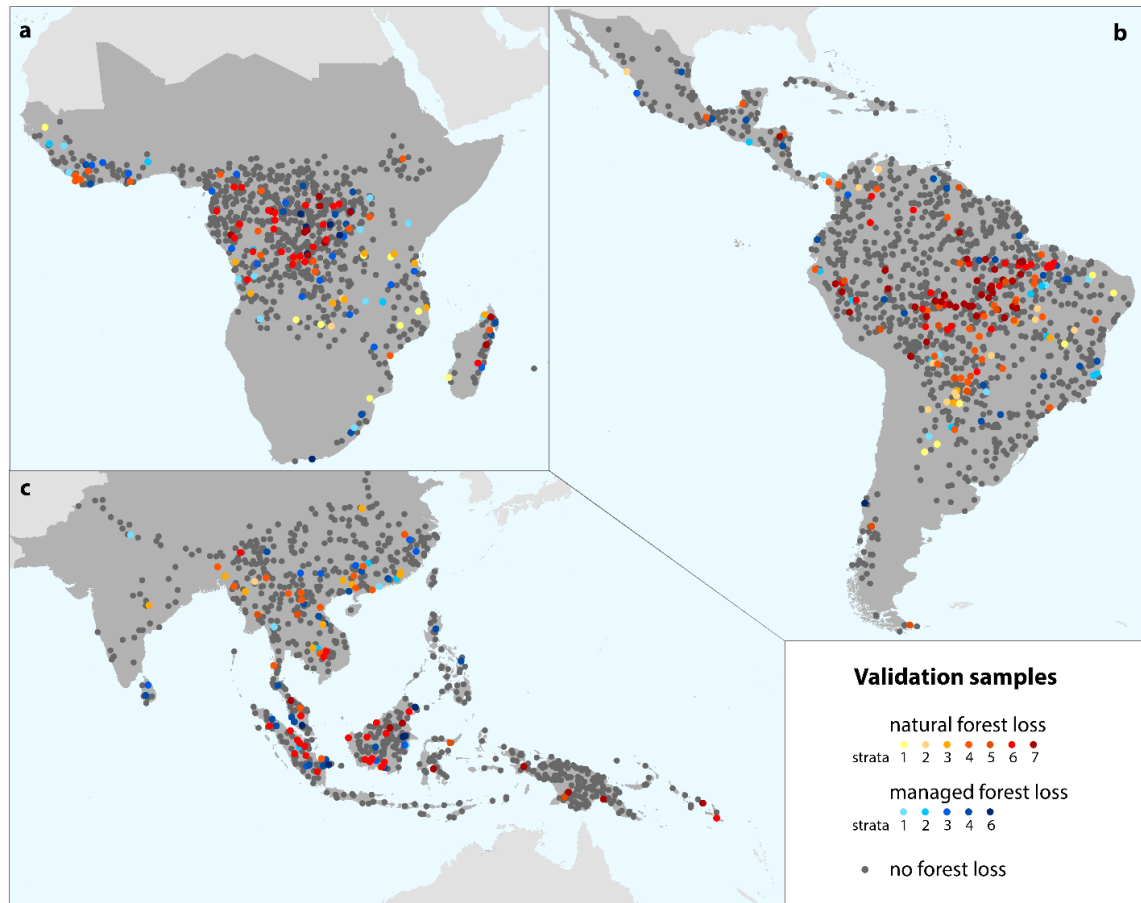


Figure 3.8 Forest loss in natural and managed forests. Sample locations classified as reference loss within natural and managed forests for each of the seven forest type strata (see figure 3.3): 1 – low cover; 2 – medium cover short; 3 – medium cover tall; 4 – dense cover short; 5 – dense cover short intact; 6 – dense cover tall; 7 – dense cover tall intact.

Total forest cover loss estimated from the reference classification of loss or no loss for the validation samples was higher compared to the estimated loss area obtained from the Hansen et al. (2013) forest loss map for each of the 3 study regions (table 3.5 and 3.4, figure 3.9). The largest increase was observed in Africa (78%). Tyukavina et al. (2013) reported a similar finding for the Democratic Republic of Congo, largely due to the scale of disturbance in smallholder landscapes and a resulting omission of forest loss. Landsat’s 30-m spatial resolution was more appropriate for accurately quantifying the industrial-scale clearings of South America and Southeast Asia. The analysis of spatial

distribution of forest loss confirms this interpretation: the ratio of the area of one-pixel boundaries around forest loss to the area of loss is 2.2 in Africa, 1.3 in South and Southeast Asia and 1.0 in Latin America. The ratio differs even more when comparing individual countries: 2.2 in the DRC, 0.88 in Indonesia and 0.79 in Brazil. For small-scale change dominated regions such as Africa, Landsat resolution assessments of forest change may lead to significant underestimation of forest carbon loss (Tyukavina *et al* 2013). Forest cover loss in the initial map was underestimated predominantly in forests with low canopy cover (strata 1 and 2, table 3.4), where the forest change signal is more ambiguous from the remote sensing perspective. Dry tropical forests are less well-studied than humid tropical forests and improved forest cover change mapping approaches are required to monitor the extent and change of open canopied woodlands and savannas.

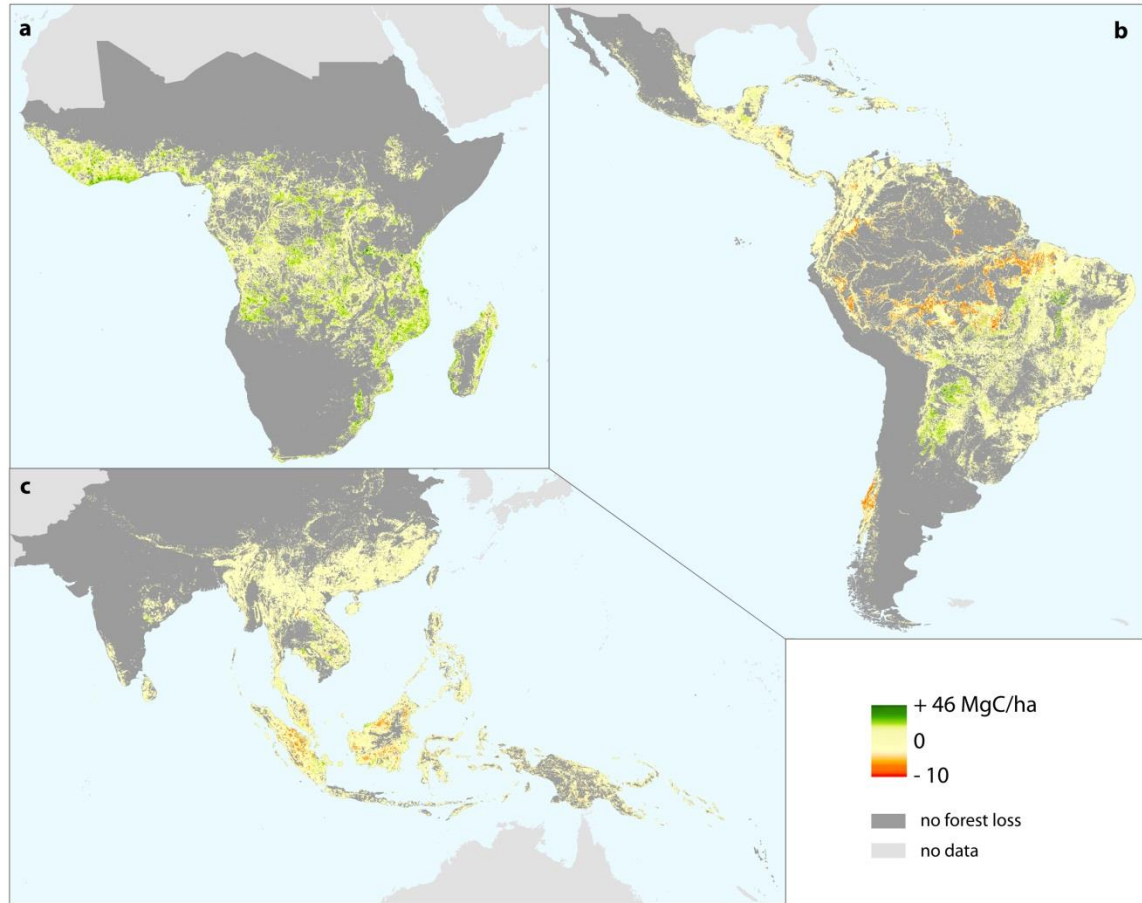


Figure 3.9 Difference between sample and map-based (Hansen et al., 2013) aboveground carbon (AGC) loss estimates. Positive values correspond to the areas where the sample estimate exceeds the map-based estimate. Difference map was derived by calculating the difference between sample- and map-based AGC loss estimates for each stratum and aggregating to a 5 km resolution for display.

3.4 Discussion and Conclusions

The most directly comparable antecedent studies (Harris *et al* 2012, Achard *et al* 2014) estimated total above- and belowground carbon loss for the tropical region (table 3.6). These two studies and the presented one each vary in geographic and temporal extent, as well as observational inputs and methods for both carbon loss and associated uncertainty (table 3.7).

Table 3.6 Comparison of gross carbon loss estimates. AGC stands for aboveground carbon; BGC – belowground carbon. Range of uncertainty represents the 95% confidence interval for the current study; 90% prediction interval derived from Monte Carlo simulations and including all critical sources of uncertainty for Harris et al. (2012), and uncertainty range derived from a sensitivity analysis related to the bias in carbon density maps for Achard et al. (2014).

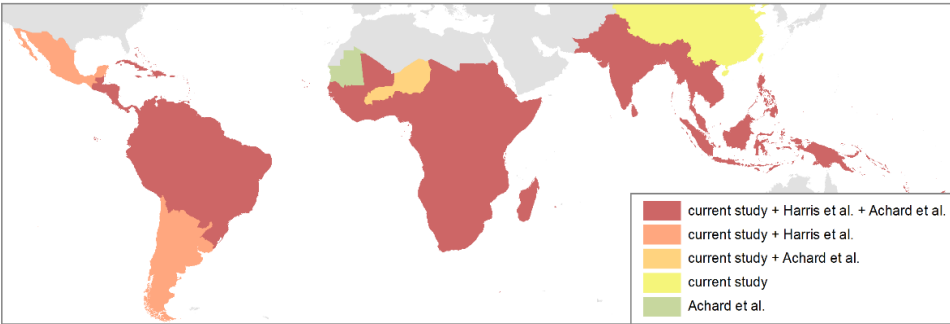
		Annual gross loss (TgC/yr)							
		AGC		AGC + BGC		AGC + BGC			
Period (2000s)		current study		current study		Harris et al. 2012		Achard et al. 2014	
		estimate	range	estimate	range	median	range	average	range
Africa	00-05					116	54 - 218		
	05-10	234	190 - 278	300	252 - 348	-	-	148	44 - 221
	10-12					-	-	-	-
Latin America	00-05					440	309 - 674		
	05-10	442	409 - 475	564	518 - 610	-	-	465	323 - 650
	10-12					-	-	-	-
South and Southeast Asia	00-05					257	208 - 345		
	05-10	346	314 - 378	439	397 - 481	-	-	267	236 - 367
	10-12					-	-	-	-
Pan-tropical total	00-05					813	570 - 1220		
	05-10	1022	958 - 1086	1303	1225 - 1381	-	-	880	602 - 1237
	10-12					-	-	-	-

Carbon loss totals from the current study are higher than that of Harris et al. and Achard et al., with the current pan-tropical and regional Africa and Southeast Asia gross carbon loss estimates outside of the range of the previous studies (table 3.6). Of the various differences in the three tropical forest carbon loss studies, possibly the most significant is the study period. Results from Hansen et al. indicated an increasing rate of forest cover loss within the 2000 to 2012 period. The study of Harris et al. covered 2000 to 2005 and Achard et al. covered 2000 to 2010. The inclusion of more recent years experiencing more forest cover loss is a likely source of variance in the respective carbon loss estimates. Additionally, carbon stock data used in the current research are not coarse resolution maps of biomass as in the previous studies. For example, Baccini et al. (2012),

which is one of the sources of carbon data in Achard et al., employed 65m GLAS-derived biomass data to subsequently calibrate 500m MODIS imagery. In this study, I use the 65m GLAS biomass data directly as the source of per stratum biomass. As the strata themselves are derived based on Landsat-derived cover, height and intactness data, this allows me to relate 30m forest cover loss with 30m forest carbon strata. I believe this to be more precise than relating forest loss to coarser biomass data that may convolve forest/non-forest pixels along fronts of change, particularly in spatially heterogeneous environments. Concerning activity data, my current area estimates are derived from examining individual 30m pixels within a probability-based sampling framework, specifically strata defined by different carbon stocks. As Tyukavina et al.'s (Tyukavina *et al* 2013) study of the Democratic Republic of Congo illustrated, map-based estimates can be biased in the case of heterogeneous, smallholder-dominated landscapes such as DRC; Landsat forest cover loss map data were found to underestimate change compared to per pixel sample-based estimation. In the presented study, Insular Southeast Asia, including Malaysia and Indonesia, and Brazil have map-based forest loss area estimates within 10% of the sample-based estimates. These countries represent areas of extensive agroindustrial development where 30m Landsat-based mapping is largely accurate, within +/-10% of the sample-based estimate. However, the proportion of total pan-tropical forest loss within these regions is reduced from 50% in the map-based estimate to 41% in the sample-based estimate (table 3.5). Regions such as Africa, Southeast Asia and Central America have finer-scale forest loss dynamics than Brazil and Insular Southeast Asia and correspondingly higher sample-based estimates than mapped-based. The consequence is an overall pan-tropical sample-based forest cover loss estimate 24%

higher than the map-based total. While discerning the exact sources of the variance between the current carbon loss estimate and that of Harris et al. and Achard et al. is difficult without a complete formal intercomparison, the aforementioned considerations (table 3.7) – study period, study area, carbon stock data, and sample-based area estimation methodology – are likely factors.

Table 3.7 Comparison of methodology in the current study, Harris et al. (2012) and Achard et al. (2014)

	Current study	Harris et al. 2012	Achard et al. 2014
Study period	2000 – 2012	2000 - 2005	2000 - 2010
Study area			
Forest definition	Height >5m; canopy cover \geq 25%	Height >5m; canopy cover \geq 25%	Area at least 3 ha (final reporting); height >5m; 100% of areas with >75% canopy cover plus 50% of areas with 30-70% canopy cover == forest area
Baseline year 2000 forest cover area	2631 Mha	1790 Mha	1574 Mha
Forest loss area estimation method	Pixel-level (30m) sample-based estimate, derived using Hansen et al. (2013) 30-m forest cover loss map as a stratifier	18.5x18.5-km block scale forest loss map (Hansen et al. 2010)	Sample-based estimate: regular sample of 10x10 km blocks, minimal mapping unit within a block – 3 ha, input satellite data ~30m resolution
Carbon pools included	AGC+BGC	AGC+BGC	AGC+BGC

AGC data	~65m point-based GLAS-modeled AGC estimates averaged over forest cover strata	Average AGC within 18.5x18.5 km blocks from the 1-km resolution map of Saatchi et al. (2011)	Average AGC within 10x10 km blocks from 500-km resolution (Baccini et al. 2012) and 1-km resolution (Saatchi et al. 2011) carbon stock maps
BGC data	Mokany et al. (2006) allometry used to estimate mean BGC for each forest stratum from the stratum-average AGC (derived from GLAS point-based estimates)	Average AGC within 18.5x18.5 km blocks from the 1-km resolution map of Saatchi et al. (2011), which uses Mokany et al. (2006) allometry	Average BGC within 10x10 km 1-km resolution map of Saatchi et al. (2011), which uses Mokany et al. (2006) allometry; the same allometry applied to derive BGC estimates from Baccini et al. (2012) AGC estimates

Brazil is the country with the largest area of natural forest loss in the study period. The officially reported forest loss in the Legal Amazon in Brazil is 17.6 Mha in 2000-2012 (INPE, www.obt.inpe.br/prodes/prodes_1988_2013.htm). I found 25.1 ± 3.8 Mha of natural loss over the same period. The difference could be due to differing methodological approaches (e.g., the minimal mapping unit of 6.25 ha in PRODES vs. the per-pixel (30m) mapping of Hansen et al. (2013)) as well the inclusion by the current study of additional natural forest loss outside of the Legal Amazon (e.g., cerrado woodland types). Recently reported primary forest loss of 6.03 Mha in Indonesia (Margono *et al* 2014) falls within the 95% confidence interval of the current natural forest loss estimate of 7.5 ± 2.2 Mha. Natural forest loss for the DRC of reported by Tyukavina et al. (2013) and consisting of terra firma and wetland primary forests and woodlands, also falls within the uncertainty of my current DRC sample-based estimate.

The utility of the presented approach under REDD+ comes from the ability to adapt it to any areal extent. Landsat is the closest existing system to an operational land imaging capability and Landsat data are available globally free of charge. While higher spatial resolution imagery are increasingly available and being tested and implemented

for national-scale REDD+ monitoring (Government of Guyana 2014), the likelihood of all tropical countries having the budgetary resources to systematically task, process and characterize annual national-scale commercial data sets now and into the future is highly uncertain. Landsat data may remain the most viable option for national-scale REDD+ monitoring for a number of countries. Using Landsat data, I followed recommended good practice guidance on the use of map-based activity data. Landsat-mapped carbon stock strata and forest cover loss were used in a stratified random sampling approach that enabled reliable estimation of pan-tropical forest cover loss area (SE of 4% for the pan-tropical gross forest loss area estimate) using a relatively small number of samples (3000 for the entire pan-tropical region). Probability sampling can also be used to assess the nature of forest loss, e.g. natural versus human-managed forests in this study, but also drivers and land use outcomes of forest clearing.

It is worth noting that the reference imagery for the sample based images may consist of high spatial resolution commercial data in place of Landsat, if resources for data acquisition and purchasing are available. For example, the Ministry of Environment of Peru recently completed a study analogous to the presented one, except that a two-stage cluster sample based on 12km by 12km blocks divided into low and high forest loss change strata was employed (Potapov *et al* 2014). Eighteen low change and twelve high change sample blocks were randomly selected within the respective strata, and RapidEye purchased for each block. The RapidEye data were compared with antecedent Landsat images in the quantification of area of forest cover loss, with primary and secondary forest loss interpreted as in the study presented here. The use of Landsat-derived products to guide the sample allocation of costlier assets is easily implemented and cost-effective.

The current Landsat-based pan-tropical estimated annual gross forest AGC loss represents 11% of the recently reported global annual estimate of carbon dioxide emissions for 2012 (IPCC 2014) (13% when including BGC estimate). Just over one-half of currently estimated carbon loss from tropical forest cover disturbance occurred within natural forests. While emissions from fossil fuels continue to grow globally (1.3% annually from 1970 to 2000 and 2.2% annually from 2000 to 2010 (IPCC 2014)), the extent of natural forests in the tropics continues to decline. Other carbon pools, particularly soil carbon in tropical peatlands (Page *et al* 2002), are a significant source of GHG emissions and are unaccounted for here. Regardless, there will be a continued diminishing fraction of global carbon dioxide emissions from natural tropical forest loss as their extent declines and fossil fuel emissions continue to rise at a more rapid pace than emissions from forest conversion. Rather than indicating a reduced importance of avoided deforestation, this fact points to the increasing significance of and need for the formal valuation of REDD+ co-benefits in the conservation of natural tropical forests (Miles and Kapos 2008, Díaz *et al* 2009, Phelps *et al* 2012, Potts *et al* 2013, Mullan 2014).

Chapter 4: Indirect mapping of forest degradation in the tropics³

4.1. Introduction

Tropical forests are unique in their provision of key ecosystem services, including climate regulation and biodiversity richness (Millennium Ecosystem Assessment 2005). However, they are under considerable pressure as an extant natural system due to exploitation and conversion to higher order land uses. The deforestation and forest degradation of tropical forests constitute the second largest source of anthropogenic emissions of carbon dioxide after fossil fuel combustion (van der Werf *et al* 2009). Stand-replacement disturbance of tropical forests is well understood with examples from national to global scale, including Brazil's annual mapping of Legal Amazon deforestation (Shimabukuro *et al* 2012) as well as annual to epochal pan-tropical mapping of forest cover loss (Hansen *et al* 2013, Kim *et al* 2014). However, the spatial extent of more subtle disturbance dynamics, including selective logging and fragmentation, is less well characterized.

Forest degradation is estimated to account for at least 15% of total carbon emissions from land cover and land use change in the tropics (Houghton 2013). Forest degradation is a complex multi-aspect phenomenon, which could be broadly defined as a human-induced, long-term reduction of intrinsic forest values (IPCC 2003a) such as biodiversity and carbon stocks. Many such degradation processes are best characterized using field data, a costly and labor-intensive endeavor at national scales (Pearson *et al*

³ The presented material is under review: Tyukavina A., Hansen M.C., Potapov P.V., Krylov A.M. (*in review*) Pan-tropical hinterland forests – mapping forests absent of disturbance. *Global Ecology and Biogeography*

2014, Berenguer *et al* 2014). Remotely sensed data sets offer an alternative to field assessments in quantifying forest degradation. In remotely sensed applications, degradation is largely defined as canopy/tree cover removal where a forest remains a forest; in other words, forest disturbance does not result in the minimum canopy threshold defining forest being crossed (Mollicone *et al* 2007). High spatial resolution optical, radar and LIDAR satellite and airborne data have been used to characterize forest degradation as a result of selective logging (Furusawa *et al* 2004, Asner 2009) and smallholder charcoal production (Rembold *et al* 2013). However, such data are unsuitable for large area degradation mapping and monitoring due to a lack of operational monitoring systems and prohibitive data costs. Freely available, systematically acquired medium spatial resolution remotely sensed imagery, specifically Landsat data, have been used to directly map areas of selective logging (Asner *et al* 2005, Souza *et al* 2005, Matricardi *et al.* 2007). The accuracy of this approach, however, depends on the degree of canopy removal and the time lag between disturbance event and image acquisition (Souza *et al* 2005).

Indirect mapping of forest degradation is an alternative approach based on the elimination of intact areas, rather than direct mapping of degraded forests (GOFC-GOLD 2013). One such approach, applied globally using Landsat data, is the Intact Forest Landscape (IFL) product (Potapov *et al* 2008b). The IFL mapping approach employs a combination of GIS data and visual interpretation of satellite imagery to map large ($\geq 500 \text{ km}^2$) contiguous forest landscapes absent of human activity (e.g. transport infrastructure, settlements, logging, agricultural activities, etc.). The IFL method advances previous wilderness mapping efforts (Bryant *et al* 1997, McCloskey and

Spalding 1989, Sanderson *et al* 2002) through the use of a consistent image source and systematic geospatial rules for intact forest delineation and has been promoted as an input to national forest monitoring and carbon accounting systems (Maniatis and Mollicone 2010, GOFC-GOLD 2013).

The IFL method has been employed at national scales to map forest degradation in Indonesia (Margono *et al* 2012, 2014) and in Central Africa (Zhuravleva *et al* 2013). In these studies, the IFL was used to subdivide primary forests, mapped using a pixel-based image classification, into degraded and intact sub-types. Rates of primary forest degradation and conversion were subsequently quantified at the national scale. However, the IFL mapping approach is labor-intensive due to the requirement of visual image interpretation in delineating areas of human activity. It is also conservative, meaning that once a forest is excluded from the IFL, it cannot be restored to an “intact” state. Logged or secondary forests that have not experienced recent disturbance may have recovered viable ecosystem functions, for example carbon stocks or biodiversity. The finding of extensive ape populations within sustainably logged forests of northern Republic of Congo (Wildlife Conservation Society 2008) and the complete recovery of pre-exploitation biomass in logging concessions within the Central African Republic (Gourlet-Fleury *et al* 2013) are two such examples. Methods that differentiate persistent forest utilization from episodic low-intensity disturbance can bring useful context to forest disturbance and degradation and/or recovery.

The outcome of degradation mapping, whether directly or indirectly characterized, is to divide existing forest cover into two subtypes, one more structurally and likely ecologically intact, and another comparatively impoverished. Methods that

automatically make this distinction over large areas may serve multiple ecological monitoring objectives, from carbon stock monitoring to protected area and land use planning (Jantz *et al* 2014). In this study, I present a method for automatically delineating such forests, which I term hinterland forests. Hinterland forests are defined as forest patches absent of and removed from disturbance in near-term history. User-defined parameters are employed to automatically generate hinterland forest extent and change over time, including minimum 1) size of hinterland forest patch, 2) corridor width, 3) distance from disturbance, and 4) extant history.

The hinterland forest product complements the IFL concept through the implementation of a defined disturbance interval. In this manner both primary and mature secondary forests can be included as hinterland forest if no disturbance is documented within the defined interval, in the case of this study the twelve year record of Hansen *et al*. (2013). The idea was prototyped earlier using Web-Enabled Landsat Data (Roy *et al* 2010) for a four year period over the contiguous United States, highlighting dramatic regional differences in landscapes dominated by forestry and long-term regrowth (Hansen *et al* 2014). I illustrate the method using year 2000 forest cover and 2000-2012 forest cover change data by Hansen *et al*. (2013) to map hinterland forests for the years 2007, 2011 and 2013 and assess 2007-2012 forest degradation over the tropics. To validate the results, I employ Lidar height metrics to estimate whether undisturbed hinterland forests are structurally different from non- hinterland forests.

4.2. Data and methods

4.2.1. Definitions

Forest is defined here as tree cover taller than 5m with canopy cover $\geq 25\%$, and dense forests as 5m tall canopy cover $\geq 75\%$. Hinterland forests are defined as recently undisturbed and unfragmented forests and may consist of either primary or mature secondary forests. Hinterland forests are thematically different from the IFL which include both forests and non-forest ecosystems (Potapov *et al* 2008b). Hinterland forests are defined primarily by the absence of disturbance in near-term history.

Criteria for the differentiation of hinterland forests are the following (figure 4.1):

a) Distance from recent stand-replacement forest disturbance: >1 km

The choice of a 1km buffer around tree cover loss and gain (which indicates prior disturbances) as the area where forest degradation is likely to occur is based on the literature review of Broadbent *et al* (2008), showing that 99% of edge effects in the tropical and temperate forests, including elevated fire frequency, are observed up to 2 km from the forest edge, including higher tree mortality up to 1 km from the forest edge, and wind disturbance up to 500 m.

b) Minimum size of forest patch: 100 km^2

Size threshold was selected following the study of Skole and Tucker (1993), who defined fragmented forest as “areas less than 100 square kilometers surrounded by deforestation”, and considering that in tropical regions forest fragments smaller than 50 km^2 are in danger of the receding edge phenomenon (Gascon *et al* 2000).

c) Connectivity of hinterland forest patches: minimum corridor width: 2 km

This criterion is also based on the review by Broadbent *et al* (2008): corridors narrower than 2 km will be entirely affected by the edge effects and are therefore likely to undergo further degradation, leading to the disconnection of the hinterland forest patches.

d) Interval of extant forest: 12 years

This criterion represents the length of the Hansen *et al.* (2013) global forest disturbance data set. Extending the interval to a longer period is a function of data availability for forest extent and disturbance. For this prototype effort, the available global record is employed.

Hinterland forest criteria are flexible: the numerical value of each criterion could be modified depending on the planned application of a hinterland forest map.

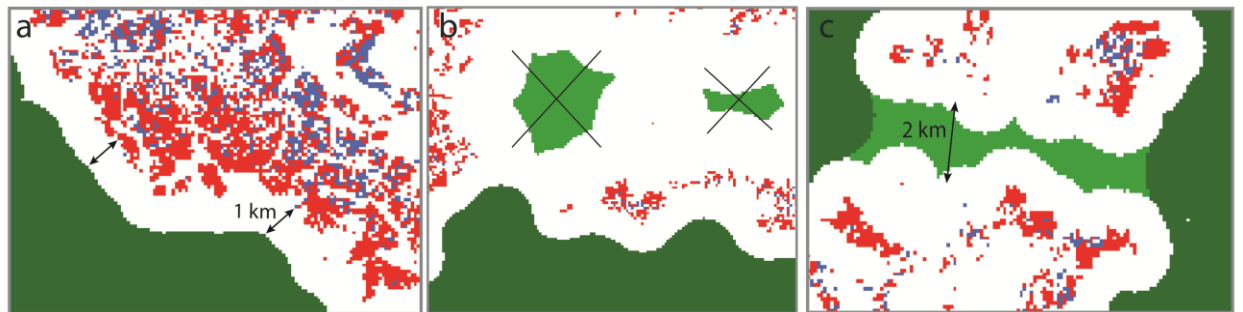


Figure 4.1 Hinterland forest criteria: a) distance to forest cover loss and gain (>1 km); b) minimum patch size (100 km²); c) minimum corridor width (2 km). Red is forest cover loss; blue – forest cover gain; dark green – hinterland forests; light green – other forests after subtracting 1-km buffer around change.

Forest degradation is defined as a change in the area of hinterland forests over time. Stand-replacement disturbance is the reference used to map hinterland change.

Such disturbances near to or within antecedent hinterland forest result in a reduction in hinterland forest extent. As with any indirect mapping approach, I am mapping areas likely to have experienced degradation per the scientific consensus on the effects of degradation dynamics including fragmentation, selective logging or fire (Hansen *et al* 2012, Souza Jr. 2012).

4.2.2. Data

To map hinterland forests, the data from the study of Hansen *et al.* (2013) were used (figure 4.3a). All input data were resampled from 30m to 90m due to computational limitations, with the final hinterland forest layers having a 90-m resolution. Forest extent was delineated by averaging to 90m (simple average) and thresholding year 2000 percent canopy cover data. Forest loss from 2000 to 2006 was used to establish baseline disturbance information for hinterland forest mapping and subsequent loss from 2007 to 2012 for mapping hinterland forest change. Additionally, forest gain from 2000 to 2012 was used as an input to hinterland forest mapping, as it reflects either disturbance prior to 2000 or afforestation. When aggregating forest loss and gain data to 90m, every 90m pixel with at least two 30-m loss or change pixels was considered change. Change areas smaller than 3 90-m pixels in a 2-km diameter circular moving window were regarded as noise and excluded from further buffering (figure 4.2). Water cover is an ancillary dataset in hinterland forest mapping, used to disaggregate forest patches split by large rivers, which work as environmental barriers. Here I used 2000-2012 Landsat-based semi-permanent water layer (Hansen *et al* 2013), which is a by-product of a quality assessment model used to produce the global forest cover change dataset.

4.2.3. Hinterland forest mapping

The process of hinterland forest mapping is schematically represented in figure 4.2. Parameters of input data could be defined depending on the available forest cover data (start and end date) and forest definition (forest canopy cover threshold). In this study hinterland forests are mapped for years 2007, 2011 and 2013 (using 2000-2006, 2000-2010 and 2000-2012 forest cover loss data respectively and 2000-2012 forest gain data), separately for all forests ($\geq 25\%$ canopy cover) and dense forests ($\geq 75\%$). The most recent hinterland forest layer (2013 hinterlands for all forests) is available online from <http://glad.geog.umd.edu/hinterland>. Processing parameters (width of buffer around change, minimum corridor width and minimum forest patch size) are defined by the hinterland forest criteria, as outlined earlier.

Hinterland forest mapping includes the following steps:

1. Buffering of combined forest cover change (loss and gain) data;
2. Subtraction of buffered change from reference forest cover;
3. Removing narrow (< 2 km wide) corridors between forest patches. This is done by applying a 1-km buffer from the forest edge inside the forest and the subsequent 1-km buffer outside;
4. Subtracting water from the intermediate results to separate forest patches divided by water bodies, visible in Landsat;
5. Removing patches with the areas smaller than the defined minimum hinterland forest patch area (100 km^2)

Hinterland/non-hinterland forests for 2007 were compared to data from NASA's Geoscience Laser Altimeter System (GLAS) processed by Baccini et al. (2012).

Available data for the years 2007 and 2008 totaled circa 2 mln. shots converted into forest height measurements. The GLAS Lidar data have a nominal 65m circular footprint, and mean forest heights were calculated for hinterland and non-hinterland forests for dense (>75%) and open canopied tree cover classes (25%-75%) for Latin American, African and Southeast Asian tropical forests.

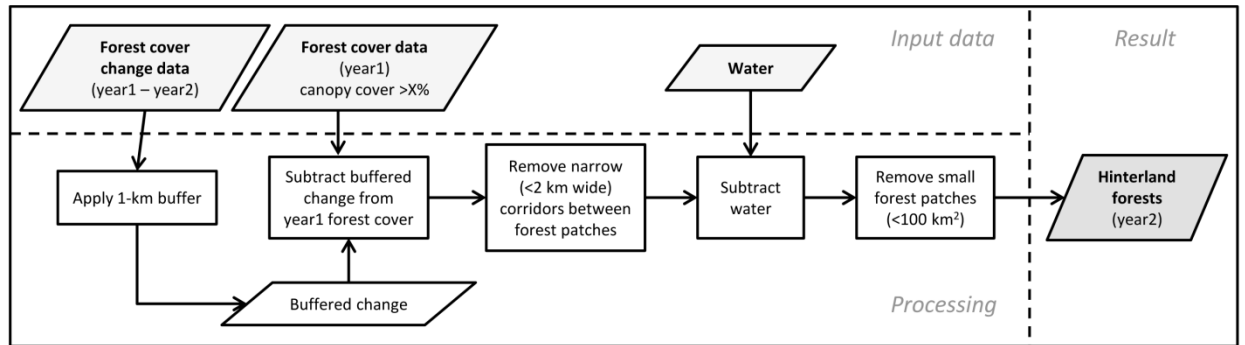


Figure 4.2 Hinterland forest mapping workflow. Input parameters: start and end years (year1 and year2) and forest canopy cover threshold (X%)

4.2.4 Forest degradation mapping

Forest degradation is mapped as the difference between hinterland forest layers for two sequential characterizations. Figure 4.3 illustrates the concept by mapping 2007-2012 tropical forest degradation as the difference between 2007 and 2013 hinterland forest layers. The forest degradation map is the result of the overlay of the two independently produced maps. Hinterland forest delineation is sensitive to errors of commission regarding forest loss and gain, particularly isolated pixels. To evaluate the initial hinterland change map, I randomly selected 500 forest degradation polygons out of 188514 polygons with an area <100km². Samples were allocated to the three continents proportionally to the number of change polygons: 250 to Latin America, 150 to Sub-Saharan Africa, and 100 to Southeast Asia. For each sample polygon a visual

assessment was performed using Landsat annual composite images (Hansen *et al* 2013) and high resolution data from Google Earth. The presence of adjacent forest cover change or forest fragmentation was interpreted as confirming forest degradation. Analysis of the sample blocks revealed (figure 4.4) that 100% of forest degradation polygons smaller than 0.08 km² and 98% of polygons smaller than 0.13 km² were identified as false change in the process of visual assessment. Hence, polygons <0.13 km² were removed from the final hinterland change map. For the remaining smaller degradation patches (0.13 – 100 km²), the error rate is estimated to be 4% (6 out of 152 polygons were identified as noise).

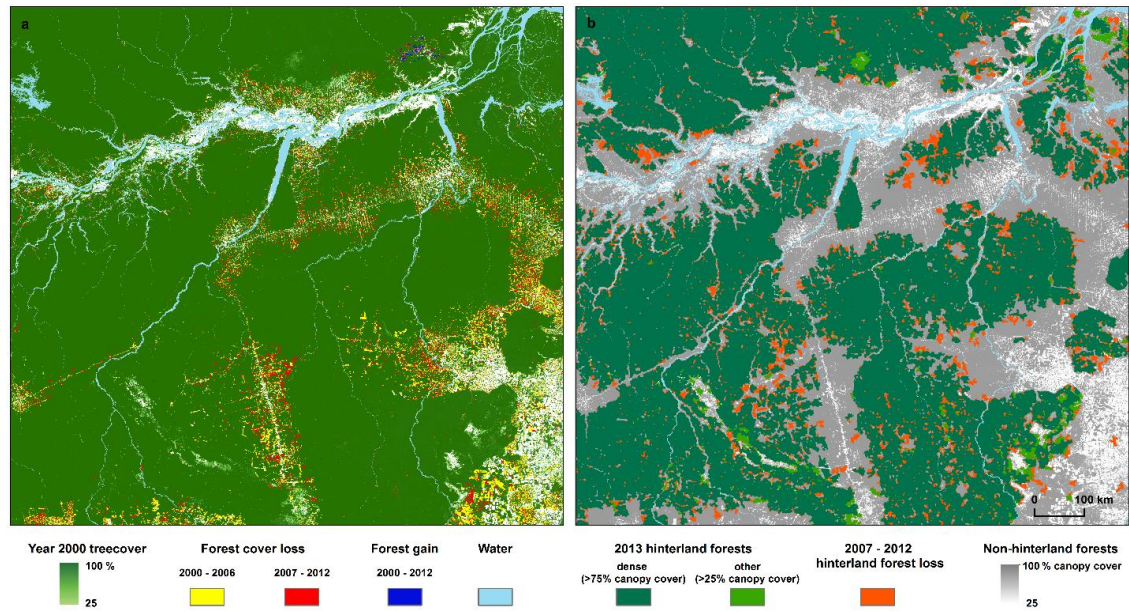


Figure 4.3 2007-2012 forest degradation (hinterland forest loss) mapping: a) hinterland forest mapping data inputs (year 2000 % canopy cover, 2000-2012 forest cover loss and gain, 2000-2012 stable water by Hansen et al. (2013)); b) 2007-2012 forest degradation mapped as a difference between 2007 and 2013 hinterland forest layers. Para. Brazil.

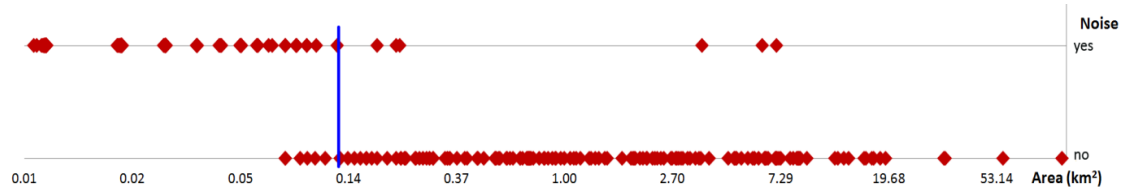


Figure 4.4 Results of the visual assessment of 2007-2012 forest degradation patches with the area $<100\text{km}^2$. Blue represents inclusion threshold: all polygons $< 0.13\text{km}^2$ were considered incorrect (noise) and excluded from the final forest degradation map. X axis (area) has log scale.

4.3 Results

4.3.1 Hinterland forest and degradation mapping

The hinterland forest map for the year 2007, produced using 2000-2006 forest loss data, is shown in figure 4.5. Dense hinterland forests represent recently undisturbed cores of tropical rainforests; other hinterlands depict lower canopy cover undisturbed humid tropical forests and remaining natural tropical woodlands. Figure 4.6 illustrates the degradation of hinterland forest in 2007-2012. In addition to degradation, some hinterland forests are directly cleared. I compared the distribution of 2007-2012 forest loss (Hansen *et al* 2013) within and outside of hinterland forests. In each of the 3 study regions, hinterland forest loss comprised less than 1% of the forest loss (0.7% in Latin America and Africa, 0.4% in Southeast Asia), indicating that clearing of previously degraded forests is much more widespread than hinterland forest clearing. Forest clearing tends to occur in proximity to previous forest loss (Alves 2002, Aguiar *et al* 2007) and it can be expected that hinterland forest clearing should be comparatively rare. In the study of Indonesia by Margono *et al* (2014) which employed the IFL to identify degraded primary forest, 98% of clearing occurred in already degraded forests. This result points out the utility of hinterland forests as areas removed from more intensive exploitation. Clearing of hinterland forests, where it occurs, represents a comparatively rare

disturbance dynamic within isolated forests. Latin America experienced the largest share of total hinterland forest loss (54.0%) followed by Africa and Southeast Asia (23.6% and 22.3% respectively).

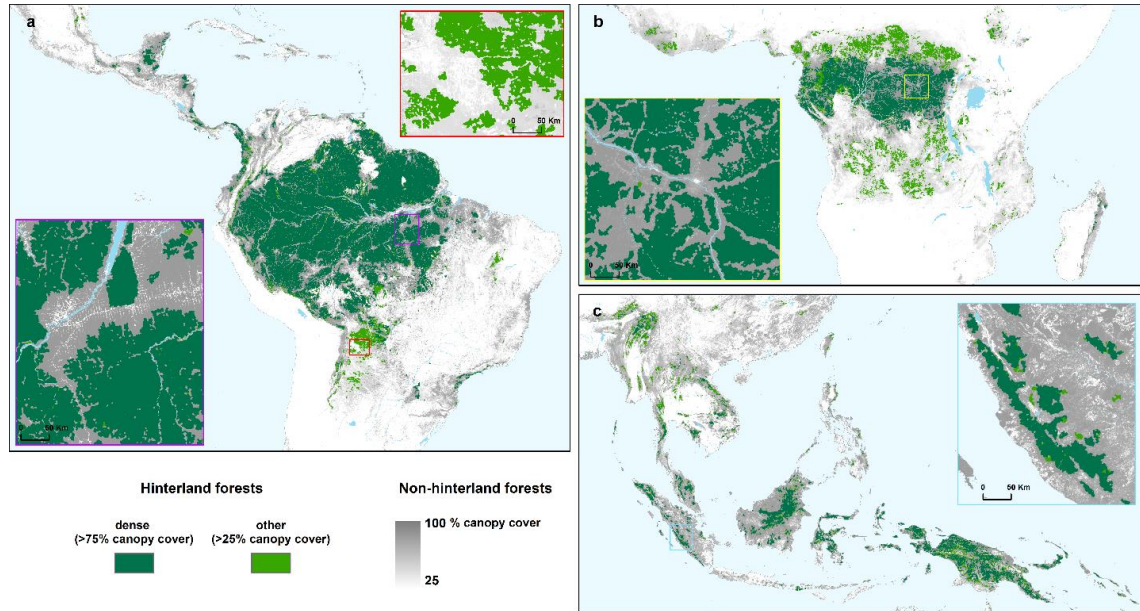


Figure 4.5 Hinterland forests 2007: a) Latin America; purple inset – Para, Brazil; red – Chaco woodlands; b) Africa; yellow inset – Kisangani, DRC; c) Southeast Asia; cyan inset – coast of Sumatra, Indonesia.

Hinterland forest loss exceeds gross forest cover loss due to stand-replacement disturbance from the map of Hansen et al. (2013) for all study regions (table 4.1), most significantly in Africa (~ 5:1). The proportion of degraded forests in proximity of change (within a 1-km buffer around change, hinterland criterion *a* from figure 4.1) to forests excluded from 2013 hinterlands due to fragmentation (hinterland criteria *b* and *c* from figure 4.1) differs among the continents (table 4.1). In Latin America and Southeast Asia, these proportions are roughly equal (50.3% degradation in proximity of change vs. 49.7% degradation due to fragmentation for South America; 48.9% to 51.4% for Southeast

Asia). Africa hinterland loss was predominantly due to fragmentation (43.5% vs. 56.5%), reflecting the more spatially heterogeneous nature of forest disturbance in Africa.

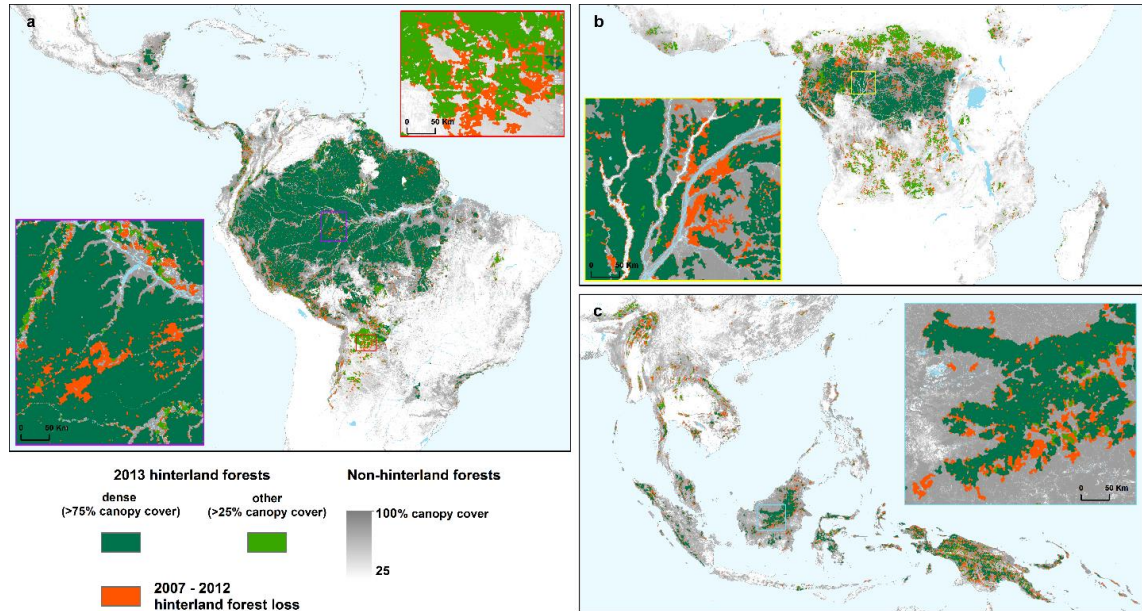


Figure 4.6 Forest degradation (2007-2012): a) Latin America; purple inset – Urucu natural gas field, Amazonas, Brazil; red – Chaco woodlands large-scale agricultural clearing, Santa Cruz, Bolivia and Boqueron and Alto Paraguay, Paraguay; b) Africa; yellow inset – smallholder-dominated agriculture, Likuola, RoC and Equateur, DRC; c) Southeast Asia; cyan inset – logging in Central Kalimantan, Indonesia and Sarawak, Malaysia.

Hinterland forest extent and loss from 2007 to 2012 is shown in table 4.2, with national-scale dynamics illustrated graphically in figure 4.7. Pan-tropically, hinterland forests accounted for just over one-third of all tree cover >25% in 2007. In the following six years, hinterland forest extent was reduced by nearly 20%, from 745 Mha to 613 Mha. Each major tropical forest region is different in terms of hinterland forest extent and loss. Of the 745 Mha of hinterland forest in 2007, 62% was located in Latin America, 25% in Africa and 13% in Southeast Asia. Despite the fact that Latin America lost the most

hinterland forest in the period of 2007 to 2012, the proportion of remaining pan-tropical hinterland forest within Latin America by 2012 increased to 67% while Africa declined to 23% and Southeast Asia to 10%.

Figure 4.7 illustrates the nations with considerable hinterland forest. For Latin America, a pan-Amazon cluster of Brazil, Venezuela, Colombia and Peru constitutes the largest extent of hinterland forest pan-tropically. The northeast coast of South America, contiguous with the Amazon Basin countries and consisting of Suriname, Guyana and French Guiana, represents the most intact tropical hinterland forest sub-region. Gabon, Republic of Congo, Central African Republic, Democratic Republic of Congo and Cameroon make up the next most extensive regional cluster of hinterland forest, however with a higher degree of loss. The third largest regional-scale hinterland forest is found in Indonesia and Papua New Guinea, with proportional loss greater still than either of the Latin American or central African core hinterland zones. Central African Republic has the largest extent of hinterland woodland (25-75% tree cover) with Angola, South Sudan and Zambia also containing considerable hinterland woodlands. In Latin America, Bolivia and Brazil have the most extensive hinterland woodland. Paraguay and Argentina contain increasingly fragmented woodland hinterlands, having lost roughly one-half of their respective extent from 2007 to 2012. In Southeast Asia, hinterland woodlands are also highly fragmented and actively reduced with remaining tracts largely found in Thailand, Myanmar and India.

Table 4.1 Estimated extent of 2007-2012 forest degradation (hinterland forest loss) in the study regions

	2007-2012 forest degradation (Mha)			Annual forest degradation (Mha/yr)	Annual gross forest cover loss (Mha/yr), Hansen et al., 2013
	total	due to proximity to disturbances	due to fragmentation		
Latin America	55.8	28.1	27.7	9.3	4.9
Africa	48.9	21.3	27.6	8.2	1.7
Southeast Asia	38.4	18.7	19.7	6.4	2.9
<i>total</i>	143.2	68.1	75.1	23.9	9.4

Table 4.2 2007 forest cover, 2007 hinterland forest extent and 2007-2012 hinterland forest loss by country. 2007 forest cover is derived from year 2000 canopy cover (Hansen et al., 2013) by thresholding (>25%) and subtracting 2000-2006 forest cover loss.

	2007 treecover	2007 hinterland		2007-2012 hinterland loss	
	Mha	Mha	% from 2007 treecover	Mha	% from 2007 hinterland
Africa					
Angola	62.86	12.44	20	5.21	42
Benin	0.58	0.00	0	-	-
Burkina Faso	0.001	0.00	0	-	-
Burundi	0.83	0.00	0	-	-
Cameroon	34.09	13.36	39	3.54	26
Central African Republic	51.54	21.51	42	5.84	27
Chad	0.94	0.05	6	0.001	3
Cote d'Ivoire	17.39	0.60	3	0.06	11
Democratic Republic of the Congo	208.68	83.43	40	16.75	20
Equatorial Guinea	2.65	1.18	44	0.48	41
Ethiopia	15.39	1.85	12	0.69	37
Gabon	24.88	16.70	67	4.68	28
Gambia	0.02	0.00	0	-	-
Ghana	7.68	0.13	2	0.07	52
Guinea	11.23	0.11	1	0.02	14
Guinea-Bissau	1.48	0.00	0	-	-
Kenya	3.86	0.24	6	0.15	60
Liberia	9.27	1.80	19	0.46	26
Madagascar	18.12	0.79	4	0.36	46
Malawi	2.17	0.00	0	-	-
Mozambique	36.38	1.70	5	0.73	43
Nigeria	12.74	1.41	11	0.49	35
Republic of Congo	28.44	16.69	59	3.19	19

	2007 treecover	2007 hinterland		2007-2012 hinterland loss	
	Mha	Mha	% from 2007 treecover	Mha	% from 2007 hinterland
Rwanda	0.70	0.04	6	0.04	100
Sierra Leone	5.99	0.06	1	0.03	44
South Sudan	16.89	3.73	22	0.52	14
Tanzania	33.52	2.05	6	0.70	34
Togo	0.79	0.00	0	-	-
Uganda	9.84	0.53	5	0.30	57
Zambia	31.32	4.68	15	1.26	27
<i>Africa total</i>	650.28	185.11	28	45.56	25
Latin America					
Argentina	38.50	3.92	10	1.73	44
Belize	1.71	0.55	32	0.08	15
Bolivia	63.85	28.83	45	7.50	26
Brazil	506.81	251.82	50	18.67	7
Colombia	81.28	40.55	50	4.17	10
Costa Rica	3.89	0.66	17	0.20	31
Cuba	4.03	0.18	4	0.05	26
Ecuador	19.03	6.71	35	0.86	13
El Salvador	0.99	0.00	0	-	-
French Guiana	8.15	7.25	89	1.27	18
Guatemala	7.41	0.90	12	0.20	22
Guyana	18.97	15.49	82	1.86	12
Haiti	0.90	0.00	0	-	-
Honduras	7.67	0.52	7	0.09	18
Jamaica	0.76	0.02	3	0.003	12
Mexico	53.89	3.22	6	0.90	28
Nicaragua	7.62	0.74	10	0.24	32
Panama	5.65	1.57	28	0.43	27
Paraguay	23.72	3.94	17	1.84	47
Peru	77.64	53.16	68	6.95	13
Suriname	13.93	11.92	86	0.85	7
Venezuela	56.54	32.29	57	2.71	8
<i>Latin America total</i>	1002.92	464.22	46	50.60	11
Asia					
Bangladesh	2.07	0.0001	0.01	0.0001	100
Bhutan	2.61	0.11	4	0.03	29
Brunei	0.52	0.25	48	0.04	17
Cambodia	8.79	1.56	18	0.72	46
China	129.57	2.11	2	1.51	71
India	41.35	2.65	6	1.05	40
Indonesia	156.16	50.06	32	14.79	30
Laos	18.87	2.76	15	1.61	58
Malaysia	27.63	4.27	15	1.83	43
Myanmar	43.06	8.38	19	4.62	55
Nepal	5.29	0.05	1	0.04	79
Papua New Guinea	42.88	18.18	42	7.17	39

	2007 treecover	2007 hinterland		2007-2012 hinterland loss	
	Mha	Mha	% from 2007 treecover	Mha	% from 2007 hinterland
Philippines	18.74	0.90	5	0.66	73
Sri Lanka	4.01	0.14	4	0.07	49
Taiwan	2.35	0.21	9	0.09	44
Thailand	20.12	2.69	13	1.26	47
Vietnam	16.61	1.53	9	0.79	51
<i>Asia total</i>	540.64	95.86	18	36.29	38
<i>Pan-tropical total</i>	2193.84	745.19	34	132.45	18

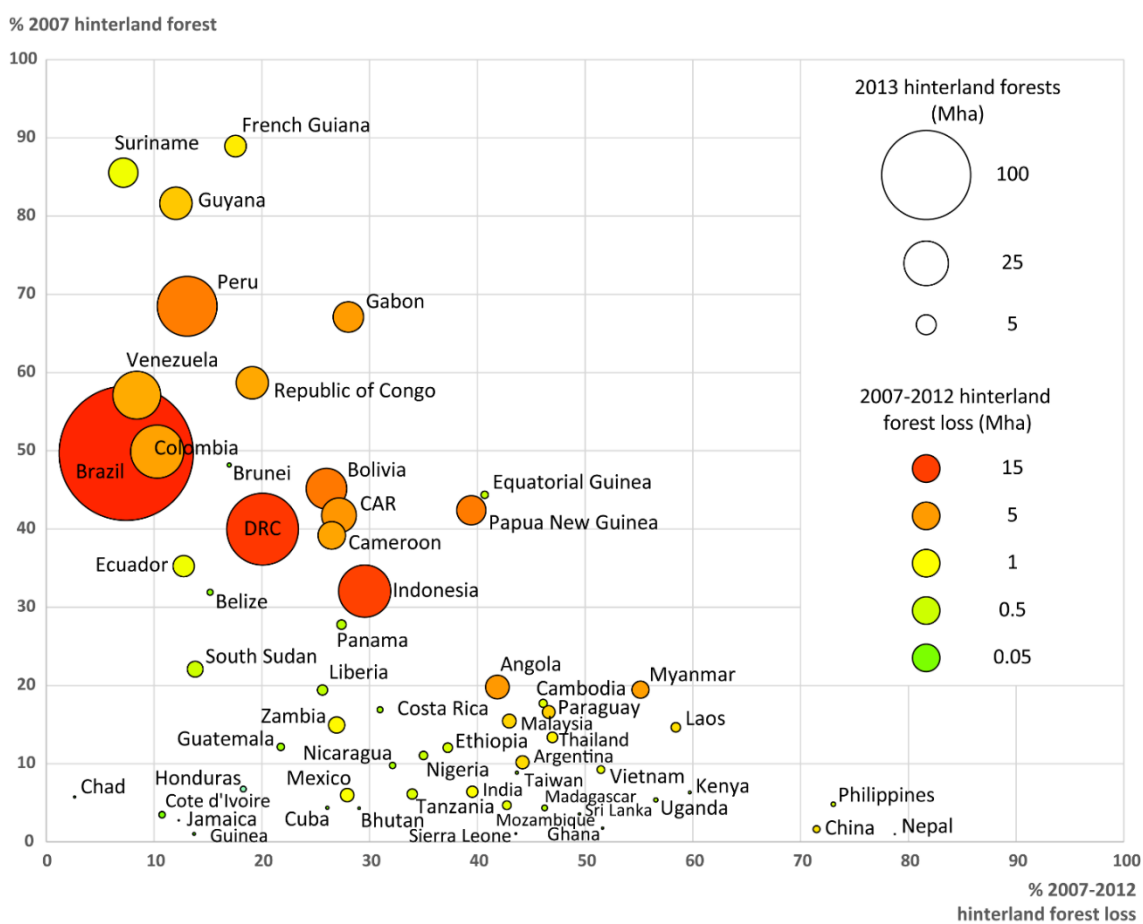


Figure 4.7 Percent of hinterland forests 2007 from total forest cover (>25%) vs. percent 2007-2013 hinterland forest loss from 2007 hinterlands. Circle size represents 2007 hinterland forest area (diameter is proportional to the square root of the area). DRC stands for the Democratic Republic of the Congo, CAR for Central African Republic. Tropical countries with hinterland forest extent <200 ha (Bangladesh, Benin, Burkina Faso, Burundi, El Salvador, Gambia, Guinea-Bissau, Haiti, Malawi, Togo) and Rwanda, which lost all of its hinterland forests by 2013, are excluded from the graph.

4.3.2 Comparison with GLAS.

The distribution of GLAS-estimated tree heights (WHRC, 2014) was analyzed for the year 2007 within and outside 2007 hinterland forests (figure 4.8). For dense forests, median tree height in hinterland forests was greater than in forests outside of hinterlands (19.7 vs. 13.7 m in Latin America, 23.0 vs. 20.3 m in Africa, 23.7 vs. 17.1 m in Southeast Asia). For forests with canopy cover of 25-75%, median tree height was greater in hinterland forests compared to non-hinterland in two regions (11.4 vs. 9.8 m in Africa, 17.7 vs. 14.1 m in Southeast Asia), and smaller in Latin America (5.4 vs. 7.2 m). The distributions of heights in the pairs of hinterland and non-hinterland forests with the same % canopy cover differed significantly (Wilcoxon-Mann-Whitney test, $p < 0.05$). This supports the hypothesis that hinterland forests mapped using the presented method are structurally different from the forests outside of the hinterlands. In most cases non-hinterland forests with the same canopy cover are shorter than hinterland forests, presumably due to degradation processes. Bereunger et al. (2014) observed from field data in the Amazon that the largest trees (≥ 50 cm DBH) are most affected by selective logging and understory fires, which corresponds with the differences in GLAS-estimated tree heights between hinterland and non-hinterland forests. Low canopy cover (25-75%) forests in Latin America represent a different case with non-hinterland forests being taller than hinterland and having wider range of tree heights (figure 4.8). Spatial distribution of these forest types in Latin America (figure 4.5) is not uniform: hinterland forests are found predominantly in Chaco woodlands, while non-hinterland forests include areas of plantation forestry, which may explain the greater mean height of non-hinterland forests in medium tree cover ecoregions.

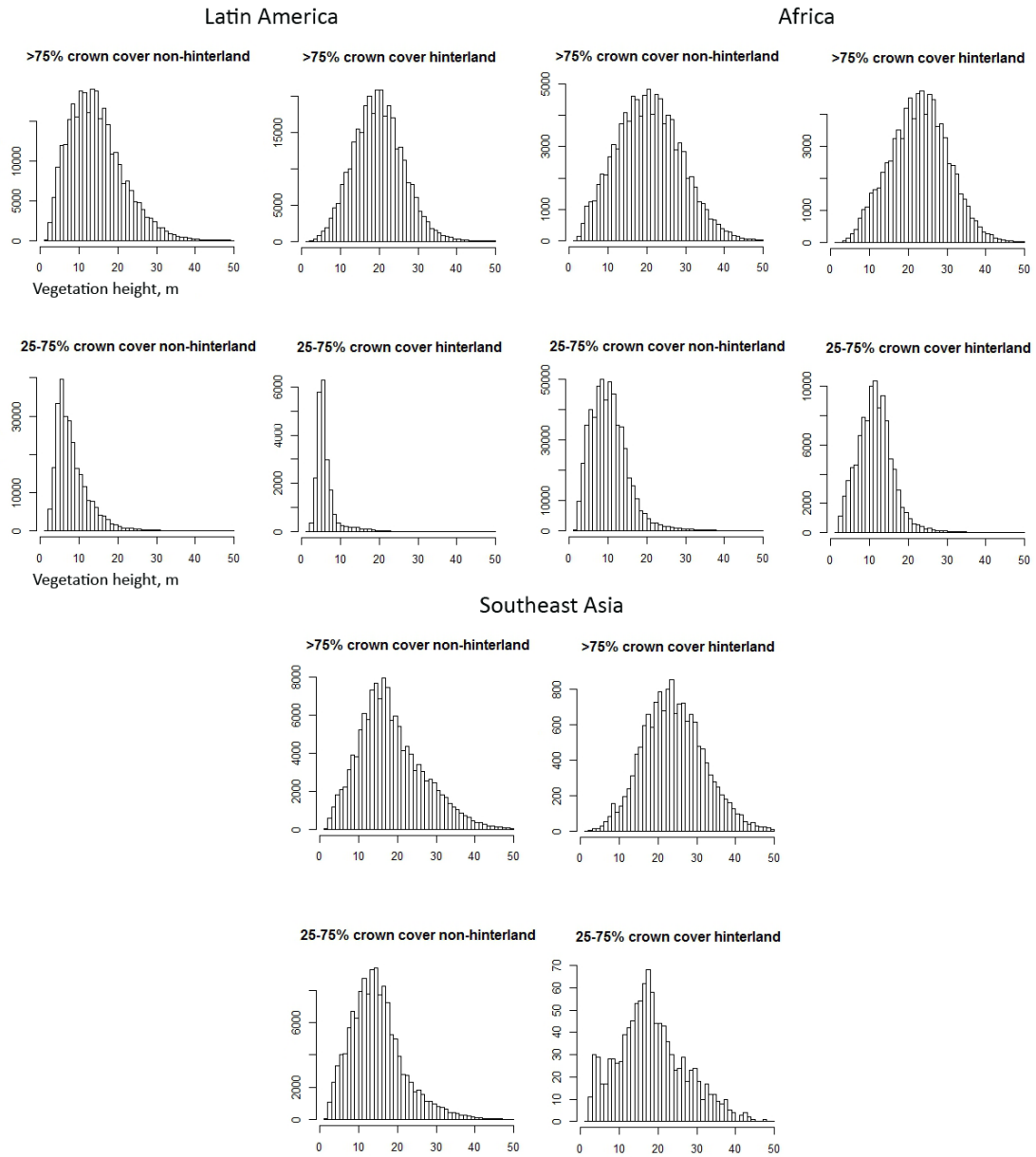


Figure 4.8 Histograms of year 2007 GLAS-estimated tree heights within and outside 2007 hinterland forests.

4.3.3 Comparison with the IFL map.

I created a 2011 hinterland forest map (using 2000-2010 forest loss data) to match and compare with previously published IFL maps for Central Africa and South-

East Asia (<http://intactforests.org/data.monitoring.html>). The basic difference between the two approaches is that IFLs include natural non-forested areas, whereas I map only forests. To account for this difference, 2010 IFL and 2011 hinterland forest maps were compared only within forests (>25% crown cover). Results of the comparison are presented in figure 4.9. The overall agreement between the two maps is 92.0% in Southeast Asia and 86.7% in Central Africa. IFL map is generally more conservative: forests, mapped as hinterland, but not included into the IFL (blue, figure 4.9) comprise 5.7 and 11.0% of the total forest area in Southeast Asia and Central Africa, while IFLs not classified as hinterlands (red, figure 4.9) make up only 2.2 and 2.3% respectively. The main sources of the disagreement are the differences in the forest cover loss data (visual interpretation of imagery vs. automated mapping results) and mapping method (table 4.3). Conceptually, the IFLs should be nested within hinterland forests, except for the inclusion of natural disturbances in the hinterland delineation. Forest canopy loss due to fire, storm damage, disease or other natural factors should manifest themselves as ephemeral in a hinterland monitoring system, similar to selective logging.

Table 4.3 Sources of disagreement between the 2010 IFL map (Potapov *et al* 2008b) and 2011 hinterland forest map (current study)

	IFL (Potapov <i>et al</i> 2008b)	Hinterland forests (current study)
Natural disturbances	Not treated as disturbances	Treated as disturbances
Secondary forests	Young secondary forests excluded	All secondary forest included
Minimum patch size	500 km ²	100 km ²
Patch width criterion	At least 10 km wide at the broadest place	No
Forest cover change buffered	No	Yes
Infrastructure (roads, pipelines, power lines, settlements) buffered	Yes	Only for new infrastructure that resulted in forest cover loss (e.g. roads established before 2000 are not buffered)

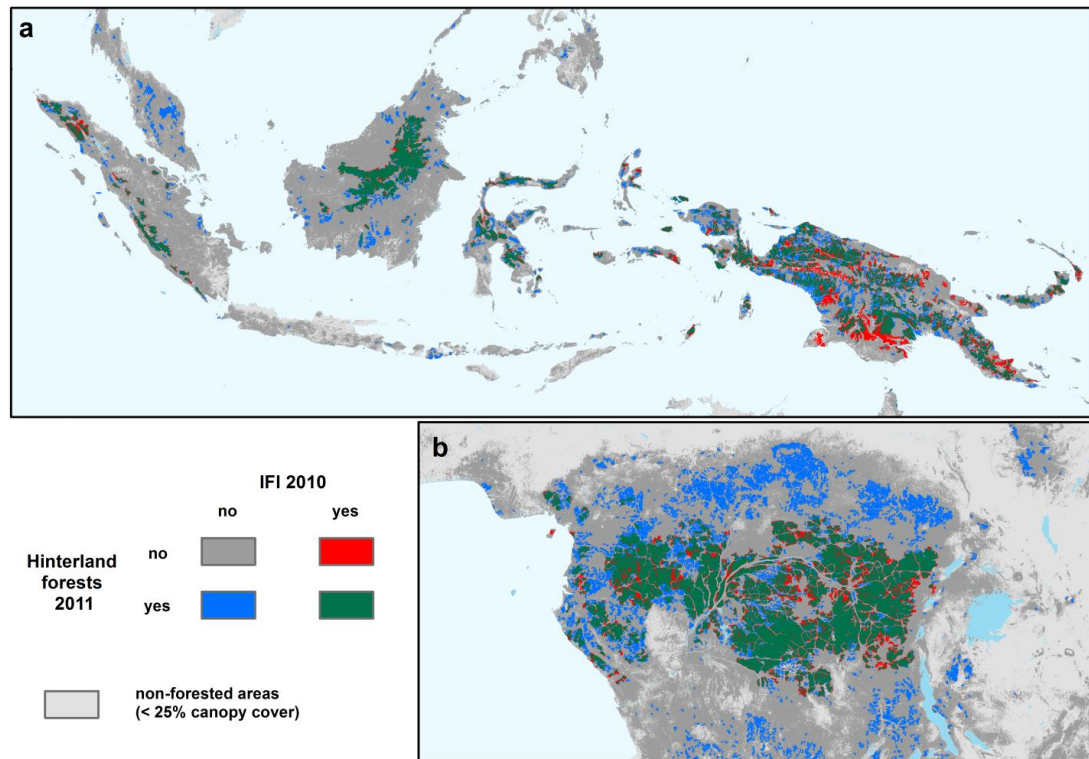


Figure 4.9 Comparison of 2010 Intact forest landscapes (IFL) map and 2011 hinterland forest map

4.4 Discussion and Conclusions

Results illustrate the dramatic loss of natural forests as the bulk of tropical forests experience land use transitions (Rudel *et al* 2005). Regions with little hinterland forest include Central America, the Caribbean, West Africa, East Africa, mainland Southeast Asia and Malaysia and the Philippines in Insular Southeast Asia. A total of 43 countries, largely from these regions, contain only 9% of all tropical hinterland forest. Two countries, Bangladesh and Rwanda, lost all remaining hinterland forests during the 2007 to 2012 period. From an ecological perspective, ensuring the preservation of remaining tracts of hinterland forest in these regions should be a priority. One example is the area of the Calakmul/Maya Biosphere Reserves in Central America, a contiguous block of hinterland forest experiencing forest loss along nearly its entire perimeter. In

West Africa, Tai National Forest in Cote D'Ivoire is the most intact remnant of Western Guinean Lowland rainforest ecoregion, constituting a discrete and largely stable zone of hinterland forest. Conversely, Brazil alone accounted for 38% of 2012 pan-tropical hinterland forest. A total of six countries accounted for 73% and seventeen 94% of all pan-tropical hinterland forests in 2012. From policy perspectives, including the UNFCCC Reducing Emissions from Deforestation and Degradation initiative (Houghton 2012), investments that take into account hinterland forest areal extent, rate of loss, ecological uniqueness, and national monitoring and management capacity, should be prioritized.

Hinterland forest maps can be used for a variety of applications, including the analysis of protected area network, prioritizing high biodiversity and high carbon stock areas (Jantz *et al* 2014), species distribution and habitat modeling (Franklin and Miller 2009), carbon monitoring (Harris *et al* 2012) and other types of geospatial analyses. The demonstrated method enables automated mapping of hinterland forests and areas likely to be experiencing forest degradation. The method is flexible regarding the baseline date of the analysis and other hinterland forest criteria. The criteria proposed here (distance from disturbance, minimum forest patch and corridor width) are based on an analysis of the literature concerning forest edge effects and fragmentation, but can be modified according to project or research needs (e.g. minimum size of forest fragment for various faunal taxonomic groups may differ from <1 to 500 km² (Turner 1996)). Automated rules for adding hinterland forest over time could also be developed, though this prototype effort did not characterize such gains. For example, Gourlet-Fleury *et al.* (2013), documented full biomass recovery for selectively logged forests of the Central African

Republic 24 years after removals. Adding such landscapes to the hinterland class, possibly labeled by age since disturbance, is feasible, but will require a longer earth observation record to implement.

Degradation is of particular importance in the context of carbon emissions and climate change mitigation. Pearson et al. (2014) estimated that carbon emissions from selective logging can lead to the loss of up to 15% of forest carbon stock. Bereunguer et al. (2014) estimated that selective logging and understory fires combined can account for the loss of 40% of aboveground carbon stock. Consistent pan-tropical mapping and monitoring of degraded forests has not yet been realized. In this study, degradation is defined as hinterland to non-hinterland forest change and consists of areas that do not exhibit disturbance directly detectable with Landsat (30-m spatial resolution). Validation and assessment of the hinterland forest change for targeting degradation is a challenge due to the fact that degradation processes are often gradual; the effects of degradation may become observable years after the creation of forest edge and/or fragmentation. Here I employed GLAS heights within and outside of hinterland forests to demonstrate the biophysical basis of the hinterland concept in discriminating likely degradation. Confirming the degree of degradation within hinterland forest change will require robust ancillary data, likely *in situ* measurements. Employing hinterland change as a stratum for allocating field inventory resources as suggested by Mollicone et al (2007) in using IFL data could facilitate quantification of forest carbon loss due to degradation for areas where resources for systematic national-scale monitoring are limited.

Limitations of the hinterland mapping method include the sensitivity to the quality of the input forest cover and change data: false positive forest change will lead to

the underestimation of the hinterland forest area and overestimation of forest degradation. Another limitation concerns the inclusion of natural forest disturbance. Excluding such change from the current automated process would require either visual interpretation or automated attribution of change factors to remove natural forest loss. For many land use applications, this is a drawback, especially for analysis change in boreal forests where the majority of the forest loss dynamic is due to wildfire (Potapov *et al* 2008a). However, the automated hinterland delineation of forests absent of recent change targets areas of relatively stable and mature forest structure, with implications for ecosystem services such as carbon stocks and biodiversity.

Chapter 5: Summary of findings, significance and future research directions

5.1. Sample-based approach to forest loss area estimation and its implications for carbon monitoring

Following the good practice recommendations (Olofsson *et al* 2014, 2013, Stehman 2013) in Chapters 2 and 3, I have employed a probability-based sampling to estimate area of forest cover loss from Landsat-resolution forest cover change maps for the DRC and for the entire pan-tropical region. Results show that area estimation based on a validation sample and exempt from map errors can significantly increase forest loss area and associated carbon loss estimates for the landscapes dominated by small-scale land dynamics, such as Central Africa. Sample-based estimation added 78% to forest loss area calculated from the map in tropical Africa (Chapter 3, tables 3.4 and 3.5), which contributed to the aboveground carbon loss estimate exceeding the previously published estimates (table 3.6). Sample-based estimations using higher spatial resolution data, e.g. 5m RapidEye time series or sub-meter optical images, may be required to adequately quantify forest cover dynamics in such environments. For the regions and countries with the predominance of large-scale industrial forest clearing, e.g. Brazil and Indonesia, I have found Landsat-based forest cover maps to perform reasonably well: sample-based loss area was within 10% of the map estimate (table 3.5).

I have also demonstrated the possibility of sample-based thematic interpretations, disaggregating loss by occurrence in natural- or human-managed forests using validation sample (Chapter 3). Only 55% of pan-tropical forest cover loss area and 58% of AGC loss were shown to originate from natural forests. Considering that the

contribution of carbon loss from natural forests to global greenhouse gas emissions is likely to continue decreasing with the decreasing extent of natural forests and increasing emissions from fossil fuels, international mechanisms like REDD+ should consider shifting the focus from carbon accounting to formal valuation of co-benefits, e.g. biodiversity and other non-carbon ecosystem services.

A sample-based approach allows identification of multiple thematic characteristics of the studied phenomenon with a minimal amount of effort instead of creating respective wall-to-wall layers. However, evaluation of the accuracy of sample-based thematic interpretations is challenging if reference datasets are nonexistent and the reference condition of the sample is defined in the interactive mode by an expert.

Map-based stratification reduces standard errors of sample-based area estimates, but to further improve estimation it may be necessary to create additional sampling substrata based on knowledge of the map properties. In Chapters 2 and 3 I have demonstrated that an additional “probable loss” stratum around mapped forest loss was effective in targeting omission errors when validating conservative national- and global-scale maps prone to forest loss omission: all validation samples with loss omission error in the DRC came from a 1-km “probable loss” buffer around mapped loss (Chapter 2, table 2.3); 78 out of 85 validation samples with loss omission error in the pan-tropical study came from a 1-pixel “probable loss” buffer (Chapter 3, table 3.2). Further evaluation is needed to understand the impact of additional sub-strata and their relative size on the area estimation, particularly sub-strata targeting likely areas of omission and commission errors.

Major advantages of the approach presented in Chapters 2 and 3 are the following:

- Flexibility regarding data inputs: publically available forest cover, change, and biomass maps, satellite data (Landsat, high resolution data from Google EarthTM), and generic carbon data may be used, although more detailed and region-specific data (e.g. national forest inventory or high resolution remotely sensed data) may be leveraged as well if available;

- Low computational requirements: sample-based analysis does not involve large amounts of data processing;

- Scalability: the approach is suitable for any spatial scale from landscape (REDD+ projects) to global;

- Error reduction: low standard errors of forest loss area estimation with a relatively small sample size due to the map-based stratification.

Some of the challenges and limitations of the method are:

- Dependence on sampling design: the result varies with the selected stratification, sample size, sampling unit and allocation of sampling units among strata. Different sample allocation scenarios can be compared using hypothetical error matrices to choose the most appropriate sampling design in each case (Stehman 2012, 2009), but the choice of the single best design is somewhat subjective and highly dependent on the specific research objectives and validation goals;

- Volatility of sample-based estimation: each realization of a probability sampling would yield slightly different estimates depending on the random sample allocation; in some cases one extremely rare sample can significantly alter the estimate (e.g. 1 omitted

loss sample out of 90 in the primary forest “probable loss” sub-stratum in the DRC brought an extra 20% to the loss area in primary forests (Chapter 2));

- Does not produce spatially explicit carbon loss maps: sample-based adjustment of forest loss area is not spatially explicit; the resulting estimate is a per stratum total (one number per stratum with the uncertainty around it);

- Uncertainties from carbon data: there is an absence of in-depth analysis of uncertainties for the carbon data, such as uncertainties from field measurements, allometric equations, model errors, etc. which could affect estimation accuracy. Carbon data are treated as a substitute of forest inventory data for the per-stratum mean carbon density calculation; standard error of the mean is calculated from a population standard deviation of the carbon data.

5.2. Potential of hinterland forest mapping in stratification for forest carbon loss estimation and in forest degradation assessment

In Chapter 4 I have demonstrated using GLAS height data that undisturbed and unfragmented hinterland forest likely have higher aboveground biomass than non-hinterland forests, and therefore hinterland forest maps can be used to improve stratifications of forest cover for carbon estimation similarly to the way the IFL map was used in a year 2000 forest cover stratification in Chapter 3. Hinterland forest mapping is highly automated and, hence, less labor-intensive compared to the original IFL mapping approach which is based on visual image interpretation. Subsequently, hinterland forest mapping is more flexible in terms of criteria and monitoring interval. At the same time, hinterland forest maps are highly reliant on the quality of the input forest cover and loss

data, e.g. forests with natural disturbances will be falsely excluded from hinterlands if a forest loss layer contains both human-induced and natural forest loss.

High biomass undisturbed forests are a primary focus of conservation efforts and deforestation prevention initiatives such as REDD+. Hinterland forest maps can help focus monitoring efforts over these priority areas, e.g. acquisition of high resolution remotely sensed imagery can be targeted along the edges of hinterland forest massifs where the expansion of human activity is most likely to occur. Time series of hinterland forest maps may be used to delineate areas of likely forest degradation and assess long-term carbon loss associated with degraded areas. Sampling of high resolution optical and LIDAR data (Asner *et al* 2010, 2014) calibrated using field surveys (Gonzalez *et al* 2010) or repeated sample-based field measurements (Berenguer *et al* 2014) may be used to quantify carbon stocks within degradation areas.

5.3. Future research directions

In paragraph 5.1. I highlighted the fact that sample-based forest loss studies, though providing crucial information on map errors and allowing estimation of forest loss area for various spatial units, are by their nature not spatially explicit. In moving from wall-to-wall maps containing errors to unbiased sample-based estimates, the spatial component is lost. One of the directions for future research is to investigate methods to return from validation data to spatially explicit maps adjusted to match sample-based estimates. To do so, it is necessary to return to the original loss probability layers, which are the outputs of the supervised classification algorithms used to derive binary forest cover maps. For example, Hansen et al. (2013) used a 50% threshold to derive a yes/no forest loss map from the loss probability layer (forest cover loss corresponds to loss

probability $\geq 50\%$). This threshold can be modified for each spatial stratum in such a way that the area of loss from the resulting adjusted map is the closest possible to the sample-based estimate. For example, for the short and medium cover strata in Africa (Chapter 3, table 3.4), where the 30-m map tends to omit forest loss, the adjusted loss probability threshold will be less conservative (below 50%), but for the dense cover tall strata in Latin America and Southeast Asia, where the map slightly overestimates forest loss, it will be more conservative (above 50%). Though this approach needs further investigation and testing, forest cover loss maps adjusted using validation sample data may become one of the standard delivery products for mapping projects, along with the original map and validation error matrix.

The hinterland forest map, one of the deliverables of Chapter 4, is planned to be used as the area of interest for prototyping near real-time forest disturbance monitoring using Landsat data. With both Landsat 7 and 8 in operation, multiple cloud-free looks within a given year are possible for the majority of hinterland areas (figure 5.1). The basic concept for near real-time monitoring is to compare Top-of-atmosphere-corrected (TOA-corrected) and normalized (using the approach from Potapov *et al* (2012)) pixel values from the current image with historical observations for the same season of the year: if the current value is outside the historic min-max range of spectral band reflectance values or indices (e.g. NDVI, NBR), a forest disturbance alert can be reported. The algorithm is planned to be prototyped for Peru and later expanded to the rest of the humid tropical domain.

There is still considerable room to improve the quantification of tropical forest dynamics and associated carbon loss, e.g. reducing the uncertainty of forest loss and gain

area estimates to improve net change estimates, improving baseline forest stratifications, attributing forest loss with drivers of change and targeting relevant emission factors of both stand-replacement disturbances and degradation for more precise carbon loss estimates. These improvements should not only aim to increase the resulting accuracy, but also to decrease the amount of effort and processing time required to derive forest area and carbon change estimates. Considering this, using information from sample-based estimates to improve map-based estimates is a promising next step in advancing forest monitoring using earth observation data. The synergistic use of sample- and map-based methods will ensure the accurate and timely generation of forest extent and change data.

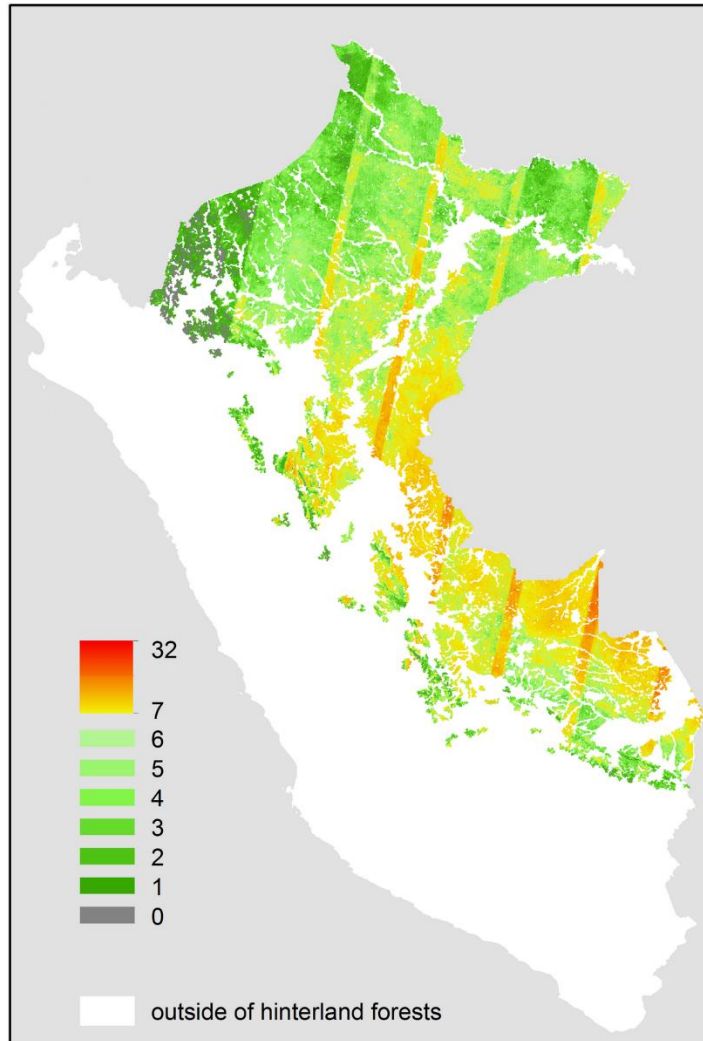


Figure 5.1 Number of cloud-free observations for each 30-m pixel during the first 288 days of the year 2014 within a hinterland forest mask in Peru.

Bibliography

- Achard F, Beuchle R, Mayaux P, Stibig H-J, Bodart C, Brink A, Carboni S, Desclée B, Donnay F, Eva H D, Lupi A, Raši R, Seliger R and Simonetti D 2014 Determination of tropical deforestation rates and related carbon losses from 1990 to 2010. *Glob. Chang. Biol.* **20** 1–15
- Achard F, DeFries R, Eva H, Hansen M, Mayaux P and Stibig H-J 2007 Pan-tropical monitoring of deforestation *Environ. Res. Lett.* **2** 045022
- Achard F, Eva H D, Stibig H-J, Mayaux P, Gallego J, Richards T and Malingreau J-P 2002 Determination of deforestation rates of the world's humid tropical forests. *Science* **297** 999–1002
- Aguiar A P D, Câmara G and Escada M I S 2007 Spatial statistical analysis of land-use determinants in the Brazilian Amazonia: Exploring intra-regional heterogeneity *Ecol. Modell.* **209** 169–88
- Alves D S 2002 Space-time dynamics of deforestation in Brazilian Amazonia *Int. J. Remote Sens.* **23** 2903–8
- Asner G P 2009 Tropical forest carbon assessment: integrating satellite and airborne mapping approaches *Environ. Res. Lett.* **4** 034009
- Asner G P, Knapp D E, Balaji A and Paez-Acosta G 2009 Automated mapping of tropical deforestation and forest degradation: CLASlite *J. Appl. Remote Sens.* **3** 033543
- Asner G P, Knapp D E, Broadbent E N, Oliveira P J C, Keller M and Silva J N 2005 Selective logging in the Brazilian Amazon. *Science* **310** 480–2
- Asner G P, Knapp D E, Martin R E, Tupayachi R, Anderson C B, Mascaro J, Sinca F, Chadwick K D, Higgins M, Farfan W, Llactayo W and Silman M R 2014 Targeted carbon conservation at national scales with high-resolution monitoring *Proc. Natl. Acad. Sci.*
- Asner G P, Powell G V N, Mascaro J, Knapp D E, Clark J K and Jacobson J 2010 High-resolution forest carbon stocks and emissions in the Amazon *Proc. Natl. Acad. Sci. U. S. A.* **107** 1–5
- Aweto A O 2013 *Shifting cultivation and secondary succession in the tropics* (Oxfordshire, UK: CABI)
- Baccini A, Goetz S J, Walker W S, Laporte N T, Sun M, Sulla-Menashe D, Hackler J, Beck P S A, Dubayah R, Friedl M A, Samanta S and Houghton R A 2012 Estimated carbon dioxide emissions from tropical deforestation improved by carbon-density maps *Nat. Clim. Chang.* **2** 182–5
- Berenguer E, Ferreira J, Gardner T A, Aragão L E O C, De Camargo P B, Cerri C E, Durigan M, Oliveira R C De, Vieira I C G and Barlow J 2014 A large-scale field assessment of carbon stocks in human-modified tropical forests. *Glob. Chang. Biol.* **2005** 1–14
- Broadbent E, Asner G, Keller M, Knapp D, Oliveira P and Silva J 2008 Forest fragmentation and edge effects from deforestation and selective logging in the Brazilian Amazon *Biol. Conserv.* **141** 1745–57
- Broich M, Stehman S V, Hansen M C, Potapov P and Shimabukuro Y E 2009 A comparison of sampling designs for estimating deforestation from Landsat

- imagery : A case study of the Brazilian Legal Amazon *Remote Sens. Environ.* **113** 2448–54
- Brown S 1997 *Estimating Biomass and Biomass Change of Tropical Forests: a Primer. UN FAO Forestry Paper 134* (Rome)
- Bryant D, Nielsen D and Tangle L 1997 *The Last Frontier Forests: Ecosystems and Economies on the Edge* (World Resources Institute, Washington, DC)
- Butler D 2014 Many eyes on Earth: Swarms of small satellites set to deliver close to real-time imagery of swathes of the planet *Nature* **505** 143–4
- Bwangoy J-R B, Hansen M C, Roy D P, Grandi G De and Justice C O 2010 Wetland mapping in the Congo Basin using optical and radar remotely sensed data and derived topographical indices *Remote Sens. Environ.* **114** 73–86
- Caccetta P, Furby S L, O’Connell J, Wallace J F and Wu X 2007 Continental Monitoring: 34 Years of Land Cover Change Using Landsat Imagery *32nd International symposium on remote sensing of environment* pp 25–9
- Céline E, Philippe M, Astrid V, Catherine B, Musampa C and Pierre D 2013 National forest cover change in Congo Basin: deforestation, reforestation, degradation and regeneration for the years 1990, 2000 and 2005. *Glob. Chang. Biol.* **19** 1173–87
- Chave J, Andalo C, Brown S, Cairns M A, Chambers J Q, Eamus D, Fölster H, Fromard F, Higuchi N, Kira T, Lescure J-P, Nelson B W, Ogawa H, Puig H, Riéra B and Yamakura T 2005 Tree allometry and improved estimation of carbon stocks and balance in tropical forests. *Oecologia* **145** 87–99
- Chave J, Condit R, Aguilar S, Hernandez A, Lao S and Perez R 2004 Error propagation and scaling for tropical forest biomass estimates. *Philos. Trans. R. Soc. Lond. B. Biol. Sci.* **359** 409–20
- Cochran W G 1977 *Sampling techniques* (New York: John Wiley & Sons, Inc.)
- Cochrane M A and Schulze M D 1999 Fire as a recurrent event in tropical forests of the eastern Amazon: effects on forest structure, biomass, and species composition *Biotropica* **31** 2–16
- Díaz S, Hector A and Wardle D A 2009 Biodiversity in forest carbon sequestration initiatives: not just a side benefit *Curr. Opin. Environ. Sustain.* **1** 55–60
- FAO 2012 *FRA 2015 Terms and Definitions. Forest Resources Assessment Working Paper 180*. (Food and Agriculture Organization of the UN, Rome, Italy)
- FAO 2010 *Global Forest Resources Assessment 2010. FAO forestry paper 163*. (Food and Agriculture Organization of the UN, Rome, Italy)
- Franklin J and Miller J A 2009 *Mapping species distributions* (Cambridge University Press, New York)
- Furusawa T, Pahari K, Umezaki M and Ohtsuka R 2004 Impacts of selective logging on New Georgia Island, Solomon Islands evaluated using very-high-resolution satellite (IKONOS) data *Environ. Conserv.* **31** 349–55
- Gascon C, Williamson B G and da Fonseca G A B 2000 Receding Forest Edges and Vanishing Reserves *Science* (80-.). **288** 1356–8
- GFOI 2014 *Integrating remote-sensing and ground-based observations for estimation of emissions and removals of greenhouse gases in forests: Methods and Guidance from the Global Forest Observations Initiative. Version 1, January 2014* (Group on Earth Observations, Geneva, Switzerland)

- Gibbs H K 2006 Major World Ecosystem Complexes Ranked by Carbon in Live Vegetation: An Updated Database Using the GLC2000 Land Cover Product. NDP-017b.
- Gibbs H K and Brown S 2007 Geographical Distribution of Woody Biomass Carbon in Tropical Africa: An Updated Database for 2000. NDP-055b
- Gibbs H K, Brown S, Niles J O and Foley J a 2007 Monitoring and estimating tropical forest carbon stocks: making REDD a reality *Environ. Res. Lett.* **2** 045023
- Goetz S and Dubayah R 2011 Advances in remote sensing technology and implications for measuring and monitoring forest carbon stocks and change *Carbon Manag.* **2** 231–44
- Goetz S J, Baccini A, Laporte N T, Johns T, Walker W, Kellndorfer J, Houghton R A and Sun M 2009 Mapping and monitoring carbon stocks with satellite observations: a comparison of methods *Carbon Balance Manag.* **4** 2
- GOFC-GOLD 2013 *A sourcebook of methods and procedures for monitoring and reporting anthropogenic greenhouse gas emissions and removals associated with deforestation, gains and losses of carbon stocks in forests remaining forests, and forestation. Version COP19-2* (GOFC-GOLD Land Cover Project Office, Wageningen University, The Netherlands)
- GOFC-GOLD 2010 *A sourcebook of methods and procedures for monitoring and reporting anthropogenic greenhouse gas emissions and removals caused by deforestation, gains and losses of carbon stocks in forests remaining forests, and forestation. Report version COP16-1.* (GOFC-GOLD Project Office, Natural Resources Canada, Alberta, Canada)
- Gonzalez P, Asner G P, Battles J J, Lefsky M A, Waring K M and Palace M 2010 Forest carbon densities and uncertainties from Lidar, QuickBird, and field measurements in California *Remote Sens. Environ.* **114** 1561–75
- Gourlet-Fleury S, Mortier F, Fayolle A, Baya F, Ouédraogo D, Bénédet F and Picard N 2013 Tropical forest recovery from logging: a 24 year silvicultural experiment from Central Africa. *Philos. Trans. R. Soc. Lond. B. Biol. Sci.* **368** 20120302
- Government of Guyana 2014 *The Reference Level for Guyana's REDD+ Program*
- Hansen M C and DeFries R S 2004 Detecting Long-term Global Forest Change Using Continuous Fields of Tree-Cover Maps from 8-km Advanced Very High Resolution Radiometer (AVHRR) Data for the Years 1982-99 *Ecosystems* **7** 695–716
- Hansen M C, Egorov A, Potapov P V, Stehman S V, Tyukavina A, Turubanova S, Roy D P, Goetz S J, Loveland T R, Ju J, Kommareddy A, Kovalsky V, Forsyth C and Bents T 2014 Monitoring conterminous United States (CONUS) land cover change with Web-Enabled Landsat Data (WELD) *Remote Sens. Environ.* **140** 466–84
- Hansen M C, Potapov P V, Moore R, Hancher M, Turubanova S a, Tyukavina A, Thau D, Stehman S V, Goetz S J, Loveland T R, Kommareddy A, Egorov A, Chini L, Justice C O and Townshend J R G 2013 High-resolution global maps of 21-st century forest cover change *Science* **342** 850–3
- Hansen M C, Potapov P V and Turubanova S A 2012 Use of Coarse Resolution Imagery to Identify Hot Spots of Forest Loss at the Global Scale *Global Forest*

- Monitoring from Earth Observation* ed F Achard and M Hansen (Taylor and Francis, New York)
- Hansen M C, Roy D P, Lindquist E, Adusei B, Justice C O and Altstatt A 2008 A method for integrating MODIS and Landsat data for systematic monitoring of forest cover and change in the Congo Basin *Remote Sens. Environ.* **112** 2495–513
- Hansen M C, Stehman S V and Potapov P V 2010 Quantification of global gross forest cover loss *Proc. Natl. Acad. Sci. U. S. A.* **107** 8650–5
- Harris N L, Brown S, Hagen S C, Saatchi S S, Petrova S, Salas W, Hansen M C, Potapov P V and Lotsch A 2012 Baseline map of carbon emissions from deforestation in tropical regions. *Science* **336** 1573–6
- Hayes D J and Cohen W B 2007 Spatial , spectral and temporal patterns of tropical forest cover change as observed with multiple scales of optical satellite data *Remote Sens. Environ.* **106** 1–16
- Herold M, Román-Cuesta R M, Mollicone D, Hirata Y, Van Laake P, Asner G P, Souza C, Skutsch M, Avitabile V and Macdicken K 2011 Options for monitoring and estimating historical carbon emissions from forest degradation in the context of REDD+. *Carbon Balance Manag.* **6** 13
- Hirschmugl M, Steinegger M, Gallaun H and Schardt M 2014 Mapping Forest Degradation due to Selective Logging by Means of Time Series Analysis: Case Studies in Central Africa *Remote Sens.* **6** 756–75
- Houghton R A 2012 Carbon emissions and the drivers of deforestation and forest degradation in the tropics *Curr. Opin. Environ. Sustain.* **4** 597–603
- Houghton R A 2013 The emissions of carbon from deforestation and degradation in the tropics: past trends and future potential *Carbon Manag.* **4** 539–46
- Houghton R A, Greenglass N, Baccini A, Cattaneo A, Goetz S, Kellndorfer J, Laporte N and Walker W 2010 The role of science in Reducing Emissions from Deforestation and Forest Degradation (REDD) *Carbon Manag.* **1** 253–9
- Houghton R A, Lawrence K T, Hackler J L and Brown S 2001 The spatial distribution of forest biomass in the Brazilian Amazon: a comparison of estimates *Glob. Chang. Biol.* **7** 731–46
- INPE 2008 *Monitoramento da cobertura florestal da Amazônia por satélites: Sistemas PRODES, DETER, DEGRAD E QUEIMADAS 2007-2008*. (São José dos Campos, SP, Brazil: Instituto Nacional de Pesquisas Espaciais)
- Instituto Nacional de Pesquisas Espaciais 2012 Monitoring of the Brazilian Amazonian Forest by Satellite, 2000-2012
- IPCC 2006 *IPCC Guidelines for National Greenhouse Gas Inventories* ed H S Eggleston, L Buendia, K Miwa, T Ngara and K Tanabe (Hayama, Japan: Institute for Global Environmental Strategies)
- IPCC 2013 *Climate Change 2013: the Physical Science Basis. Contribution of Working Group I to the Fifth Assessment Report of the Intergovernmental Panel on Climate Change* (Cambridge University Press, Cambridge, UK and New York, NY, USA)
- IPCC 2014 *Climate Change 2014: Mitigation of Climate Change. Contribution of Working Group III to the Fifth Assessment Report of the Intergovernmental Panel on Climate Change*

- IPCC 2003a *Definitions and Methodological Options to Inventory Emissions from Direct Human-induced Degradation of Forests and Devegetation of Other Vegetation Types* (Hayama, Japan: Institute for Global Environmental Strategies)
- IPCC 2003b *Good practice guidance for land use, land-use change and forestry* (IPCC National Greenhouse Gas Inventories Programme, Hayama, Japan)
- Jantz P, Goetz S and Laporte N 2014 Carbon stock corridors to mitigate climate change and promote biodiversity in the tropics *Nat. Clim. Chang.* **4**
- Khorram S 1999 *Accuracy Assessment of Remote Sensing-Derived Change Detection* ed S Khorram (Bethesda, MD: American Society for Photogrammetry and Remote Sensing)
- Kim D-H, Sexton J O, Noojipady P, Huang C, Anand A, Channan S, Feng M and Townshend J R 2014 Global, Landsat-based forest-cover change from 1990 to 2000 *Remote Sens. Environ.*
- Kindermann G E, McCallum I, Fritz S and Obersteiner M 2008 A global forest growing stock, biomass and carbon map based on FAO statistics *Silva Fenn.* **42** 387–96
- Laporte N T, Stabach J A, Grosch R, Lin T S and Goetz S J 2007 Expansion of industrial logging in Central Africa *Science* (80-.). **316** 1451
- Lefsky M A, Harding D J, Keller M, Cohen W B, Carabajal C C, Espirito-santo F D B, Hunter M O and Jr R D O 2005 Estimates of forest canopy height and aboveground biomass using ICESat *Geophys. Res. Lett.* **32** L22S02
- Lehmann E A, Caccetta P A, Zhou Z-S, McNeill S J, Wu X and Mitchell A L 2012 Joint Processing of Landsat and ALOS-PALSAR Data for Forest Mapping and Monitoring *IEEE Trans. Geosci. Remote Sens.* **50** 55–67
- Malhi Y, Wood D, Baker T R, Wright J, Phillips O L, Cochrane T, Meir P, Chave J, Almeida S, Arroyo L, Higuchi N, Killeen T J, Laurance S G, Laurance W F, Lewis S L, Monteagudo A, Neill D A, Vargas P N, Pitman N C A, Quesada C A, Salomao R, Silva J N M, Lezama A T, Terborgh J, Martinez R V and Vinceti B 2006 The regional variation of aboveground live biomass in old-growth Amazonian forests *Glob. Chang. Biol.* **12** 1107–38
- Maniatis D and Mollicone D 2010 Options for sampling and stratification for national forest inventories to implement REDD+ under the UNFCCC. *Carbon Balance Manag.* **5** 9
- Margono B A, Potapov P V, Turubanova S A, Stolle F, Hansen M C and Stole F 2014 Primary forest cover loss in Indonesia over 2000 to 2012 *Nat. Clim. Chang.* **4** 730–5
- Margono B A, Turubanova S, Zhuravleva I, Potapov P, Tyukavina A, Baccini A, Goetz S and Hansen M C 2012 Mapping and monitoring deforestation and forest degradation in Sumatra (Indonesia) using Landsat time series data sets from 1990 to 2010 *Environ. Res. Lett.* **7** 034010
- Mccloskey J M and Spalding H 1989 A Reconnaissance-Level Inventory of the Amount of Wilderness Remaining in the World *Ambio* **18**
- Miles L and Kapos V 2008 Reducing greenhouse gas emissions from deforestation and forest degradation: global land-use implications. *Science* **320** 1454–5
- Millennium Ecosystem Assessment 2005 *Ecosystems and Human Well-being: Current State and Trends, Volume 1*

- Mitchard E T A, Feldpausch T R, Brien R J W, Lopez-Gonzalez G, Monteagudo A, Baker T R, Lewis S L, Lloyd J, Quesada C A, Gloor M, ter Steege H, Meir P, Alvarez E, Araujo-Murakami A, Aragão L E O C, Arroyo L, Aymard G, Banki O, Bonal D, Brown S, Brown F I, Cerón C E, Chama Moscoso V, Chave J, Comiskey J a., Cornejo F, Corrales Medina M, Da Costa L, Costa F R C, Di Fiore A, Domingues T F, Erwin T L, Frederickson T, Higuchi N, Honorio Coronado E N, Killeen T J, Laurance W F, Levis C, Magnusson W E, Marimon B S, Marimon Junior B H, Mendoza Polo I, Mishra P, Nascimento M T, Neill D, Núñez Vargas M P, Palacios W A, Parada A, Pardo Molina G, Peña-Claros M, Pitman N, Peres C a., Poorter L, Prieto A, Ramirez-Angulo H, Restrepo Correa Z, Roopsind A, Roucoux K H, Rudas A, Salomão R P, Schiatti J, Silveira M, de Souza P F, Steininger M K, Stropp J, Terborgh J, Thomas R, Toledo M, Torres-Lezama A, van Andel T R, van der Heijden G M F, Vieira I C G, Vieira S, Vilanova-Torre E, Vos V A, Wang O, Zartman C E, Malhi Y and Phillips O L 2014 Markedly divergent estimates of Amazon forest carbon density from ground plots and satellites *Glob. Ecol. Biogeogr.* 1–12
- Mitchard E T A, Saatchi S S, Baccini A, Asner G P, Goetz S J, Harris N L and Brown S 2013 Uncertainty in the spatial distribution of tropical forest biomass: a comparison of pan-tropical maps *Carbon Balance Manag.* **8**
- Mokany K, Raison R J and Prokushkin A S 2006 Critical analysis of root : shoot ratios in terrestrial biomes *Glob. Chang. Biol.* **12** 84–96
- Mollicone D, Achard F, Federici S, Eva H D, Grassi G, Belward A, Raes F, Seufert G, Stibig H-J, Matteucci G and Schulze E-D 2007 An incentive mechanism for reducing emissions from conversion of intact and non-intact forests *Clim. Change* **83** 477–93
- Mullan K 2014 *The Value of Forest Ecosystem Services to Developing Economies. CGD Working Paper 379.* (Washington, DC: Center for Global Development)
- Olofsson P, Foody G M, Herold M, Stehman S V, Woodcock C E and Wulder M A 2014 Good practices for estimating area and assessing accuracy of land change *Remote Sens. Environ.* **148** 42–57
- Olofsson P, Foody G M, Stehman S V. and Woodcock C E 2013 Making better use of accuracy data in land change studies: Estimating accuracy and area and quantifying uncertainty using stratified estimation *Remote Sens. Environ.* **129** 122–31
- Ometto J P, Aguiar A P, Assis T, Soler L, Valle P, Tejada G, Lapola D M and Meir P 2014 Amazon forest biomass density maps: tackling the uncertainty in carbon emission estimates *Clim. Change*
- Page S E, Siegert F, Rieley J O, Boehm H V, Jayak A and Limink S 2002 The amount of carbon released from peat and forest fires in Indonesia during 1997 *Nature* **420** 61–5
- Pan Y, Birdsey R A, Fang J, Houghton R, Kauppi P E, Kurz W A, Phillips O L, Shvidenko A, Lewis S L, Canadell J G, Ciais P, Jackson R B, Pacala S W, McGuire A D, Piao S, Rautiainen A, Sitch S and Hayes D 2011 A large and persistent carbon sink in the world's forests *Science* **333** 988–93
- Pearson T R H, Brown S and Casarim F M 2014 Carbon emissions from tropical forest degradation caused by logging *Environ. Res. Lett.* **9** 1–11

- Pflugmacher D, Cohen W, Kennedy R and Lefsky M 2008 Regional applicability of forest height and aboveground biomass models for the Geoscience Laser Altimeter System *For. Sci.* **54** 647–57
- Phelps J, Webb E L and Adams W M 2012 Biodiversity co-benefits of policies to reduce forest-carbon emissions *Nat. Clim. Chang.* **2** 497–503
- Popescu S C 2007 Estimating biomass of individual pine trees using airborne lidar *Biomass and Bioenergy* **31** 646–55
- Popescu S C, Zhao K, Neuenschwander A and Lin C 2011 Satellite lidar vs. small footprint airborne lidar: Comparing the accuracy of aboveground biomass estimates and forest structure metrics at footprint level *Remote Sens. Environ.* **115** 2786–97
- Potapov P, Hansen M C, Stehman S V, Loveland T R and Pittman K 2008a Combining MODIS and Landsat imagery to estimate and map boreal forest cover loss *Remote Sens. Environ.* **112** 3708–19
- Potapov P, Turubanova S and Hansen M C 2011 Regional-scale boreal forest cover and change mapping using Landsat data composites for European Russia *Remote Sens. Environ.* **115** 548–61
- Potapov P V, Dempewolf J, Talero Y, Hansen M C, Stehman S V, Vargas C, Rojas E J, Castillo D, Mendoza E, Calderón A, Giudice R, Malaga N and Zutta B R 2014 National satellite-based humid tropical forest change assessment in Peru in support of REDD+ implementation *Environ. Res. Lett.* **9** 124012
- Potapov P V, Turubanova S A, Hansen M C, Adusei B, Broich M, Altstatt A, Mane L and Justice C O 2012 Quantifying forest cover loss in Democratic Republic of the Congo, 2000–2010, with Landsat ETM+ data *Remote Sens. Environ.* **122** 106–16
- Potapov P, Yaroshenko A, Turubanova S, Dubinin M, Laestadius L, Thies C, Aksenov D, Egorov A, Yesipova Y, Glushkov I, Karpachevskiy M, Kostikova A, Manisha A and Tsybikova E 2008b Mapping the world's intact forest landscapes by remote sensing *Ecol. Soc.* **13** 51
- Potts M D, Kelley L C and Doll H M 2013 Maximizing biodiversity co-benefits under REDD+: a decoupled approach *Environ. Res. Lett.* **8** 1–5
- Pütz S, Groeneveld J, Henle K, Knogge C, Martensen A C, Metz M, Metzger J P, Ribeiro M C, de Paula M D and Huth A 2014 Long-term carbon loss in fragmented Neotropical forests *Nat. Commun.* **5** 5037
- Rembold F, Oduori S M, Gadain H and Toselli P 2013 Mapping charcoal driven forest degradation during the main period of Al Shabaab control in Southern Somalia *Energy Sustain. Dev.* **17** 510–4
- Romijn E, Herold M, Kooistra L, Murdiyarso D and Verchot L 2012 Assessing capacities of non-Annex I countries for national forest monitoring in the context of REDD+ *Environ. Sci. Policy* **19–20** 33–48
- Roy D P, Ju J, Kline K, Scaramuzza P L, Kovalskyy V, Hansen M C, Loveland T R, Vermote E and Zhang C 2010 Web-enabled Landsat Data (WELD): Landsat ETM + composited mosaics of the conterminous United States *Remote Sens. Environ.* **114** 35–49
- Rudel T K, Coomes O T, Moran E, Achard F, Angelsen A, Xu J and Lambin E 2005 Forest transitions: towards a global understanding of land use change *Glob. Environ. Chang.* **15** 23–31

- Saatchi S S, Harris N L, Brown S, Lefsky M, Mitchard E T A and Salas W 2011 Benchmark map of forest carbon stocks in tropical regions across three continents *PNAS* **108** 9899–904
- Sanderson E W, Jaiteh M, Levy M A, Redford K H, Wannebo A V and Woolmer G 2002 The Human Footprint and the Last of the Wild *Bioscience* **52**
- Schoene D, Killmann W, von Luepke H and LoycheWilkie M 2007 *Definitional issues related to reducing emissions from deforestation in developing countries. Forest and Climate Change Working Paper 5*. (Food and Agriculture Organization of the UN, Rome, Italy)
- Shimabukuro Y E, Batista G T, Mello E M K, Moreira J C and Duarte V 1998 Using shade fraction image segmentation to evaluate deforestation in Landsat Thematic Mapper images of the Amazon Region *Int. J. Remote Sens.* **19** 535–41
- Shimabukuro Y E, dos Santos J R, Formaggio A R, Duarte V and Rudorff B F T 2012 The Brazilian Amazon Monitoring Program: PRODES and DETER Projects *Global Forest Monitoring from Earth Observation* (CRC Press) p 354
- Skole D and Tucker C 1993 Tropical Deforestation and Habitat Fragmentation in the Amazon: Satellite Data from 1978 to 1988 *Science* (80-.). **260** 1905–10
- Souza C M, Roberts D A and Monteiro A L 2005 Multitemporal Analysis of Degraded Forests in the Southern Brazilian Amazon *Earth Interact.* **9** 1–25
- Souza Jr. C 2012 Monitoring of Forest Degradation: A Review of Methods in the Amazon Basin *Global Forest Monitoring from Earth Observation* ed F Achard and M C Hansen (Taylor and Francis, New York)
- Stehman S V 2013 Estimating area from an accuracy assessment error matrix *Remote Sens. Environ.* **132** 202–11
- Stehman S V 2012 Impact of sample size allocation when using stratified random sampling to estimate accuracy and area of land-cover change *Remote Sens. Lett.* **3** 111–20
- Stehman S V 2009 Sampling designs for accuracy assessment of land cover *Int. J. Remote Sens.* **30** 5243–72
- Stehman S V and Czaplewski R L 1998 Design and Analysis for Thematic Map Accuracy Assessment : Fundamental Principles *Remote Sens. Environ.* **64** 331–44
- Stehman S V. 2014 Estimating area and map accuracy for stratified random sampling when the strata are different from the map classes *Int. J. Remote Sens.* **35** 4923–39
- Sun G, Ranson K, Kimes D, Blair J and Kovacs K 2008 Forest vertical structure from GLAS: An evaluation using LVIS and SRTM data *Remote Sens. Environ.* **112** 107–17
- Thiel C J, Thiel C and Schmullius C C 2009 Operational Large-Area Forest Monitoring in Siberia Using ALOS PALSAR Summer Intensities and Winter Coherence *IEEE Trans. Geosci. Remote Sens.* **47** 3993–4000
- Treuhaft R N, Chapman B D, dos Santos J R, Gonçalves F G, Dutra L V, Graça P M L A and Drake J B 2009 Vegetation profiles in tropical forests from multibaseline interferometric synthetic aperture radar, field, and lidar measurements *J. Geophys. Res.* **114** D23110
- Turner I M 1996 Species Loss in Fragments of Tropical Rain Forest : A Review of the Evidence *J. Appl. Ecol.* **33** 200–9

- Tyukavina A, Stehman S V, Potapov P V, Turubanova S a, Baccini A, Goetz S J, Laporte N T, Houghton R A and Hansen M C 2013 National-scale estimation of gross forest aboveground carbon loss: a case study of the Democratic Republic of the Congo *Environ. Res. Lett.* **8** 1–14
- UNFCCC 2014 *Report of the Conference of the Parties on its nineteenth session, held in Warsaw from 11 to 23 November 2013*. (United Nations Office at Geneva, Switzerland)
- UNFCCC 2006 *Report of the Conference of the Parties serving as the meeting of the Parties to the Kyoto Protocol on its first session, held at Montreal from 28 November to 10 December 2005*. (United Nations Office at Geneva, Switzerland)
- UN-REDD 2011 *Expert meeting on assessment of forest inventory approaches for REDD+. Meeting report*. (Rome)
- Walker W S, Member A, Stickler C M, Kellndorfer J M, Member S, Kirsch K M and Nepstad D C 2010 Large-Area Classification and Mapping of Forest and Land Cover in the Brazilian Amazon : A Comparative Analysis of ALOS / PALSAR and Landsat Data Sources **3** 594–604
- Van der Werf G R, Morton D C, DeFries R S, Olivier J G J, Kasibhatla P S, Jackson R B, Collatz G J and Randerson J T 2009 CO₂ emissions from forest loss *Nat. Geosci.* **2**
- Wildlife Conservation Society 2008 Massive Numbers Of Critically Endangered Western Lowland Gorillas Discovered In Republic Of Congo *ScienceDaily*
- Wulder M A, Masek J G, Cohen W B, Loveland T R and Woodcock C E 2012 Opening the archive: How free data has enabled the science and monitoring promise of Landsat *Remote Sens. Environ.* **122** 2–10
- Zheng D L, Prince S D and Wright R 2003 NPP Multi-Biome: Gridded Estimates for Selected Regions Worldwide, 1989-2001, R1. Data set.
- Zhuravleva I, Turubanova S, Potapov P, Hansen M, Tyukavina A, Minnemeyer S, Laporte N, Goetz S, Verbelen F and Thies C 2013 Satellite-based primary forest degradation assessment in the Democratic Republic of the Congo, 2000–2010 *Environ. Res. Lett.* **8** 1–13
- Zolkos S G, Goetz S J and Dubayah R 2013 A meta-analysis of terrestrial aboveground biomass estimation using lidar remote sensing *Remote Sens. Environ.* **128** 289–98